NASA TECHNICAL TRANSLATION

NASA TT F-247




# PROBLEMS OF THE MOVEMENT OF LARGE METEORIC BODIES IN THE ATMOSPHERE

*by V. A. Bronshten*

*Izdatel'stvo Akademii Nauk SSSR,*
*Moscow,* 1963

NATIONAL AERONAUTICS AND SPACE ADMINISTRATION • WASHINGTON, D. C. • NOVEMBER 1964

# PROBLEMS OF THE MOVEMENT OF LARGE METEORIC BODIES IN THE ATMOSPHERE

By V. A. Bronshten

Translation of "Problemy dvizheniya v atmosfere krupnykh meteoritnykh tel"

Izdatel'stvo Akademii Nauk SSSR,
Moscow, 1963

NATIONAL AERONAUTICS AND SPACE ADMINISTRATION

For sale by the Office of Technical Services, Department of Commerce,
Washington, D.C. 20230 -- Price $2.75

CONTENTS

## FROM THE AUTHOR

The movement of meteorites, that is, of bodies of considerable mass, through the atmosphere of the earth takes place at enormous velocities—from 11 to 72 km/sec. At such velocities the flying meteorite forms a very strong shock wave, comparable with the shock waves of nuclear explosions and considerably exceeding in amplitude the shock waves formed in the course of flow about supersonic aircraft, missiles or rockets, as well as models in aerodynamic experiments.

On the other hand, in the shock wave of a flying meteorite there is an interaction of the shock wave with the body leading to the melting and evaporation of that body. This circumstance differentiates the shock waves of meteorites from explosion waves.

Meteoric bodies of smaller size, engendering meteoric phenomena and having, naturally, the same velocities as do meteorite-forming bodies, fly under different conditions of flow and do not form a shock wave.

All this differentiates the problem of the movement of meteorites in the atmosphere from problems connected with the study of shock waves and the hypersonic flow about bodies at velocities of less than 11 km/sec, as well as the movement of meteors. The complexity of the problem under consideration lies in the necessity for taking into account nonequilibrium processes in the shock waves, interaction of the wave with a body subjected to ablation (evaporation) and the almost total lack of experimental data.

This work does not claim to be an attempt at creating a theory of the movement of a meteorite in the atmosphere; the development of such a theory will yet require no small amount of effort on the part of large teams of specialists. Our objective is a more modest problem: to systematize and bring into clear focus the basic elementary processes originating in the shock wave and in the course of its interaction with the meteorite. We have devoted particular attention to the kinetics of ionization, and to its influence on the temperature distribution within the shock wave. Unfortunately, to now calculations of the thermal action of the shock wave on a meteorite have taken either no account at all of ionization, or only very rough estimates were made, it being possible for the errors of these estimates to attain one order of magnitude in the value of the temperature, and several orders in the estimates of the heat flow. This applies also to the effect of thermal blocking.

No consideration is given by us to questions connected with the properties of the ballistic waves of meteorites at considerable distances from the body, and with the action of these ballistic waves on terrestrial objects.

We assume that the reader is familiar with the basic physical theory of meteors within the scope of B. Yu. Levin's monograph "Fizicheskaya teoriya meteorov i meteornoye veschestvo v solnechnoy sisteme" (The Physical Theory of Meteors and Meteoric Substance in the Solar System), as well as with the general principles of gasdynamics.

We take this opportunity to express deep gratitude to the scientific editor of the book, Prof. K. P. Stanyukovich, for constant attention and assistance in the work, to Doctor of Physical and Mathematical Sciences, B. Yu. Levin, Doctor of Physical and Mathematical Sciences, Yu. P. Rayzer, Doctor of Physical and Mathematical Sciences, L. M. Biberman, Doctor of Physical and Mathematical Sciences, S. B. Pikel'ner, Professor G. I. Pokrovskiy for helpful creative discussions and remarks, Candidates of Physical and Mathematical Sciences, O. M. Bolotsenkovskiy, and N. M. Kuznetsov for the presentation of valuable materials.

The author thanks programmer A. N. Chigorin for compiling the necessary computations on the "Strela" electronic computer, as well as the Council of the Moscow Division of the All-Union Astronomical and Geodetic Society and the Astronomical Council of the Academy of Sciences USSR for making these calculations possible.

The author will gratefully accept all remarks and requests connected with the present work; these should be directed to the following address: Moscow, K-9, p/ya(P.O. Box)1268, VAVO, V. A. Bronshten.

V. A. Bronshten

# INTRODUCTION

## Section 1. Formulation of the Problem

The problem of the movement in the terrestrial atmosphere of large cosmic bodies capable of penetrating the atmosphere and landing on the earth in the form of meteorites is at present of great theoretical and practical interest. The theoretical value of this problem is determined by the multiformity of the physical phenomena accompanying the movement of a large body through the atmosphere at a cosmic velocity (the formation of a strong shock wave, heating, the dissociation and ionization of air behind the front of the shock wave, heat transfer, ablation of the meteoric body, etc.). The practical value of this problem is connected with the development of space flights and the problem of the return of space ships to earth.

By now, because of the research of many specialists, in particular I. Khoppe, B. Yu. Levin, K. P. Stanyukovich and Öpik, a theory of the phenomena accompanying the flight of meteors in the atmosphere, which has received the name of the physical theory of meteors, has been worked out in detail. This theory is applicable to meteoric bodies with a diameter of not more than 1 cm, which engender the conventional and bright meteors. Such bodies are completely destroyed in the atmosphere, thereby not reaching the earth's surface.

In a considerably less developed condition is the theory of the movement of large, meteorite-forming masses in the atmosphere; actually speaking, such a theory has not yet been developed. The multiformity of the problems that must be solved, in order that such a theory be developed, is so broad that for their solution the participation of large teams of scientists of different specialties is required.

In order to provide a conception of the place of the phenomenon under consideration, among others of a similar nature that are connected with motion with respect to a large body through rarefied gas, we shall construct a schematic mass, the velocity diagram (Figure 1), on which we shall enter, on the basis of mass and velocity arguments, the areas occupied by bodies of various classes.

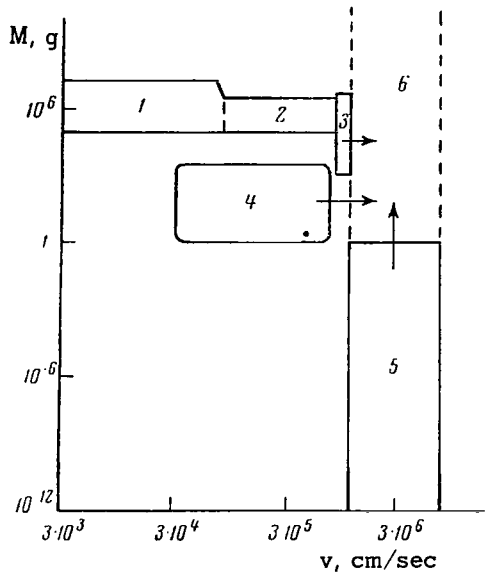


Figure 1. Diagram, in the plane M, v, of the movement of various bodies under supersonic conditions.

1. Aircraft. The masses of modern aircraft are from 100 kg to 200 tons, i.e., from $10^5$ to $2 \cdot 10^8$ g; the velocities attained are up to 1 km/sec, and more.

2. Meteorological, geophysical, and ballistic rockets. The masses are of the same order as in the case of aircraft; the velocities range from 1 to 8 km/sec, because when orbital velocity is exceeded this rocket passes into the next class of bodies.

3. Artificial earth satellites and space rockets. The masses are from 1.5 kg to 6.5 tons, i.e., from $1.5 \cdot 10^3$ to $6.5 \cdot 10^6$ g; the velocities range from 8 to 12 km/sec.

4. Models used in aerodynamic experiments (in wind tunnels and supersonic tunnels, etc.). The approximate range of masses is 1 to $10^4$ g; the velocity range is 0.3 to 7 km/sec.

5. Meteors. The mass range of bodies engendering conventional and telescopic meteors is from $10^{-6}$ to 1 g; the velocity range is 11 to 72 km/sec.[1]

---

[1]Finer meteoric bodies do not create luminescence and, decelerating in the atmosphere, fall to the earth without loss of mass. These bodies, called micrometeorites, will not be considered by us.

6. Meteorites. This class of bodies does not have a sharp boundary with the preceding class, since the path of a meteoric body, in other words, the possibility of reaching the earth's surface, depends not only on the initial mass, but also on the velocity. We shall assume conditionally that the masses of meteorites range from 1 g to $10^7$ tons (1 to $10^{13}$ g).[1] Their velocities upon entry into the terrestrial atmosphere have the same limits as in the case of meteors: 11–72 km/sec.

From an examination of Figure 1 it is clear that the domain of meteorites on the mass-velocity diagram does not overlap, but merely touches the domain of meteors on the side of lesser masses, and on the side of lesser velocities does not overlap, but merely touches the domains of space rockets, artificial satellites and aerodynamic experiments.

This in the final count defines the qualitative distinction between phenomena accompanying the movement of large meteorite-forming masses in the atmosphere and phenomena studied, on the one hand, by meteor physics and, on the other hand, by hypersonic aerodynamics in its classical form (i.e., with account not taken of nonequilibrium phenomena).

It must also be noted here that besides the two selected criterial parameters (mass and velocity), it is necessary to take into account a third—the density of the gas through which the body moves. The influence of density will be considered in Section 3.

Now let us consider not the formal, but the physical differences between the movement in the atmosphere of meteorite-forming masses (which we shall, for the sake of brevity, simply call meteorites) and the movement of other classes of bodies, the domains of which touch the domain of meteorites.

As is known, during the movement of a meteor in the upper strata of the atmosphere, a cushion of compressed air is formed in front of the meteor body. This phenomenon is connected with the fact that oncoming molecules of air, in bouncing away from the body, encounter new oncoming molecules, etc. In the movement of a meteorite it is not a cushion that is formed, but a shock wave. This difference is connected with the difference in flow conditions and will receive detailed consideration in Section 3.

When rockets, missiles and supersonic aircraft move in the atmosphere, as well as in aerodynamic experiments, shock waves are also formed. The basic distinction of shock waves formed

---

[1]It should be noted for the sake of definiteness that here we have in mind neither the initial nor the terminal masses of the meteorites, but the entire range of masses, i.e., from the very greatest initial masses to the very smallest masses corresponding to meteorites falling on the surface of the earth. Nevertheless the lower limit is conditional.

by meteorites lies in the fact that these waves are strong ones, the temperatures at the front of the shock wave attain tens and hundreds of thousands of degrees, and behind the front of the wave there takes place not only molecule dissociation, but also atom ionization which, as a rule, is multiple. As a result, behind the front there is formed a nonequilibrium region where the air loses the properties of plasma, and the ensuing, recombining radiation exerts a substantial influence on the structure of the wave.[1]

From this point of view, the closest analogy can be found in the case of shock waves originating as a result of powerful explosions (including atomic explosions). However, the structure of the shock wave of a flying meteorite differs from the structures of an explosion wave, and the phenomena originating during its flight—heating, ablation, deceleration—have so far been studied only for lower speeds where the nonequilibrium phenomena enumerated above originate very seldom.

The basic problem of the physical theory of the movement of meteorites in the atmosphere may be formulated in a manner similar to that used for the basic problem of the theory of meteors, as a determination of the laws of change of the velocity and mass of a meteoric body in its movement through the atmosphere. The path toward a solution of this problem lies, in our opinion, in a manifold study of the properties of a strong shock wave and the interaction of the shock wave with the meteor body.

In this book we shall try to develop the overall pattern of the phenomena that determine the interaction of the shock wave with the meteor body, devoting our main attention to the processes of ionization and recombination behind the front of the shock wave, on the temperature distinction behind the front, and on determination of the flow of radiation obtained by the body from the shock wave. In concluding the book, we shall attempt to sketch out problems and to present a program of further research in this field.

## Section 2. Application of the Physical Theory of Meteors

The fullest exposition of the physical theory of meteors and a survey of the works in this field published to 1956 is contained in the monograph of B. Yu. Levin (Ref. 1).

Considering the movement of a meteoric body with respect to the molecules of air, we can assume that the meteoric body is decelerated by the impulse transmitted by counterblows of the

---

[1] In the range of densities and temperatures studied by us, plasma may, generally speaking, be regarded as an ideal gas, but only when an equilibrium state has been attained. In the case at hand this condition is not always fulfilled.

molecules, while heating and loss of mass of the body as a result of melting or evaporation take place because of transmission to the body of the energy of the oncoming air molecules. From these considerations are derived the basic equations of the physical theory of meteors, which have the following form:

$$M \frac{dv}{dt} = -\Gamma S \rho v^2 \tag{2.1}$$

(deceleration equation),

$$\frac{dM}{dt} = -\Lambda \frac{S \rho v^3}{2Q} \tag{2.2}$$

(equation of mass loss),

where M is the mass, v is the velocity, S is the area of the midsection of the meteorite; $\Gamma$ and $\Lambda$ are the coefficients of resistance and heat transfer; $\rho$ is the density of air; and Q is the energy expended for the removal (ablation) of a unit mass (into this enters the expenditure of heat for warming the mass, and its evaporation or melting; equation (2.2) does not take into account the heating of the body in depth).

Coefficients $\Gamma$ and $\Lambda$ depend on the nature of the process of the transmission of the impulse and energy by the air molecules in the meteor body, and are, generally speaking, variables. But since the range of their variation is not large, they are usually assumed to be constant in the first approximation.

It is obvious that the heat transfer coefficient $\Lambda < 1$, since only part of the energy of the oncoming air molecules is expended for removal of mass (ablation) from the meteorite. The corresponding portion of the energy is expressed in terms of the coefficient of accommodation $\alpha$, which for iron and stone meteorites is from 0.75 to 1. Besides, air molecules flying off the body after collisions, and then, also evaporating molecules from the meteoric body, bring about an enclosure effect which reduces the quantity of molecules reaching the body's surface and transferring impulse and heat to it. This effect is expressed by the coefficient of thermal enclosure $\alpha\Lambda$ and the coefficient of deceleration enclosure $\alpha\Gamma$. Thus $\Lambda = \alpha\alpha\Lambda$.

Regarding the deceleration coefficient $\Gamma$, it may be either larger or smaller than unity, depending on the shape and dimensions of the body, the conditions of flow about it by the oncoming airstream, and the presence of a reactive impulse of the rebounding molecules.

V. G. Fesenkov (Ref. 2) has taken into account that the diminution of meteorite mass smoothly ceases when the velocity approaches a certain value $v_m$, and has supplemented equation (2) by the multiplier $(v^2 - v_m^2)/v^2$:

$$\frac{dM}{dt} = -\Lambda \frac{S\rho v^3}{2Q} \frac{v^2 - v_m^2}{v^2}. \tag{2.3}$$

Dividing (2.2) and (2.3) by (2.1) and integrating, we obtain solutions of the mass loss equation for the cases of $v_m = 0$ and $v_m > 0$, respectively:

$$\frac{M}{M_0} = e^{\frac{\sigma}{2}(v^2 - v_0^2)}, \tag{2.4}$$

$$\frac{M}{M_0} = \left(\frac{v}{v_0}\right)^{-\frac{\sigma v_m^2}{2}} e^{\frac{\sigma}{2}(v^2 - v_0^2)}. \tag{2.5}$$

The subscript 0 signifies the initial values of mass and velocity, and the letter $\sigma$ denotes the value

$$\sigma = \frac{\Lambda}{2\Gamma Q}. \tag{2.6}$$

Parameter $\sigma$ may be found from observations if the velocity and acceleration of the meteor are measured, and the brightness curve E(t) of the meteor is obtained. Then, assuming the brightness E(t) to be proportional to the mass loss of the meteor body and to the square of the velocity, it is possible to determine $(dM/dt)_n$ for the moment $t_n$ on the basis of $E(t_n)$, and then from equations (2.1), (2.2) and (2.4), to determine the value $\sigma$. It stands to reason that $\Gamma$ and $\Lambda$ are here assumed constant.[1] The formula for determining $\sigma$ has the form:

$$\sigma = \frac{E}{\tau v^2}\left[\int_t^{t_n} \frac{E}{\tau v^2}\, dt\right]^{-1}\left(v \frac{dv}{dt}\right)^{-1}, \tag{2.7}$$

where $\tau$ is the coefficient of luminosity transmission, usually assumed proportional to the velocity: $\tau = \tau_0 v$ (then in the denominator $v^3$ stands everywhere in place of $\tau v^2$).

We introduce the designations:

$$u = \frac{\sigma v^2}{6}; \quad u_0 = \frac{\sigma v_0^2}{6}; \quad u_m = \frac{\sigma v_m^2}{6}; \quad U = \frac{u}{u_0} = \left(\frac{v}{v_0}\right)^2. \tag{2.8}$$

---

[1] Considerable complexity is introduced into this question when consideration is given to the disintegration of meteoric bodies, in which case both deceleration and mass loss are sharply intensified. In addition, whereas photometric determination of E(t) yields the total mass of the fragments, the value of deceleration corresponds to the average mass of one fragment. Therefore, lack of knowledge of the law of disintegration can distort the results for $\sigma$.

Substituting them into formula (2.5), we reduce it to the form of

$$\frac{M}{M_0} = U^{-3u_m} e^{-3u_0 (1-U)}. \tag{2.9}$$

The law of the change of velocity with altitude may be obtained by integrating equation (2.1) along the path of the meteorite. Assuming $S/S_0 = (M/M_0)^{2/3}$, and bearing in mind that

$$\frac{dv}{dt} = v \frac{dv}{dH} \cos i,$$

where H is the altitude and i is the angle of inclination of the meteorite trajectory to the vertical, after substituting (2.9) into (2.1) and integrating, we obtain:

$$U^{-u_m} \int_u^{u_0} e^{-(u_0 - u)} \frac{du}{u} = \frac{2\Gamma S_0 \sec i}{M_0} \int_H^{\infty} \rho dH. \tag{2.10}$$

Assuming the distribution of air density to be according to the barometric formula $\rho = \rho_0 e^{-H/H^*}$, where $H^*$ is the altitude of a homogeneous atmosphere, and introducing a coefficient of the form $A = S_0/M_0^{2/3}$, we reduce expression (2.10) to the form of

$$U^{-u_m} \int_U^1 e^{-u_0 (1-U)} \frac{dU}{U} = \frac{2\Gamma A \rho_0 H^* \sec i}{M_0^{1/3}} e^{-H/H^*}, \tag{2.11}$$

whence, taking account of (2.9),

$$\int_U^1 \left(\frac{M}{M_0}\right)^{1/3} \frac{dU}{U} = Ke^{-H/H^*}, \tag{2.12}$$

where K denotes a constant multiplier in the right-hand part of (2.11). Then for a given mass ratio $M/M_0$ and velocity ratio $v/v_0$, it is possible to find a corresponding altitude:

$$H = -H^* \ln \frac{1}{K} \int_U^1 \left(\frac{M}{M_0}\right)^{1/3} \frac{dU}{U}. \tag{2.13}$$

The integral, which enters into the left-hand part of formula (2.10), is equal to

$$I = e^{-u_0} [\mathrm{Ei}(u_0) - \mathrm{Ei}(u)], \tag{2.14}$$

where Ei(u) is an integral index function. Thus,

$$H = -H^* \ln \frac{I}{KU^{u_m}}. \tag{2.15}$$

At the moment the meteorite reaches the earth's surface, H = 0, and the condition

$$I = KU^{u_m} \tag{2.16}$$

will be fulfilled.

Given some most probable values of the parameters $\sigma$, $\Gamma$, $\Lambda$, as well as of the angle i, and assuming specific initial values of $M_0$, $v_0$, it is possible on the basis of formulas (2.16) and (2.14) to find the terminal velocity, $v_k$, of the meteorite, and then according to formula (2.9), the terminal mass, $M_k$. The multiplier $U^{u_m}$ is usually close to unity, since $u_m \ll 1$. Therefore, assuming with V. G. Fesenkov that $v_m = 1$ km/sec, we obtain $u_m = 0.002$; if, on the other hand, we take the estimate of Ceplecha (Ref. 3), based on observations of the flight of Pribram meteorite, $v_m = 7$ km/sec, we shall nevertheless have $u_m = 0.08$. For meteorites undergoing considerable deceleration in the atmosphere, the multiplier $U^{u_m}$ should be taken into account.

Some authors have made attempts to investigate the movement of meteors in the atmosphere on the basis of the stated physical theory of meteors. Thus, in 1951, Thomas and Whipple (Ref. 4) carried out an investigation of the probable conditions of the fall of the meteorite. Judging by the small dimensions of the crater formed by this meteorite in landing (in which it still lies), the geocentric velocity of the Gobi meteorite was minimal; this was taken into account. In spite of the introduction of some concepts from aerodynamics and heat-exchange theory, Thomas and Whipple based their calculations on the use of equations (2.1) and (2.2), assuming that $\Gamma = 0.5$, and taking the value of $\sigma$ from the work of Jacchia (Ref. 5), which contained 55 determinations of this value for 36 bright meteors. In some variants of the solution, they adopted the mean value of $\log \sigma$ ($\log_{mean} \sigma = -11.75$), and in other variants they adopted its maximum value ($\log_{max} \sigma = -11.28$).

The method described above was used in 1951 by V. G. Fesenkov (Ref. 2) for studying the movement of the Sikhote-Alinskiy meteorite, and in 1960 by V. A. Bronshten for ascertaining the probable conditions of the fall of the Tungusskiy and the Kaaliyarvskiy meteorites (Refs. 6, 7).

Here, different values of initial masses, differing by one order of magnitude, were selected, and solutions were obtained for a considerable range of initial velocities. The results (terminal masses, velocities and kinetic energies of fall) were compared with estimates of the energy of destruction taking place on the site as a result of the fall. On the basis of these rather approximate comparisons, it was nevertheless possible to estimate the probable values of the initial masses with an accuracy of up to 33 percent, and the values of the initial velocities with an accuracy of up to 50 percent.

Much indeterminacy is introduced into these estimates through lack of knowledge of the precise values of the parameters $\Gamma$ and $\Lambda$ (or of $\sigma$). In most of the investigations, $\Gamma$ and $\Lambda$ were assumed constant. Nevertheless, the assumption concerning the constancy of $\Gamma$ and $\Lambda$ is not justified, since $\Gamma$ apparently depends on the shape, and particularly, on the velocity of the meteor body, while $\Lambda$ depends on the predominance of one process or another of heat exchange and the removal of the mass of the meteorite (ablation). Moreover, substantial differences of opinion exist among various authors concerning the evaluation of these coefficients.

Baker (Ref. 8), on the basis of the experimental data of Hodges, Jensen, and others, assumes that for large meteorite bodies moving under conditions of continuous flow (see Section 3), $\Gamma = 0.46$. A value of $\Gamma$ close to 0.5 is adopted by Thomas and Whipple (Ref. 4), as well as by B. Yu. Levin (Ref. 1), considering it to be most probable for large meteoric bodies. The lower limit of $\Gamma$, according to Thomas and Whipple is equal to 0.2–0.3, and the upper limit is 1. B. Yu. Levin allows for the possibility that in the case of very small bodies and with intensive evaporation $\Gamma > 1$ (due to the reactive action of the evaporating molecules of the meteoric body).

In 1950, K. P. Stanyukovich (Ref. 9), investigating the movement of small meteoric bodies at altitudes in excess of 80 km, used the formula of the aerodynamic coefficient of resistance

$$c_x = 2\Gamma = \frac{2}{3}\frac{8+1}{\sqrt{\pi}}\sqrt{\gamma - 1}, \tag{2.17}$$

where $\gamma$ is the indicator of the adiabatic air curve. For high altitudes, where the free-path length, l, of molecules, is large in comparison to the dimension D of the meteoric body, and their impacts are nonelastic, K. P. Stanyukovich assumes that $\gamma = 5/4$, and, consequently, that $c_x = 2.1$, $\Gamma = 1.05$ (it is usually assumed in aerodynamics that $c_x = 2$). For lower altitudes, where $l \ll D$, and a shock wave is formed in front of the flying meteoric body, K. P. Stanyukovich assumes $\gamma = 6/5$, from which is obtained $c_x = 1.87$ and $\Gamma = 0.94$.

On the basis of the same aerodynamics formula (2.17), which expresses the deceleration pressure on a smooth sphere at supersonic velocities, V. G. Fesenkov (Ref. 2), assuming $\gamma = 7/5$, obtained[1] $\Gamma = 1.3$. Subsequently, in calculating the movement of the Sikhote-Alinskiy meteorite, he used various values of $\Gamma$, 0.5, 1 and 2, giving preference to the latter value. "For a body of irregular shape and, particularly, one producing, due to the speed of its movement, intensive vortex nuclei in its immediate vicinity which are transported with it and considerably increasing the size of the effective cross section, the coefficient $\Gamma$ should still increase considerably, but may under no circumstances diminish" (in comparison to $\Gamma = 1.3$), states V. G. Fesenkov.

---

[1]As we shall see in Section 7, Table 5, the estimates of the isentropic exponent $\gamma$, adopted by K. P. Stanyukovich, are closer to actuality than is the estimate of V. G. Fesenkov, although in the general case this value depends on the velocity of the meteorite (via the temperature in the shock wave).

In 1960, K. P. Stanyukovich (Ref. 10), as a result of investigating the effect of the reactive impulse of evaporated and escaping molecules, obtained a formula of the form

$$\Gamma = 1 + \frac{\varkappa}{2v}[v_1 + v_2 f(v)], \tag{2.18}$$

where $v_1$ and $v_2$ are the velocities of its escaping and evaporated molecules; and $\varkappa$ is a coefficient depending upon the shape of the meteorite (for a sphere, $\varkappa = 0.5$). Application of formula (2.18) yielded $1.8 < \Gamma < 2.5$ for the basic range of meteoric velocities.

G. I. Pokrovskiy (Ref. 11), in summarizing the results of experiments with cumulative charges--with the action of rapidly expanding (several km/sec) plasma of electrical discharge onto ballistic pendulums, as well as meteoric data--came to the conclusion that within the range of Mach 3 to Mach 10, $c_x$ diminishes as the Mach number increases, and may be considered to be approximately inversely proportional to the velocity. Furthermore, when Ma > 10, $c_x$ on the contrary grows with an increase in Ma, and is approximately in proportion to the velocity; it attains values of the order of 10 (i.e., $\Gamma = 5$).

The only determination of $\Gamma$ from observations of the bolide which terminated in the falling of the Pribram meteorite was made by Ceplecha (Ref. 3). This bolide was photographed by meteor patrols from two Czechoslovak stations, and the photographs were processed in detail. The trajectories of various parts of the bolide (which broke up in the air) were identified from fallen fragments of the meteorite. The final masses of the fragments, as well as the density and composition of the meteorite, were known, thereby facilitating the investigation. As a result, $\Gamma = 0.43$ was obtained (for velocities of 1 to 7 km/sec), which is in good agreement with the experimental data of Baker, as well as with that of Thomas and Whipple for this velocity range.

The values of $\Gamma$ for greater velocities were then obtained by another method, i.e., from a comparison of the altitude of burnout and the length of the last ("dark") section of the trajectory. For various pieces of the meteorite (0.1–4.5 kg in mass), $\Gamma = 0.55$–$1.20$ were found.

In a somewhat better position is the question of estimating the value $\sigma$; this value, as has been stated above, may be found from photographs on the basis of the curve-of-brightness change and the velocity of the meteor along its path, according to formula (2.7).

By such a method Jacchia (Ref. 12) obtained over 1,000 determinations of $\sigma$ for 438 meteors. Individual values are not presented in that work; rather, the mean group values are listed for 8 groups corresponding to various ranges of velocity $\sigma$, and for 11 groups corresponding to various intervals of the logarithm of integral brightness $E_\infty$. The mean group values of $\sigma$ for the various velocities (expressed in terms of g/erg) lie within the limits of

$$2 \cdot 10^{-12} < \sigma < 10^{-11}.$$

In earlier works of Jacchia (Ref. 5), on the basis of 36 photographs, 55 values of $\sigma$ were obtained which lay within the limits of

$$5 \cdot 10^{-13} < \sigma < 4 \cdot 10^{-12}.$$

Some of the divergence between these domains of the values of $\sigma$ are to be explained first of all by the fact that in Ref. 12, 355 of the 438 meteors were photographed by powerful high-speed Super-Schmidt cameras and, with the exception of 3 of these meteors, have $E_\infty < 10$ (the brightness of a star of zero magnitude was adopted as a unit of $E_\infty$). The remaining 83 meteorites were photographed by small cameras with a wider field of vision; therefore, in their case the probability that bright meteors will get into the photograph is greater, and for them $10 < E_\infty < 1{,}000$. In Ref. 5 only photographs taken with small cameras were used, and consequently, this material pertains to brighter meteors. Furthermore, as has already been stated, according to Ref. 12 the limits for $\sigma$ pertain to mean group values, and the scattering of individual values should be greater. The following values of $\sigma$ were obtained by Jacchia (n is the number of meteors).

| | |
|---|---|
| $\log \sigma = -11.22$ | ([12], n = 355, Super-Schmidts) |
| $\log \sigma = -11.41$ | ([12], n = 83, small cameras) |
| $\log \sigma = -11.75$ | ([ 5], n = 36, small cameras) |

In Ref. 12 the dependence of $\sigma$ on $E_\infty$ was traced, and a distribution of $\sigma$ with a transition to brighter (i.e., more massive) meteors was discovered.

On the basis of processing photographs of the bolide of the Pribram meteorite (Ref. 3), Ceplecha obtained for the velocity range $v \leq 20$ km/sec, a variable $\sigma$, increasing with velocity:

| | | | | | |
|---|---|---|---|---|---|
| v, km/sec ..... | 7 | 10 | 14 | 17 | 20 |
| $\sigma \cdot 10^{12}$ ..... | 0.2 | 0.4 | 0.6 | 0.8 | 0.9 |

The order of magnitude of the $\sigma$ obtained by Ceplecha fits into the range of values found in the early work of Jacchia for bright meteors (Ref. 5).

This data provided a basis for V. A. Bronshten, in his investigation of the movement of the Tungusskiy and Kaaliyarvskiy meteorites (Refs. 6, 7) in the atmosphere, to assume that $\sigma = 10^{-12}$. In Ref. 6 he investigated the influence of the estimates of parameters $\Gamma$ and $\sigma$ on the terminal meteorite masses and on the velocities which were obtained in the calculations, as well as the influence of $\Gamma$ on the deceleration process.

The results of this investigation are reduced to the following: The course of deceleration and of the distribution of mass with altitude at given $M_0$ and $\Gamma$ is determined only by the product

$\sigma v_0^2$ and, consequently, depends on the parameter $\sigma$. Variation of this value leads to the fact that all of the velocities obtained in the calculation change in inverse proportion to $\sqrt{\sigma/\sigma_0}$, where $\sigma_0 = 10^{-12}$. Estimates of $\Gamma$ and of the initial mass $M_0$ determine the zero point on the altitude scale; in other words, the deceleration and mass-loss curves will be shifted upward or downward without changing their form.[1] Moreover, since $\Gamma$ and $M_0$ enter into formulas (2.10) and (2.15) in the combination $\Gamma M_0^{-1/3}$, doubling the estimate of $\Gamma$ (or more precisely, increasing it by a factor of 2.16) is equivalent to diminishing the estimate of the initial mass $M_0$ by one order of magnitude. Physically this signifies that a small mass of "streamline" shape, with a small $\Gamma$, is decelerated in the same manner as a large mass of irregular shape with a large $\Gamma$. Adoption of one estimate or the other of $\Gamma$ will exert considerable influence on the terminal mass $M_k$ of the meteorite, and still greater influence on its terminal velocity, $v_k$. Doubling of $\Gamma$ at high velocities may reduce $M_k$ and $v_k$ by an order of magnitude and more.

Variation of the coefficient of heat transfer $\Lambda$ (at constant $\Gamma$) is equivalent to variation of $\sigma$, since $\Lambda = 2\Gamma Q\sigma = 0.16 \cdot 10^{12}\sigma\Gamma$. As B. Yu. Levin (Ref. 1) states, in the case of large bodies dozens of centimeters in size, $\Lambda \leq 0.05$. At the same time Ceplecha (Ref. 13) obtained the result that, for the Pribram meteorite at the terminal sector of the paths, $\Lambda$ diminished with the velocity (from 0.068 at v = 20 km/sec to 0.025 at v = 10 km/sec).

At a constant $\sigma = 10^{-12}$, $\Lambda = 0.08$, 0.16, 0.32 correspond to $\Gamma = 0.5$, 1 and 2.

Unfortunately, meteor physics cannot provide sufficiently reliable estimates of the highly important parameters $\Gamma$ and $\Lambda$ for studying the movement of meteorites, since the theory and the observation material pertain to meteors, i.e., to bodies of smaller mass, and a rather scant body of experimental material pertains to considerably lower velocities in comparison to meteorites.

The work of Ceplecha is as yet the only of its kind, and it is scarcely possible to expect that it will again be possible to photograph a meteorite in flight from two stations by special meteor patrols. Therefore, basic efforts must be directed at creating a theory of the movement of meteorites in the atmosphere, as well as the carrying out of experimental operations.

## Section 3. Flow Conditions

A large (meteorite-forming) meteoric body (which we shall, as before, for brevity call simply a meteorite), moves in the atmosphere under different conditions than does the conventional

---

[1]This is because not only the density of air, but also the relative mass and velocity of the meteorite change with altitude according to an exponential law, and follow directly from formula (2.15).

meteoric body engendering the appearance of a meteor. In the movement of a body at hypersonic velocity in a medium (in the case at hand, in air), various conditions of flow about the body of the head-on current are possible.

In 1946, Tsien (Ref. 14) introduced the modern classification of hypersonic flow conditions that are cited in many works, particularly by Baker (Ref. 8) and V. A. Bronshten (Ref. 6). Often introduced as a parameter is the so-called Knudsen Number K, equal to the ratio of the free-path length $l_0$ of the stream to the characteristic dimension of the body D. Specifically, in the case of a meteorite we are dealing with the mean free-path length of evaporated molecules $l_e$ in relation to the head-on molecule of air. Thus

$$\mathrm{K} = \frac{l_e}{D}. \tag{3.1}$$

Another parameter determining the flow conditions is a combination of the Mach number (Ma) with the Reynolds number (Re): Ma/Re or $\mathrm{Ma}/\sqrt{\mathrm{Re}}$. These values are connected with each other by the following relationships:

$$l_e \cong l_0 \frac{\bar{v}_e}{v}; \quad \frac{l_0}{D} \cong \frac{\mathrm{Ma}}{\mathrm{Re}}; \quad \mathrm{K} \cong \frac{\mathrm{Ma}}{\mathrm{Re}} \frac{\bar{v}_e}{v} = \frac{1}{\mathrm{Re}} \frac{\bar{v}_e}{c}, \tag{3.2}$$

where $v_e$ is the mean velocity of evaporated molecules and c is the speed of sound.

Very frequently the thickness $\delta$ of the boundary layer is used in place of D as the characteristic dimension. At small Reynolds numbers ($\mathrm{Re} \ll 1$), $D/\delta \approx 1$ and, consequently,

$$\frac{l}{D} \approx \frac{l}{\delta} \approx \frac{\mathrm{Ma}}{\mathrm{Re}}. \tag{3.3}$$

For the contrary case ($\mathrm{Re} \gg 1$) the relationships

$$\frac{D}{\delta} \approx \sqrt{\mathrm{Re}}; \quad \frac{l}{\delta} \approx \frac{\mathrm{Ma}}{\sqrt{\mathrm{Re}}}. \tag{3.4}$$

are in force.

In Tsien's classification, the following basic conditions of flow about a body by a hypersonic gas stream are to be distinguished:

1) conditions of free molecular flow, when the body undergoes the impacts of individual molecules, but the collisions of these molecules with one another may be disregarded;

2) transient conditions, when the free-path length is comparable to the dimensions of the body, and collisions of molecules with one another may be taken into account;

3) conditions of flow with slip, when the tangential component of the stream velocity at the surface of the body is small, but finite (gas does not adhere to the wall of the body);

4) conditions of continuous flow, when slip is absent and the gas may be regarded as a solid medium.

Table 1 presents the conditions characterizing each of the flow regimes.

It stands to reason that these boundaries are conditional, and various authors give various values for them. Therefore, according to Schaaf (Ref. 15), the boundaries of regimes II and III correspond to $K_\delta = 10^{-1}$, and those of regimes III and IV to $K_\delta = 10^{-2}$. Baker (Ref. 8) and V. A. Bronshten (Refs. 6, 16) correspondingly adopted $10^{-1}$ and $10^{-3}$.

Table 1

Boundaries of Flow Regimes (according to Tsien)

| Regimes | $K = l/D$ | $K_\delta = l/\delta$ | Ma/Re | $Ma/\sqrt{Re}$ | Remarks |
|---|---|---|---|---|---|
| I | $K > 10$ | $K_\delta > 10$ | $>10$ | — | |
| II | $1/\sqrt{Re} < K < 10$ | $1 < K_\delta < 10$ | $\begin{cases} <10 \\ 1-10 \end{cases}$ | $>1$ — | with $Re \gg 1$ with $Re < 1$ |
| III | $10^{-2}/\sqrt{Re} < K$ $K < 1/\sqrt{Re}$ | $10^{-2} < K_\delta < 1$ | — | $10^{-2}$—1 | |
| IV | $K < 10^{-2}/\sqrt{Re}$ | $K_\delta < 10^{-2}$ | — | $<10^{-2}$ | |

A detailed examination of the classification of the flow regimes and of the conditions of the application to them of various equations of gasdynamics is contained in Refs. 17–19, as well as in the monograph of Hayes and Probstein (Ref. 20).

If in the oncoming stream the concentration of molecules is $n_0$, and the effective cross section of a molecule is $\pi\sigma^2$, the frequency of their collisions with evaporating molecules of the body will be equal (per 1 molecule) to

$$\nu_{e0} = vn_0\pi\sigma^2, \tag{3.5}$$

and the free-path length of evaporating molecules with respect to that of the oncoming ones will be equal to

$$l_e = \frac{\bar{v}_e}{n_0 v \pi \sigma^2}, \tag{3.6}$$

and furthermore

$$\bar{v}_e = \left(\frac{8kT_{\text{evap}}}{\pi m}\right)^{1/2}, \tag{3.7}$$

while the free-path length of molecules of the oncoming stream with respect to one another is

$$l_0 = \frac{1}{\sqrt{2}\, n_0 \pi \sigma^2}. \tag{3.8}$$

On the basis of (3.6), (3.7) and (3.8)

$$l_e = \sqrt{2}\, \frac{\bar{v}_e}{v} l_0 = \frac{4}{\sqrt{\pi}} T_{\text{evap}}^{1/2} \left(\frac{k}{m}\right)^{1/2} \frac{l_0}{v}. \tag{3.9}$$

Replacing $v = c \cdot Ma$ and bearing in mind the expression for the velocity of sound

$$c = \sqrt{\gamma \frac{kT}{m}}, \tag{3.10}$$

we finally obtain

$$l_e = \frac{4}{\sqrt{\pi\gamma}} \left(\frac{T_{\text{evap}}}{T}\right)^{1/2} \frac{l_0}{Ma}. \tag{3.11}$$

Since $\sqrt{\pi\gamma} \approx 2$, $T_{evap}/T \approx 10$, the approximate relationship

$$l_e \cong \frac{6{,}3}{Ma} l_0. \tag{3.12}$$

holds true. Hence $l_0/D > 1.6$ Ma corresponds to the condition $l_e/D > 10$, and analogously for the other conditions characterizing the flow boundaries cited in Table 1.

Thus, the mean free-path length of molecules 1, entering into the Knudsen Number, must not be taken for a free stream, but rather for a boundary layer, i.e., the free-path length of evaporated molecules at an evaporation temperature of $T_{evap}$. Since when $T_{evap} = 3{,}000°K$ $v_e/c \approx 5$, it may also be approximately assumed, on the basis of (3.2), that

$$K \cong \frac{5}{Re}. \tag{3.13}$$

Figure 2 shows Reynolds numbers for the case of the motion of a body with a diameter of 1 cm at velocities of 10–70 km/sec to an altitude of 120 km. Since the Reynolds number is proportional to the diameter of the body, it is possible from Figure 2 to find Re for other values of D as well. In order to present a more graphic presentation, Figure 3 shows a family of lines of equal Re in the function of altitudes above sea level and the diameter of the body (up to $D = 10^4$ cm) for v = 20 and 60 km/sec. In Figure 3 are also marked off the boundaries of the basic flow regimes.

As may be seen from Figure 3, a meteoric body with a diameter of 10 cm, at a lower altitude than 80 km, is moving already under conditions of continuous flow, and for larger bodies these conditions start at an even higher altitude. On the other hand, the flight of ordinary meteors with a mass of M < 1g takes place under conditions of flow with slip. Therefore, it is not proper to transfer rules established for ordinary meteors to the flight of large meteorites in the atmosphere.

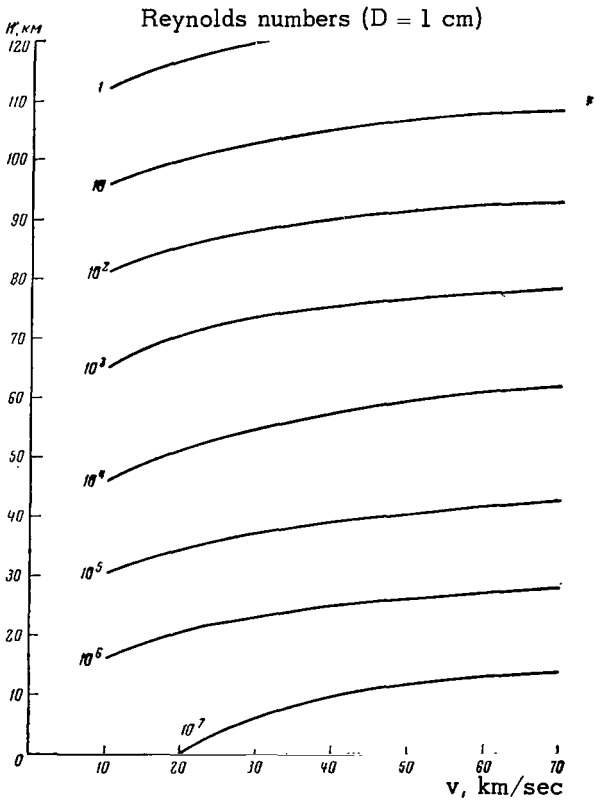


Figure 2. Reynolds numbers in the function H, v (D = 1 cm).

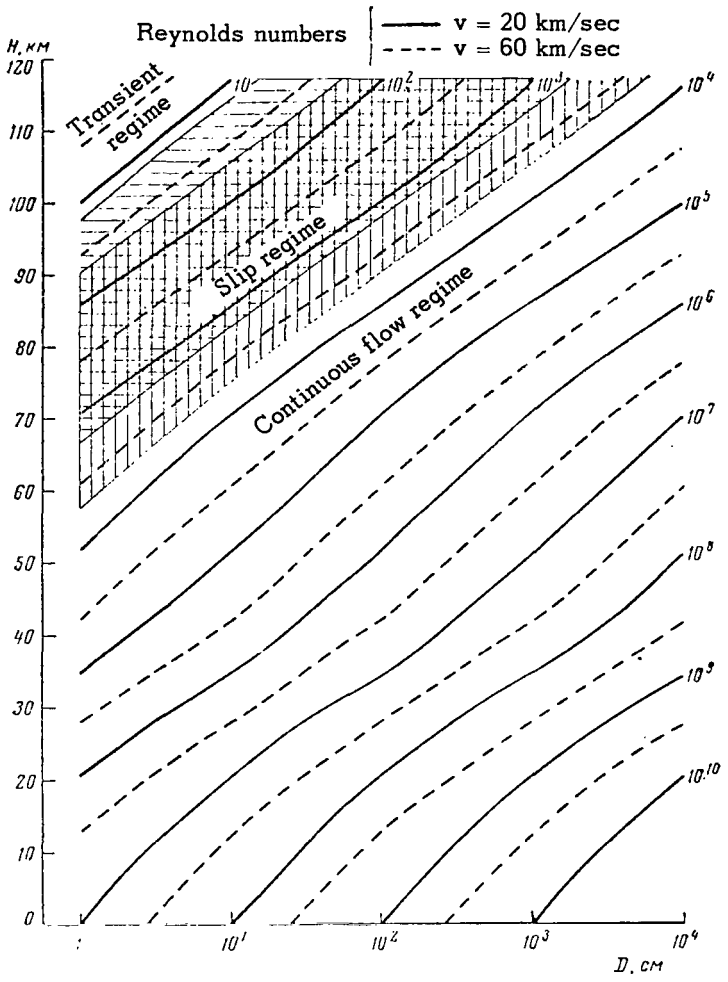


Figure 3. Reynolds numbers in the function H, D (v = 20 and 60 km/sec).

To the study of the movement of meteorite-forming bodies in the atmosphere, it is necessary to apply the equations of hypersonic aerodynamics and those of the theory of heat exchange during flight at hypersonic velocities.

# CHAPTER 1. MOVEMENT OF A METEORITE UNDER CONDITIONS OF CONTINUOUS FLOW

## Section 4. The Formation of a Shock Wave

It is known that when a large body moves in a continuum at a hypersonic velocity, a detached shock wave is formed. Since meteorites move at velocities many times exceeding that of sound (Mach 30-200), the shock wave accompanying the meteorite will be a strong one. Therefore, in studying the movement of large meteorites it is necessary not only to make use of the developments of hypersonic aerodynamics, but also to use the theory of strong shock waves.

In the past 10 years hypersonic aerodynamics has undergone extensive development in numerous research projects in the USSR and abroad. A summary of the basic results of foreign research is contained in the thorough surveys of Karman (Ref. 21), Lees (Ref. 22), Ferri (Ref. 23), Patterson (Ref. 24), and others (translated into Russian), as well as in the monograph of Hayes and Probstein (Ref. 20). The most important results of research on gas streams with a high supersonic velocity in the USSR are summarized in the monograph of G. G. Chernyy (Ref. 25).

However, the overwhelming majority of the works that have appeared in this field in recent years are directed toward the study of movement at velocities not in excess of the second cosmic velocity (11 km/sec); this determines the formulation of the question. Air is usually regarded as an ideal gas, or else some deviations of the properties of air from the properties of an ideal gas are investigated, such as, for example, those connected with dissociation. The influence of ionization, which sets in only at very high velocities, is as a rule not considered.

The formation of shock waves in the flight of meteorites has been dealt with in the USSR by K. P. Stanyukovich (Refs. 9, 26) and O. V. Dobrovol'skiy (Ref. 27). In Ref. 9 some general formulas were given which determine the pressure density and the temperature behind the front of the wave and on the surface of the meteorite body; and, the influence of the shock wave on the evaporation of the body was briefly treated. Ref. 26 dealt with the effect of the ballistic wave of the flying meteorite, and of the blast wave formed when the meteorite strikes the surface of the earth or terrestrial objects, as well as the mutual interaction of these two waves. O. V. Dobrovol'skiy (Ref. 27) attempted to take into account the influence of the evaporation of the meteorite body

upon the shock wave, considering that the evaporation process is of so intensive a nature that it may be compared with a blast process continually developing along the trajectory of the meteorite (as in a blasting fuse). The "blast" wave brought about by the rapid evaporation of the meteoric body is, in the opinion of O. V. Dobrovol'skiy, stronger than the ballistic shock wave.

We cannot agree with the interpretation of O. V. Dobrovol'skiy, since the expenditure of energy on the evaporation of a meteor body comprises but some fraction of the total energy of the shock wave, and the evaporation process itself is brought about by heating of the meteoric body by the shock wave. Thus, these can be merely some redistribution of energy, and not a summation of the energy of two waves.

In all of the enumerated works, the physics of the phenomena taking place in the shock wave of the flying meteorite is scarcely considered. The most complete investigation of the interaction of a shock wave and a meteoric body, with account taken of dissociation, ionization and radiation, was made in 1960 by K. P. Stanyukovich and V. P. Shalimov (Ref. 28). In their work the solution of the deceleration equation and of the mass loss of the meteorite under conditions of intense evaporation is given; the question of the heating of the meteoric body and of the so-called "thermal explosion" is considered. An analysis of some of the results of this work will be presented in Section 17.

For the moment let us consider qualitatively the pattern of the formation of a shock wave, considering the meteorite to be stationary and assuming the counterstream of air to be coming at it (Figure 4). The following basic elements of a shock wave may be distinguished (Ref. 29).

1. The front of the shock wave (the shock front) is a comparatively thin layer within which occurs a sharp change in the thermodynamic values (temperature, pressure and density) and transfer of the energy to the forward motion of air molecules to the energy of excitation of internal degrees of freedom: rotational and vibrational energy of molecules, chemical energy (including dissociation energy), the energy of electronic excitation and ionization.

Two layers may be distinguished in the shock front in a viscous compression wave in which the directed motion of the molecules of the stream is transformed into random motion and shock compression is effectuated, and a relaxation layer in which excitation of the intrinsic energy of the particles takes place.

2. The compressed layer 2 is the region of compressed gas behind the front of the shock wave, which on first approximation is in a state of equilibrium. However, this equilibrium is disrupted at high altitudes because of the relatively large relaxation times (for the establishment of an equilibrium state) for the basic reactions. In addition, the thickness of the shock front and of the boundary layer increases at high altitudes.

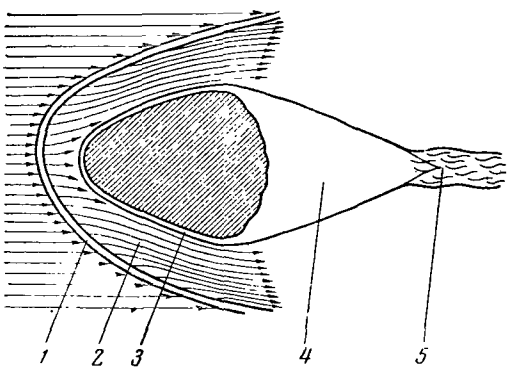


Figure 4. Diagram of the basic elements of a shock wave.

1 – front; 2 – compressed layer; 3 – boundary layer;
4 – stagnation zone; 5 – trail

3. The boundary layer 3 is a thin viscous layer, adhering to the body, in which the tangential component of velocity falls from the local value in the compressed layer of gas to zero on the surface of the body (on the wall). In the boundary layer there takes place an interaction of the evaporated molecules of the body with the atoms and ions of the oncoming stream and equalization of the temperatures of the gas and of the body. Therefore, strictly speaking, one should distinguish an aerodynamic and a thermal boundary layer.

4. The stagnation zone 4 is the region immediately behind the body; in the ideal case it constitutes a vacuum, while in the actual case this zone is filled with evaporating molecules of the body, as well as with molecules present as a result of flow stall from inhomogeneities and projections on the body, rotation of the body and other causes.

5. The trail 5 is the region of high-temperature turbulent flow with low density behind the body. The trail is formed as a result of diffusion expansion of the streams flowing about the body inwards, and the "convergence" of the flow of the masses of gas at some distance behind the body. For meteoric bodies this distance exceeds the dimensions of the body by approximately one order of magnitude.

## Section 5. Shape of the Shock Wave and the Flow Field

We are first of all interested by the question of the geometrical parameters of the shock wave, its shape and the value of its detachment, as well as by the flow fields behind the wave

front. Unfortunately, an analytical solution of this problem in general form does not as yet exist, and the shape of the shock wave is determined by numerical methods.

Even considering only the value of the detachment of the shock wave (the width of the compressed layer) $\delta_s$, in the determination of this value either approximate formulas or numerical methods of solution are used. Thus, with a hemispherical nose in the first approximation (Ref. 22):

$$\frac{\delta_s}{R_0} = \eta, \tag{5.1}$$

where $R_0$ is the radius of the sphere, $\eta = \rho_1/\rho_2$, $\rho_1$ and $\rho_2$ constitute the air density before and behind the front of the shock wave. In the second approximation Hayes (Ref. 34) obtained

$$\frac{\delta_s}{R_0} = \frac{\eta}{1 + 2\sqrt{\eta}}. \tag{5.2}$$

The monograph of Hayes and Probstein (Ref. 20) also cites the following expression for the ratio of $\delta_s$ to the radius of the shock wave on the axis $R_s$ of the body

$$\frac{\delta_s}{R_s} = \frac{\eta}{1 + \sqrt{\frac{8\eta}{3}}}, \tag{5.3}$$

which, since $\delta_s = R_s - R_0$, is reduced to the form of

$$\frac{\delta_s}{R_0} = \frac{\eta}{1 - \eta + \sqrt{\frac{8\eta}{3}}}. \tag{5.4}$$

We compare the results yielded by these formulas with the precise solution obtained by O. M. Belotserkovskiy (Ref. 37); we assume here that $\eta = 1/6$, $M\alpha = \infty$:

Formula (5.1) . . . . . $\delta_s/R_0 = 0.167$,
Formula (5.2) . . . . . $\delta_s/R_0 = 0.106$,
Formula (5.4) . . . . . $\delta_s/R_0 = 0.111$,
Precise Solution . . . . . $\delta_s/R_0 = 0.128$.

A detailed survey of this question may be found in Refs. 20 and 22. Consideration is also given to analogous expressions for blunt bodies of various shapes. Frequently, instead of solving the direct problem of the shape of the shock wave for a body of a given shape, the converse

problem was solved, i.e., the shape of the shock wave was given and the body parameters corresponding to it were computed (Ref. 20).

A method of precise solution of the direct problem was proposed in 1956 by A. A. Dorodnitsyn (Ref. 35) and was worked out in detail by O. M. Belotserkovskiy (Ref. 36). This is the method of integral relationships, which is explained in the following manner. Flow about an axially symmetric body by an oncoming stream is described in spherical coordinates by a system of differential equations in terms of partial derivatives equivalent to the equations of motion, continuity and energy. The origin of the coordinates is taken to be in the center of curvature of the nose part of the body, and between the body and the wave these are drawn N-1 lines equidistant along the radius, dividing the area of integration into N strips.

The initial equations are integrated along the radii from the contour of the body to the boundaries of the strips, as a result of which 2 N independent integral relationships are obtained. Approximating the integrals by interpolational polynomials and integrating, we obtain an approximating system consisting of 3 N conventional differential equations and N-1 final relationships.

In the first approximation (N = 1), integration is carried on from the boundary of the body all the way to the boundary of the wave. In the second approximation (N = 2) one additional line is introduced, etc. Investigation of the question and comparison with experimental data (Ref. 36) has shown that the second approximation is entirely sufficient. In such a case it is necessary to solve a system of 6 conventional differential equations and one final relationship. Computation formulas for this case have been derived by O. M. Beltoserskovskiy (Ref. 37). In the same work are given tables of the parameters of the shock wave, determining its shape, the stream function, the distribution of pressure on the body, as well as tables of the flow fields for flow about spheres and ellipsoids of revolution with semiaxis ratios of 1:2 and 3:2, at Mach numbers of $M\alpha$ = 3, 4, 6, 10 and $\infty$ (the limiting case).

In the Computer Center of the Academy of Sciences, USSR, for the calculation of plane and axially symmetric flows of gas, intensive use is also made of the method of characteristics, perfected and adapted to this purpose by P. I. Chushkin (Ref. 38) and described in detail in Ref. 39. This method was used to calculate supersonic flows past blunt-nosed cones, tables for which have been published by P. I. Chushkin and N. P. Shulishnina (Ref. 40). In these tables the coordinates of the shock wave, the distribution of pressure, Mach numbers and the coefficient of wave resistance on the surface of blunt-nosed cones are given. The shape of the blunting is spherical or ellipsoidal, with the same semiaxis ratios as in Ref. 37, with half-angles of aperture from 0° (blunt cylinder) to 40°. The same Mach numbers were chosen as in Ref. 37.

In calculating all of the indicated tables, air was considered to be an ideal gas with an isentropic exponent $\gamma = 1.40$. Besides, O. M. Belotserkovskiy calculated analogous tables for the

values $\gamma = 1.15$, 1.29 and 1.67, containing the coordinates of the shock wave and the distribution of pressure on the body.

Comparison of these tables shows that as $\gamma$ diminishes, the wave approaches closer to the body, as is shown in Figure 5. On the basis of Table 5 (Section 7), it is possible to conclude that in a majority of cases, in the shock waves of meteorites $\gamma$ will lie between the values of 1.15 and 1.29.

However, for an actual case of a flying meteorite, use of the tables on Refs. 37 and 40 encounters the following difficulties:

1) the meteorite usually has an irregular shape, although some meteorites in the process of interaction with air acquire an oriented shape, that of a blunt-nosed cone; the half-angle of aperture of such as the Karakol and Zabvod'ye meteorites is, however, very large ($\sim 50°$), and this complicates calculations;

2) the air behind the shock wave of a meteorite, as we have already noted, cannot be considered as being an ideal gas, and in such a case $\gamma$ is a variable; a way out of this situation can be found in using some effective value $\gamma_{eff}$.

The complexity of the true shape of the meteorite forces us to consider, as a first approximation, bodies of an idealized shape, i.e., spheres, ellipsoids of revolution, blunt-nosed cones and cylinders.

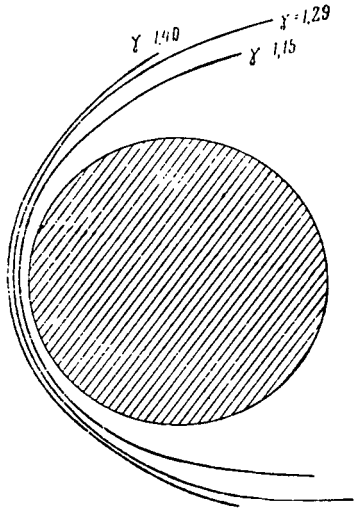


Figure 5. Shape of the shock wave for $\gamma = 1.40$, 1.29 and 1.15.

To solve the problem of the distribution of temperatures in a shock wave, which will be dealt with in Chapter II, it will be necessary to follow through the flow in the shock wave for any not very large time scale corresponding to the movement of particles in the immediate vicinity of the body.

In the tables in Ref. 37, values are cited which characterize the flow fields behind the front of a shock wave. Adopting a spherical system of coordinates (r, $\theta$), with the center in the center of curvature in the nose part of the body (Figure 6), and taking for each ray $\theta$ = const five points corresponding to the values of $\xi = 0$ (the body), 0.25, 0.50, 0.75 and 1 (the wave), where

$$\xi = \frac{r - r_0(\theta)}{\varepsilon(\theta)}, \tag{5.5}$$

O. M. Belotserkovskiy cites for each point ($\xi$, $\theta$) the velocity components along r and $\theta$, as well as the values of the stream function $\psi$ determined by the equation

$$d\psi = \rho r \sin\theta(vdr - urd\theta). \tag{5.6}$$

Since the condition

$$\frac{dr}{u} = \frac{rd\theta}{v}, \tag{5.7}$$

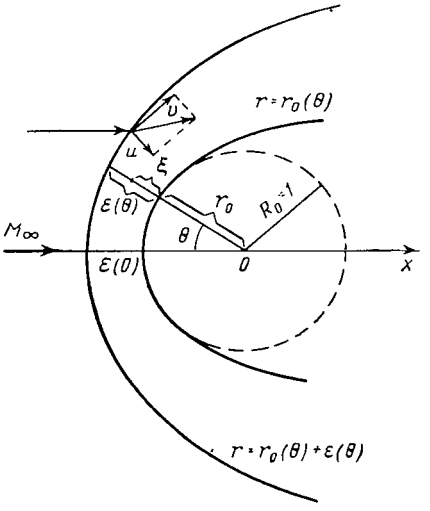


Figure 6. Basic parameters of a shock wave (r, $\xi$, $\theta$).

is satisfied along the flow lines, the function $\psi$ is constant along the flow lines. Therefore, on the basis of the values of $\psi$ it is possible to reestablish the direction of the flow lines, and on the basis of the values of u, v it is possible to reestablish the velocity vectors.

## Section 6. Processes Taking Place Behind the Shock Wave Front

When molecules intersect the oncoming stream of the front of a shock wave, a gradual redistribution of energy takes place. The kinetic energy of the forward motion of the molecules of the streams (in the system of coordinates connected with the body) is transformed at first into the energy of a disordered forward motion of the molecules ($\epsilon_{forw}$); and subsequently into the energy of excitation of internal degrees of freedom of the molecules, rotational motion and atom vibrations ($\epsilon_{ext}$); and, in case of a large amplitude of the shock wave, into dissociation energy ($\epsilon_{dis}$), electronic excitation ($\epsilon_{el}$) and, finally, into ionization energy ($\epsilon_{ion}$). Thus, the specific intrinsic energy is, in the general case, equal to

$$\epsilon = \epsilon_{forw} + \epsilon_{ext} + \epsilon_{dis} + \epsilon_{el} + \epsilon_{ion}. \tag{6.1}$$

A detailed treatment of these phenomena is contained in the survey of Ya. B. Zel'dovich and Yu. P. Rayzer (Ref. 42). Of great importance to us is that the equilibrium states, with respect to one degree of freedom or another, are not established behind the wave front instantaneously, but rather over some period of time (relaxation time). For the establishment of a Maxwell velocity distribution several (one to three) collisions are sufficient, and for the attainment of an equilibrium of rotational motion, five to ten collisions suffice. The number of collisions required for the establishment of a vibrational equilibrium depends to a great extent on temperature; when T = 3,000°, about $10^5$ collisions are required, and when T = 5,800°, about 100. The effects of vibrational and dissociative relaxation have been studied in detail by many authors, both theoretically and experimentally. A survey of the research in this field has been published by S. A. Losev and N. K. Osipov (Ref. 43).

Vibrational relaxation time $\tau_{vibr}$ has been measured in oxygen and in nitrogen at the following temperatures (Ref. 43) (the results are reduced to p = 1 atm):

| | °K | sec | | °K | sec |
|---|---|---|---|---|---|
| Oxygen | 300 | $3 \cdot 10^{-3}$ | Nitrogen | 780 | $2 \cdot 10^{-3}$ |
| " | 2,500 | $5 \cdot 10^{-6}$ | " | 3,000 | $4 \cdot 10^{-5}$ |
| " | 10,000 | $2 \cdot 10^{-7}$ | " | 5,600 | $5 \cdot 10^{-6}$ |

It can be seen that with an increase in temperature, $\tau_{vibr}$ diminishes rapidly. In the case of strong shock waves corresponding to temperatures of $10^4$ to $10^5$°K, the fall of $\tau_{vibr}$ is retarded, but this value remains very small ($< 10^{-7}$ sec), and vibrational relaxation need not be taken into account.

The dissociation of oxygen takes place at temperatures of 2,500 to 4,000° when $p_1 = 1$ atm, and at 2,000 to 3,000° when $p_1 = 10^{-3}$ atm. For nitrogen the temperature values corresponding to the start and completion of dissociation[1] amount to 4,500 to 9,000° for $p_1 = 1$ atm, and to 3,500 to 6,000° for $p_1 = 10^{-3}$ atm (Ref. 31).

Dissociative relaxation time $\tau_{dis}$ at $T < 6{,}000$°K considerably exceeds $\tau_{vibr}$ and diminishes rapidly as temperature increases. According to the data of Duff and Davidson (Ref. 44), the time for the establishment of dissociative equilibrium in the air behind a strong shock wave when $p_1 = 1$ mm Hg, and $T_1 = 300$°K amounts to

| $T_2$, °K | $\tau_{dis}$, sec |
|---|---|
| 5,000 | $8 \cdot 10^{-3}$ |
| 7,000 | $2 \cdot 10^{-3}$ |
| 10,000 | $6 \cdot 10^{-4}$ |

In waves of large amplitude, dissociation takes place very rapidly (at $T = 10^5$° several collisions are sufficient for dissociation), and we may thus regard gas in the shock wave as being fully dissociated and consisting of nitrogen and oxygen atoms (in the small admixtures of argon may be disregarded).

Then the processes of excitation and ionization occur. They are the subject of detailed consideration in Chapter II. Here we shall merely remark that the expenditure of energy for excitation in a shock wave is many orders of magnitude lower than for ionization ($\epsilon_{el} \ll \epsilon_{ion}$). This is connected with the fact that with a Boltzmann distribution in the temperature range under consideration, the share of excited atoms is small; in addition, ionization takes place starting basically with the upper levels (see Section 10), diminishing their population. Therefore, in the presence of a high degree of ionization, there will be comparatively few excited atoms in a gas. In this respect the pattern in a shock wave in air differs radically from the condition in the formative stages of plasma (Ref. 54).

It would seem that atom collisions should constitute the basic mechanism of the initial stage of ionization. However, attempts to provide a quantitative explanation of the initial stage of

---

[1]By start and completion of dissociation, we conventionally understand to mean the state wherein the share of the atomic and of the molecular component amounts, respectively, to 1 percent.

ionization on the basis of the processes of atomic collisions, as well as on the basis of photoionization, has as yet not been successful (Ref. 43). It is, however, well known that at the ionization stage of $x = 10^{-3}$, the basic mechanism leading to further ionization is already the electron impact. We shall consider this process in Chapter II.

A very substantial property of strong shock waves is the presence of strong radiation, originating basically as a result of the processes of electron recombination and deceleration in an ion field. Here, although the density of the radiation energy $U_p$ and the radiation pressure $U_p/3$ are very small in comparison to the intrinsic energy and pressure of the substance behind the wave front, the stream of radiation energy in strong waves is comparable to the stream of energy transferred by the substance, and exerts a substantial influence on the structure of the shock wave front.

A rigorous theory of a shock wave, taking radiation into account, was developed by Ya. B. Zel'dovich (Ref. 46) and Yu. P. Rayzer (Ref. 47). The results of this research are cited in the survey of Ref. 42 and will be used by us further on.[1]

Refs. 46 and 47 give solutions of the hydrodynamic equations and equations of radiation under the assumption of the absence of deexcitation (the radiation flux across the surface of the shock wave is equal to zero). The works of S. A. Kaplan and I. A. Klimishin (Ref. 33), as well as of Kogure and Osaki (Ref. 41), deal with the case of deexcitation (see Section 8).

The question of the influence of radiation on the structure of a shock wave has also been dealt with in the work of Sen and Guess (Ref. 48); however, they studied shock waves of such small amplitude ($Ma \leq 4$), that the influence of radiation in them is, contrary to the opinion of the authors, infinitesimal.

The basic manifestation of the interaction of radiation with the substance in a shock wave is expansion of the shock wave front. The same effect, as is clear from the preceding, is exerted by the retarded excitation of part of the thermal capacity connected with the finiteness of the relaxation times $\tau_{vibr}$, $\tau_{dis}$ and $\tau_{ion}$, the last of these having the greatest value.

Concerning the part played by the other factors in the expansion of the shock front, it should be noted that viscosity plays a primary part in the formation of a shock wave. But in the wider

---

[1]The influence of radiation on the structure of the shock wave front has been investigated in detail by V. A. Prokof'yev (Ref. 45), in whose work are cited the general equations of the motion of a material medium with account taken of radiation. However, their solution in Ref. 45, has been shown by Ya. B. Zel'dovich (Ref. 46) to be incorrect.

relaxation layer, where vibration excitation and dissociation take place, the part played by viscosity and thermal conductivity in the case of strong waves is insignificant.[1]

Thus, an involved complex of phenomena, for which experimental and reliable theoretical data are available, occur behind the front of a shock wave. Many of these phenomena occur simultaneously, rather than in sequence, and furthermore, influence one another (the excitation of vibrations and dissociation, ionization and radiation). Of these processes, we shall select two and submit them to more detailed scrutiny, i.e., ionization and radiation, since as has been shown above, the remaining processes need not be taken into account in our problem.

Let us estimate the energy Q, which is expended for the dissociation and ionization of a unit of mass of gas (the specific energy of dissociation and ionization).

The number of ions of the r-th ionization in a unit of mass of gas is equal to $n_r/\rho_2$. The energy expended for one r-th ionization will be equal to

$$Q_r = \frac{n_r}{\rho_2} I_r, \tag{6.2}$$

where $I_r$ is the ionization potential. But since the ions of the r-th multiple have up to this point been ionized r – 1 times, the total expenditure of energy on their ionization comprises

$$Q_{1,r} = \frac{n_r}{\rho_2} \sum_{i=1}^{r} I_i, \tag{6.3}$$

and the total ionization energy per unit of mass is

$$Q_{\text{ion}} = \frac{n_a}{\rho_2} \sum_r \left( y_r \sum_{i=1}^{r} I_i \right) = \frac{N}{\mu_a} \sum_r \left( y_r \sum_{i=1}^{r} I_i \right), \tag{6.4}$$

where $y_r = n_r/n_a$, $n_a$ is the number of atoms in a unit of volume; $\mu_a$ is the atomic weight of air; and N is Avogadro's number. Analogously, the energy expended on total dissociation will be equal to

$$Q_{\text{dis}} = \frac{n_M}{\rho_2} I_{\text{dis}} = \frac{N}{\mu_M} I_{\text{dis}}, \tag{6.5}$$

---

[1]For the time being, we have in view thermal conductivity by means of collisions of heavy particles, i.e., molecules, atoms and ions. The part played by electronic thermal conductivity will be discussed in Section 15.

where $n_m$ is the molecule concentration; $\mu_m = 2\mu_a$ is the molecular weight of air, $I_{dis}$ is the dissociation potential. Adding $Q_{dis}$ and $Q_{ion}$, we obtain

$$Q = Q_{dis} + Q_{ion} = \frac{N}{\mu_M}\left[I_{dis} + 2\sum_r \left(y_r \sum_{i=1}^{r} I_i\right)\right]. \tag{6.6}$$

Substituting constants, we obtain Q in ergs per gram:

$$Q = 3.32 \cdot 10^{10}\left[I_{dis} + 2\sum_r \left(y_r \sum_{i=1}^{r} I_i\right)\right], \tag{6.7}$$

where $I_{dis}$ and $I_i$ are expressed in electron volts. We adopt here and in the future the values of $I_{dis}$, $I_r$ for nitrogen, oxygen and air, considering the latter to be a single-component gas equivalent to a mixture of 78 percent nitrogen and 22 percent oxygen, given in Table 2.

Table 2

Potentials of Dissociation and Ionization

| Gas | $I_{dis}$ | $I_1$ | $I_2$ | $I_3$ | $I_4$ | $I_5$ | $I_6$ |
|---|---|---|---|---|---|---|---|
| Nitrogen | 9,76 | 14,49 | 29.49 | 47.24 | 77.09 | 97.47 | — |
| Oxygen | 5,08 | 13,56 | 35.00 | 54.71 | 77.08 | 113.38 | 137.48 |
| Air | 8.73 | 14.29 | 30.70 | 48,88 | 77.09 | 100.97 | 137.48 |

The sixth ionization of nitrogen has a potential of $I_6 = 551$ ev and does not take place under the conditions we are dealing with. Therefore, we have assumed $I_6$ for air to be equal to the corresponding value for oxygen, and for the relative concentrations of oxygen we shall, where necessary, introduce the correction factor 0.22.

The values of $Q_{dis}$ and $Q_r$ for fully completed consecutive stages of ionization are cited in Table 3.

Table 3

Expenditure of Energy for Dissociation and Ionization

| | $Q_{dis}$ | $Q_1$ | $Q_2$ | $Q_3$ | $Q_4$ | $Q_5$ | $Q_6$ |
|---|---|---|---|---|---|---|---|
| $Q_r$ | $2.9 \cdot 10^{11}$ | $9.5 \cdot 10^{11}$ | $2.0 \cdot 10^{12}$ | $3.2 \cdot 10^{12}$ | $5.1 \cdot 10^{12}$ | $6.7 \cdot 10^{12}$ | $9,1 \cdot 10^{12}$ |
| $Q$ | $2.9 \cdot 10^{11}$ | $1,2 \cdot 10^{12}$ | $3.3 \cdot 10^{12}$ | $6,5 \cdot 10^{12}$ | $1.2 \cdot 10^{13}$ | $1,8 \cdot 10^{13}$ | $2.0 \cdot 10^{13}$ |

For calculations of the total expenditure of energy on ionization in the case of establishment of equilibrium, it is necessary to determine the specific energy of equilibrium ionization $Q_{eq}$. In

order to estimate the value of $Q_{eq}$, it is necessary to know the degree of equilibrium ionization. The method of determining this value is well known (see, for instance, Ref. 51), and consists in the computation of equilibrium constants for various conditions and stages of ionization. The equilibrium constants $K_r$ are in their turn expressed in terms of the statistical sums of ions $u_r$ and electrons $u_{el}$:

$$K_r = \frac{u_{r+1}u_{el}}{u_r} e^{-I_r/kT} \tag{6.8}$$

where $I_r$ is the ionization potential. Moreover, on the basis of the mass action law

$$K_r = \frac{\alpha_{r+1}\alpha_{el}}{\alpha_r}, \tag{6.9}$$

where $a_r$ and $a_{el}$ express the corresponding concentration of ions and electrons in terms of one initial molecule. Obviously the following conditions must be fulfilled:

$$\sum_{r=0}^{n} \alpha_r = 2; \qquad \sum_{r=1}^{n} r a_r = a_{el}. \tag{6.10}$$

Equilibrium constants for all possible stages of nitrogen and oxygen ionization for the temperature range of (2–500) · $10^{-3}$ ° and values of relative density (in units of air density at sea level) $\rho^* = 10–10^{-3}$ are cited in the work of V. V. Selivanov and I. Ya. Shlyapintokh (Ref. 30). Determination of ion concentration $a_r$ and electron concentration $a_{el}$ on the basis of them is reduced to solving the equation system (6.9) and (6.10); this may be carried out, for instance, in the following manner. Since

$$\alpha_1 = \alpha_0 \frac{K_0}{\alpha_{el}}; \quad \alpha_2 = \alpha_0 \frac{K_0K_1}{\alpha_{el}^2}; \ldots; \quad \alpha_n = \alpha_0 \frac{K_0K_1 \ldots K_{n-1}}{\alpha_{el}^n}, \tag{6.11}$$

it is possible to write

$$\alpha_0 \left(1 + \frac{K_0}{\alpha_{el}} + \frac{K_0K_1}{\alpha_{el}^2} + \cdots + \frac{K_0K_1 \ldots K_{n-1}}{\alpha_{el}^n}\right) = 2. \tag{6.12}$$

Assigning a number of values to $a_{el}$, we compute $a_0$ for them on the basis of (6.12), and then on the basis of (6.11) we compute other instances of $a_r$, after which on the basis of the second formula (6.10), we obtain $a'_{el}$, it being generally the case that $a'_{el} \neq a_{el}$ (the initial value). The equality $a'_{el} = a_{el}$ will hold true only for the value of $a_{el}$ that is the desired one. It is found by interpolation, after which with it will be repeated a calculation already of the final values of $a_r$.

The value $Q_p$ is found according to formula (6.7), where $y_r$ should be assumed equal to $(a_r^N + a_r^O)/2$.

By this method we have calculated, on the basis of Ref. 30, the values of $\alpha_r$, $\alpha_{el}$ for $\rho^* = 10^{-1}$–$10^{-3}$, i.e., for altitudes of 33–68 km. In addition, thanks to the courtesy of I. Ya. Shlyapintokh and N. M. Kuznetsov, we were able to make use of the results of analogous calculations performed in the Institute of Chemical Physics, Academy of Sciences, USSR, embracing

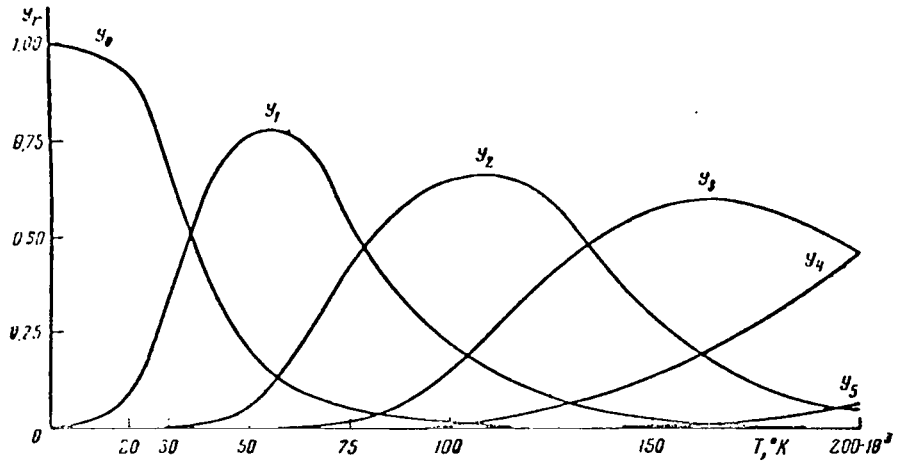


Figure 7. Change of equilibrium concentrations of air ions with temperatures for $\rho^* = 10$.

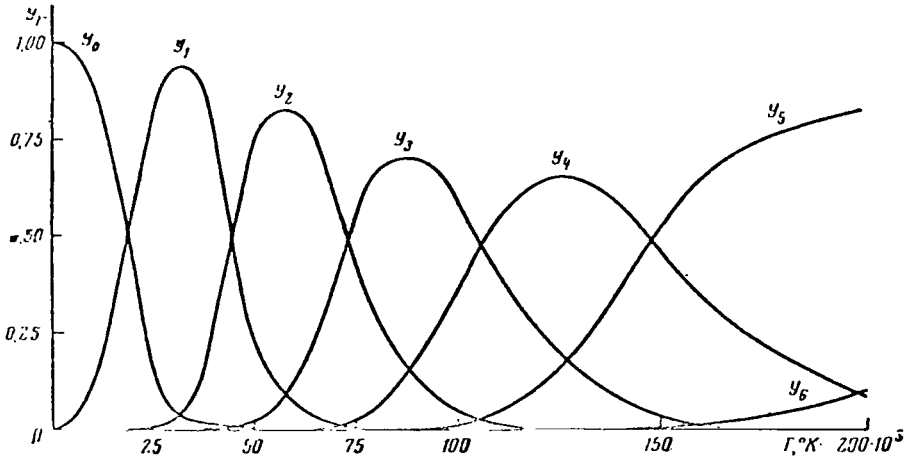


Figure 8. Change of equilibrium concentrations of air ions with temperatures for $\rho^* = 10^{-1}$.

the range of $\rho^* = 10–10^{-4}$, i.e., for the altitude range of 0–83 km (we assume the compression in the shock wave to be approximately $\rho^* = 10$). Both series of calculations were in excellent agreement for coinciding points.

Figures 7–9 show the change of equilibrium concentrations of air ions $y_r$ for the temperature range of $(20–200) \cdot 10^3$ degrees and various values of $\rho^*$. It is easy to see from the graphs that ions with two, and in rare cases with three, multiples of ionization can be represented simultaneously in a gas.

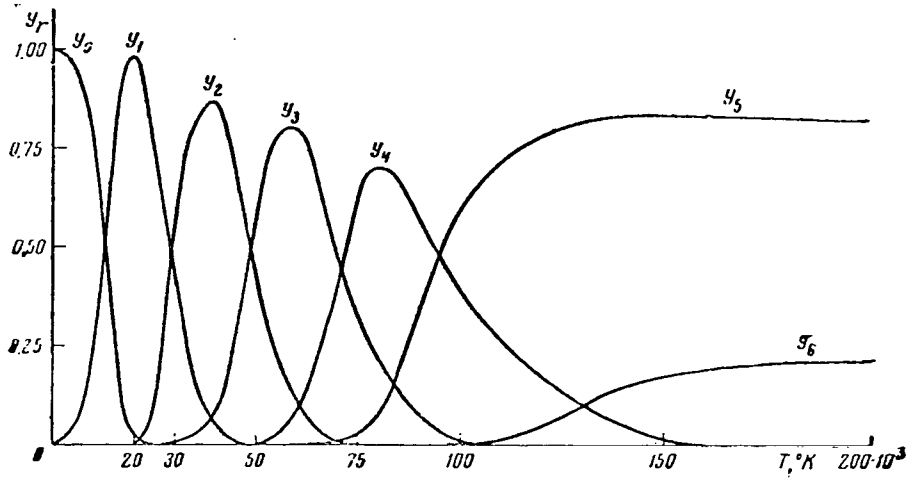


Figure 9. Change of equilibrium concentrations of air ions with temperatures for $\rho^* = 10^{-3}$.

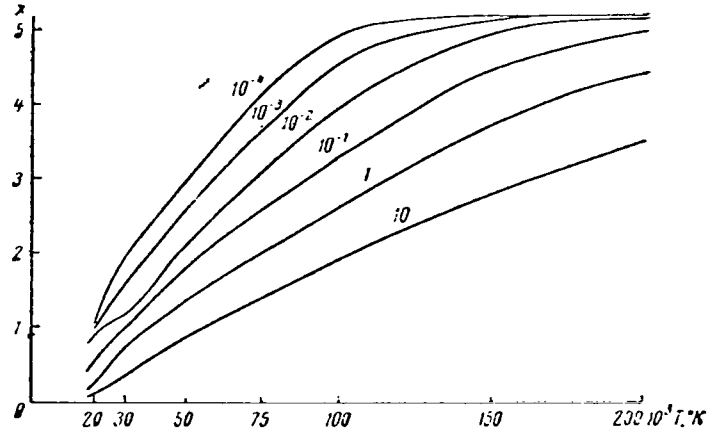


Figure 10. Changes of equilibrium electron concentrations for various $\rho^*$.

Change of the overall degree of equilibrium ionization, expressed by the ion concentration $x = a_{el}/2$, with air density and temperatures is shown in Figure 10; here, it can be seen that x increases not only with temperature, but also with altitude (i.e., with a diminution of $\rho^*$).

However, in real conditions, because of a reduction in the number of collisions behind the wave front per unit of time, actual ionization will diminish as altitudes increase, and at high altitudes an equilibrium state will not be obtained. The nonequilibrium zone may then extend to the very body of the meteorite. In order to study conditions in the nonequilibrium zone, it is necessary to solve the system of equations of the kinetics of ionization in a shock wave. This question will be considered in Section 9.

## Section 7. The Basic Relationships in a Shock Wave in the Presence of Dissociation and Ionization

The basic equations of the conservation of mass, impulse and energy in passage through the front of the shock wave have the form:

$$\begin{gathered} \rho_2 v_2 = \rho_1 v_1, \\ p_2 + \rho_2 v_2^2 = p_1 + \rho_1 v_1^2, \\ \varepsilon_2 + \frac{p_2}{\rho_2} + \frac{v_2^2}{2} = \varepsilon_1 + \frac{p_1}{\rho_1} + \frac{v_1^2}{2}. \end{gathered} \tag{7.1}$$

Here, p, $\rho$, v, and $\epsilon$ are pressure, density, and the specific intrinsic energy of the gas; the subscript 1 represents an unperturbed flow, the subscript 2 represents the compressed layer. From the first two equations of (7.1) we obtain the pressure behind the wave front:

$$p_2 = p_1 + \rho_1 v_1^2 \left(1 - \frac{\rho_1}{\rho_2}\right). \tag{7.2}$$

Since $p_2 \gg p_1$, it is possible to assume that $p_1 = 0$, and to consider the pressure $p_2$ as being directly proportional to the square of the velocity of the meteorite. The value in the parentheses is close to 0.9, since the compression $\rho_2/\rho_1$ at meteoric velocities is of the order of 10 and over.

Usually the value of gas compression in a shock wave is determined by a formula stemming from the Rankin-Hugoniot relationships:

$$\rho_2^* \equiv \frac{\rho_2}{\rho_1} = \frac{(\gamma + 1)\, p_2 + (\gamma - 1)\, p_1}{(\gamma + 1)\, p_1 + (\gamma - 1)\, p_2}, \tag{7.3}$$

which at large Mach numbers, i.e., for $p_2 \gg p_1$, assumes the form of

$$\frac{\rho_2}{\rho_1} = \frac{\gamma + 1}{\gamma - 1}, \tag{7.4}$$

where $\gamma$ is the isentropic exponent of gas. For a diatomic ideal gas, $\gamma = 7/5$; for a monatomic gas, $\gamma = 5/3$; consequently, the limit compressions in this case will be sixfold and fourfold, respectively. The ratio of the pressures is expressed by a formula analagous to (7.3):

$$\frac{p_2}{p_1} = \frac{(\gamma + 1)\rho_2 - (\gamma - 1)\rho_1}{(\gamma + 1)\rho_1 - (\gamma - 1)\rho_2}. \tag{7.5}$$

However, the relationships (7.3) and (7.5) are valid only for ideal gases. Meanwhile, the air in the shock wave formed by a meteorite differs considerably from an ideal gas with respect to its properties, this in particular being manifested by the fact that the isentropic exponent $\gamma$ becomes available—a function of temperature and pressure (for greater detail, see Ref. 31). Under conditions of dissociation and ionization, the density and pressure ratios in passage through the front of a strong shock wave may be found by a more complex method, i.e., through numerical calculation of the adiabatic shock wave. The method used in determining these and other thermodynamic values (entropy, intrinsic energy, etc.) is described in the works of V. V. Selivanov and I. Ya. Shlyapintokh (Ref. 30), and Ye. V. Stupochenko, et al. (Ref. 31). In Ref. 32 detailed tables are given of the gasdynamic functions of air behind a straight shock wave for temperatures of 6,000–12,000°, and initial pressures $p_1$ from $1–10^{-5}$ atm. Ref. 30 includes tables of these functions for a wide range of temperatures, 20,000 to 500,000°, and relative densities $\rho^*$, from 10 to $10^{-3}$.

Let us find the expression for the specific intrinsic energy behind the wave front $\epsilon_2$. For this we use the basic equations (7.1), disregarding the initial pressure $p_1 \ll p_2$, and the initial intrinsic energy $\epsilon_1 \ll \epsilon_2$. We obtain

$$\varepsilon_2 = \frac{p_2}{2\rho_2}(\rho_2^* - 1) = \frac{1}{2}\frac{p_2}{\rho_1}\frac{\rho_2^* - 1}{\rho_2^*}. \tag{7.6}$$

If the specific energy Q, expended for dissociation and ionization, is known, the compression $\rho_2^*$ may be found by substituting into the left part of (7.6) the sum of Q and the energy of forward motion $\epsilon_{forw}$, which is equal to

$$\varepsilon_{forw} = \frac{1}{\gamma_0 - 1}\frac{p_2}{\rho_2} = \frac{3}{2}\frac{p_2}{\rho_2}, \tag{7.7}$$

since for a fully dissociated gas $\gamma_0 = 5/3$. Carrying out the substitution, we obtain

$$Q + \frac{3}{2}\frac{p_2}{\rho_2} = \frac{1}{2}\frac{p_2}{\rho_2}(\rho_2^* - 1), \tag{7.8}$$

whence

$$\rho_2^* = 4 + \frac{2\rho_2}{p_2} Q = 4 + \frac{3Q}{\varepsilon_{\text{forw}}}. \tag{7.9}$$

Thus, as the shock of the energy expended for ionization is increased, relative compression $\rho_2^*$ grows.

Table 4 presents the values of $\rho_2^* = \rho_2/\rho_1$, computed according to the data of Refs. 30, 32, for various temperatures and initial pressures $p_1$.

Table 4

Compression of $\rho_2^*$ in a Shock Wave

| $T_2$ | $p_1$ | | | | | |
|---|---|---|---|---|---|---|
| | 1 | $10^{-1}$ | $10^{-2}$ | $10^{-3}$ | $10^{-4}$ | $10^{-5}$ |
| $10 \cdot 10^3$ | 11.42 | 13,56 | 14,82 | 15,27 | 16.10 | 18,30 |
| 15 | 11.26 | 12,52 | 13,58 | 15,66 | 17,85 | 18.66 |
| 20 | 10.10 | 12,12 | 13,71 | 14,85 | 15,13 | 15,19 |
| 25 | 9,93 | 11,83 | 12.75 | 13,04 | 13,87 | 16,38 |
| 30 | 9,75 | 11,21 | 11,68 | 12.62 | 14,97 | 16,41 |
| 50 | 8,97 | 10,20 | 11,43 | 12.44 | 14,32 | 14,74 |
| 75 | 8,75 | 9,82 | 11,22 | 12,53 | 14,00 | 14,18 |
| 100 | 8,62 | 9,75 | 11,07 | 12.38 | 13,49 | 12,29 |
| 150 | 8,43 | 9,52 | 10,51 | 11.14 | 10,88 | 8,46 |
| 200 | 8.08 | 8,88 | 9.41 | 9,47 | 8.68 | 7,40 |
| 250 | 7,80 | 8,32 | 8,64 | 8,42 | 7,75 | 7,12 |

Having determined from Table 4 the value of compression $\rho_2^*$ according to the arguments $p_1$, and the equilibrium temperature $T_2$ behind the shock-wave front, it is possible from tables appearing in Ref. 30 to find the pressure $p_2$, the entropy $S_2$, the intrinsic energy $\epsilon_2$, and, furthermore, the velocity $v_1$ of the oncoming stream according to the formula

$$v_1 = \sqrt{\frac{p_2}{\rho_1}\frac{\rho_2^*}{\rho_2^* - 1}}. \tag{7.10}$$

In our case, on the contrary, we are given the velocity $v_1$ (the velocity of the meteorite), while the pressure $p_2$ may be found according to formula (7.2). As regards the equilibrium temperature $T_2$, its determination will be discussed below.

We introduce the effective isentropic exponent $\gamma_{eff}$ from the condition[1]

$$\gamma_{eff} = 1 + \frac{p}{\rho\varepsilon}. \tag{7.11}$$

On the basis of (7.6) and (7.11), we obtain the value of $\gamma_{eff}$ behind the wave front

$$\gamma^*_{eff} = \frac{\rho^*_2 + 1}{\rho^*_2 - 1}. \tag{7.12}$$

From (7.12) we find the expression $\rho^*_2$ in terms of $\gamma^*_{eff}$:

$$\rho^*_2 = \frac{\gamma^*_{eff} + 1}{\gamma^*_{eff} - 1}. \tag{7.13}$$

On the basis of (7.12) and Table 4, we find the table of the values of $\gamma^*_{eff}$ (Table 5).

Thus, for the conditions that interest us, $\gamma^*_{eff} = 1.11-1.33$. It should, however be stipulated that the tables of Ref. 30 are compiled under the assumption of the presence, behind the wave front, of the equilibrium of substance with radiation.

Equilibrium radiation may be regarded as ideal gas with an isentropic exponent of $\gamma = 4/3$. Since for a proton gas, $\gamma = 4/3 = 1.33$ and $\rho^*_2 = 7$, the values of $\gamma^*$ and $\rho^*_2$ in Tables 4 and 5 at high temperatures tend toward these values. If under real conditions equilibrium with radiation is not attained, $\gamma^*_{eff}$ will be smaller, and $\rho^*_2$ will be larger than the values in Tables 4 and 5. The acts of energy exchange between radiation and substance may be (in order of their significance in strong waves) photoionization and recombination with radiation, deceleration radiation, and absorption as a result of free-free transactions, radiation and absorption in lines.

Similar to the other relaxation processes considered above, the establishment of radiation equilibrium requires a definite time, that is, equilibrium is established at some distance from the wave front. Estimates of this distance are available in Ref. 41. We shall return to a discussion of this question in Section 11.

We shall now consider in greater detail the action of dissociation and ionization on the basic gasdynamic values, viz., on pressure, density, and flow velocity behind the wave front.

Both of the processes under consideration are reduced to energy absorption. In this case, for strong shock waves the following relationships hold true (Ref. 49).

---

[1]This definition of $\gamma_{eff}$ is that of Ya. B. Zel'dovich and Yu. P. Rayzer.

Table 5

Effective Indicator of the Adiabatic Curve Behind the Wave Front $\gamma^*_{eff}$

| $T_2$ | $p_1$ | | | | | |
|---|---|---|---|---|---|---|
| | 1 | $10^{-1}$ | $10^{-2}$ | $10^{-3}$ | $10^{-4}$ | $10^{-5}$ |
| $10 \cdot 10^3$ | 1.19 | 1.16 | 1.14 | 1.14 | 1.13 | 1.12 |
| 15 | 1.21 | 1.17 | 1.16 | 1.14 | 1.12 | 1.11 |
| 20 | 1.22 | 1.18 | 1.16 | 1.14 | 1.14 | 1.14 |
| 25 | 1.22 | 1.18 | 1.17 | 1.16 | 1.16 | 1.13 |
| 30 | 1.23 | 1.20 | 1.19 | 1.17 | 1.14 | 1.13 |
| 50 | 1.25 | 1.22 | 1.19 | 1.17 | 1.15 | 1.14 |
| 75 | 1.26 | 1.23 | 1.20 | 1.17 | 1.14 | 1.15 |
| 100 | 1.26 | 1.23 | 1.20 | 1.17 | 1.16 | 1.18 |
| 150 | 1.27 | 1.24 | 1.21 | 1.20 | 1.20 | 1.27 |
| 200 | 1.28 | 1.25 | 1.24 | 1.24 | 1.25 | 1.31 |
| 250 | 1.29 | 1.27 | 1.25 | 1.27 | 1.30 | 1.33 |

$$p_2' = \rho_1 v_1^2 \left( \frac{2}{\gamma + 1} + \Delta \right), \tag{7.14}$$

$$\frac{\rho_1}{\rho_2'} = \frac{v_2'}{v_1} = \frac{\gamma - 1}{\gamma + 1} - \Delta, \tag{7.15}$$

$$u' = v_1 \left( \frac{2}{\gamma + 1} + \Delta \right), \tag{7.16}$$

the parameter $\Delta > 0$ is expressed in terms of the quantity of absorbed energy (per unit of mass) Q, in the following manner:

$$\Delta = \frac{\Delta_1 - 1}{\gamma_* + 1}; \quad \Delta_1 = \sqrt{1 + \frac{2(\gamma_*^2 - 1)\, Q}{v_1^2}}, \tag{7.17}$$

where $\gamma_*$ is the isentropic exponent behind the wave front; and, $v_1$ and u are, respectively, the speed of the shock wave and the velocity of the medium behind the wave front in a system of coordinates connected with unperturbed gas. All values for the case of energy absorption, $(Q > 0)$, are marked with a prime. Obviously, if $Q = 0$, then $\Delta = 0$ and formulas (7.14)–(7.16) will assume their trivial form (see formulas (7.2) and (7.4)). From formulas (7.14)–(7.17) it follows (with formulas (7.1) taken into account):

$$\frac{p_2'}{p_2} = \frac{u'}{u} = \frac{1 + \Delta_1}{2}, \tag{7.18}$$

$$\frac{\rho_2'}{\rho_2} = \frac{v_2}{v_2'} = \frac{\gamma_* - 1}{\gamma_* - \Delta_1}, \tag{7.19}$$

$$\frac{T_2'}{T_2} = \frac{1 + \Delta_1}{2} \frac{\gamma_* - \Delta_1}{\gamma_* - 1}. \tag{7.20}$$

It is very easy to see that when Q = 0, these ratios become equal to unity; however, if Q > 0, then

$$p_2' > p_2,\ \rho_2' > \rho_2,\ u' > u,\ v_2' < v_2. \tag{7.21}$$

In other words, pressure, density on the front, and flow velocity behind the front (with respect to motionless gas) are greater in the case of a wave behind in which dissociation and ionization are taking place.

In a system of coordinates connected with the shock wave and the heat of a meteorite, the flow velocity behind the wave at the deceleration sector, $v_2 = v_1 - u$, on the contrary, will in this case be less. The temperatures behind the wave front will obviously also be less.

In the expression for $\Delta_1$, (7.17) is included the ratio of the specific energy of dissociation and ionization Q to the specific kinetic energy of the oncoming stream $v_1^2/2$, that is, the value $Q^* = 2Q/v_1^2$; we cite here a table of this value for various stages of ionization and velocities of the meteoric body (or, similarly, of the oncoming stream) $v_1$ (Table 6).

Table 6

Relative Specific Energy of Dissociation and Ionization Q*

| $v_1$, km/sec | $Q^*_{dis}$ | $Q_1^*$ | $Q_2^*$ | $Q_3^*$ | $Q_4^*$ | $Q_5^*$ | $Q_6^*$ |
|---|---|---|---|---|---|---|---|
| 10 | 0,58 | — | — | — | — | — | — |
| 20 | 0,14 | 0.62 | — | — | — | — | — |
| 40 | 0,036 | 0.156 | 0.40 | 0,82 | — | — | — |
| 60 | 0.016 | 0,068 | 0.182 | 0,36 | 0.64 | — | — |
| 80 | 0,0090 | 0,040 | 0,102 | 0.20 | 0.36 | 0.58 | 0.60 |

On the basis of the values for Q* cited in Table 6, it is not difficult to calculate the values $\Delta_1$ and $\Delta$ for fully completed stages of ionization.

Obviously, $Q^* < 1$, from which, on the basis of (7.17), we obtain for any $\gamma$ the condition $1 < \Delta_1 < \gamma$. Therefore, in cases where values of $Q^* > 1$ were obtained from formula (7.17), a dash was entered in Table 6. Physically, this signifies that, at the corresponding velocities $v_1$, the given styles of ionization either do not occur at all, or occur only partially.

In Table 7, for three values of $\gamma$, according to the argument Q*, are shown the values of $\tilde{p}_2 = p_2'/p_2$; $\tilde{\rho}_2 = \rho_2'/\rho_2$; $\tilde{v}_2 = v_2'/v_2$.

From Table 7 it can be seen that the values $\tilde{p}_2$, $\tilde{\rho}_2$, $\tilde{v}_2$ depends only slightly on $\gamma$, but the relative density increases perceptibility, and the velocity falls with the growth of Q*. This result agrees qualitatively with the conclusions of V. A. Prokof'yev (Ref. 45, Figures 2 and 4). It is true that in Ref. 45 the ratios $\tilde{\rho}_2$ and $\tilde{v}_2$ have, respectively, a maximum and a minimum according to the argument $p_2^* = p_2/p_1$, but this is explained by the fact that its calculations were performed for a monatomic gas (hydrogen), where after completion of the first ionization, Q ceased to grow, and therefore, with a further increase in the amplitude of the shock wave, the ratios $2Q/v_1^2$ began to diminish.

Table 7

Influence of Dissociation and Ionization on the Gasdynamics Parameters Behind the Wave Front

| Q* | $\gamma = 1.10$ | | | $\gamma = 1.25$ | | | $\gamma = 1.40$ | | |
|---|---|---|---|---|---|---|---|---|---|
| | $\tilde{p}_2$ | $\tilde{\rho}_2$ | $\tilde{v}_2$ | $\tilde{p}_2$ | $\tilde{\rho}_2$ | $\tilde{v}_2$ | $\tilde{p}_2$ | $\tilde{\rho}_2$ | $\tilde{v}_2$ |
| 0,02 | 1,001 | 1,02 | 0,98 | 1,003 | 1.02 | 0,98 | 1,005 | 1.02 | 0.98 |
| 0.2 | 1.010 | 1,27 | 0.79 | 1.030 | 1.28 | 0,78 | 1.046 | 1,30 | 0.77 |
| 0,4 | 1.020 | 1.70 | 0.59 | 1,054 | 1.75 | 0.57 | 1.088 | 1.79 | 0.56 |
| 0.6 | 1.030 | 2,56 | 0.39 | 1.078 | 2.63 | 0,38 | 1,128 | 2,78 | 0.36 |
| 0,8 | 1,040 | 5.25 | 0.19 | 1,102 | 5.45 | 0.18 | 1,164 | 5,60 | 0.18 |
| 0.9 | 1,045 | 10,5 | 0.10 | 1,114 | 10.9 | 0,09 | 1,182 | 11.3 | 0,09 |

Study of the dependence of Q* on the amplitudes of the wave for air, and changes of the value under actual conditions require solution of the equations of ionization kinetics, and this will be done in Section 9.

Let us consider in greater detail the question of the temperature in the shock wave under conditions of dissociation and ionization.

Since the process of ionization is accompanied by the loss of energy, the temperature behind the shock-wave front must fall from some value, $T_y$, at the wave front to the equilibrium value, $T_2$.

If the processes of the excitation of vibrations and dissociation did not take place in a shock wave, the temperature at the wave front would be determined according to the well-known formula derived from the general equations of a shock wave (7.1), and the equation of the state of an ideal gas (Ref. 49):

$$T_y = T_1 \frac{p_2}{p_1} \frac{\rho_1}{\rho_2}, \tag{7.22}$$

or, with (7.4) takes into account,

$$T_y = T_1 \frac{p_2}{p_1} \frac{\gamma - 1}{\gamma + 1}, \tag{7.23}$$

where $\gamma$ is the indicator of the adiabatic gas curve behind the breakaway.

However, in strong waves the temperature at the front never attains the value $T_y$ due to energy expenditures for excitation of internal degrees of freedom and for dissociation, and also due to the increase in the number of particles. Therefore, the actual temperature of the shock wave front, $T_f$, will be

$$T_f = T_1 \frac{p_2'}{p_1} \frac{\rho_1}{\rho_2'} \alpha, \tag{7.24}$$

where p' and $\rho'$ are determined by formulas (7.14) and (7.15); $\alpha$ is a multiplier that takes into account the changes in the number of particles and of the isentropic exponent in the case of complete dissociation.

Let $\gamma_0$ be the isentropic exponent for diatomic gas previous to dissociation, and let $\gamma_1$ be the same for monatomic gas. We have the energy equation

$$E = \frac{1}{\gamma - 1} \frac{p}{\rho} \tag{7.25}$$

and the equation of state for a variable number of particles

$$\frac{p}{\rho} = \frac{N}{N_0} RT. \tag{7.26}$$

From (7.25) and (7.26) it follows (since $\gamma_0 = 7/5$, $\gamma_1 = 5/3$, and $N/N_0 = 2$), that

$$\alpha = \frac{\gamma_1 - 1}{\gamma_0 - 1} \frac{N_0}{N} = \frac{5}{6}, \tag{7.27}$$

and, in this manner,

$$T_f = \frac{5}{6} T_1 \frac{p_2'}{p_1} \frac{\rho_1}{\rho_2'}. \tag{7.28}$$

Substituting (7.14), (7.15) and (7.17) into (7.28), we find

$$T_f = \frac{5}{6} T_1 \frac{\rho_1}{p_1} v_1^2 \left[\frac{2}{\gamma_* + 1} + \Delta\right] \left[\frac{\gamma_* - 1}{\gamma_* + 1} - \Delta\right] \tag{7.29}$$

or

$$T_f = \frac{25}{12} \frac{v_1^2}{c_v} \frac{(\gamma_* - \Delta_1)(1 + \Delta_1)}{(\gamma_* + 1)^2}, \tag{7.30}$$

where $\gamma_*$ is the effective isentropic exponent at the wave front, determined from (7.12); $\Delta$ and $\Delta_1$ are determined by formula (7.17) with substitution of the specific dissociation energy, $Q_{dis}$, for Q; $c_v$ is the heat capacity of air before the front,[1] equal to $7.15 \cdot 10^6$ ergs/g · deg.

Equilibrium temperature $T_2$, which becomes established simultaneously with the establishment of equilibrium ionization, is also determined according to formula (7.29), or formulas (7.30) and (7.17), but now in formula (7.17) one should assume that $Q = Q_{eq}$ when $Q_{eq}$ is the expenditure of energy for the attainment of equilibrium ionization (per unit of mass), computed according to formula (6.7), with substitution of equilibrium values of the degrees of ionization.

Although $T_y$ is a fictitious value for strong waves, it makes sense to compare it with $T_f$, initially, in order to obtain a clear conception of the influence of dissociation on temperature and on the consequences of not taking this influence into account, and secondly, for convenience, since $T_y$ is easily computed, and the transition from $T_y$ to $T_f$ and $T_2$ is simpler than direct computation of these values according to formulas (7.17), (7.29) and (7.30).

On the basis of (7.22) and (7.28), we find for the desired temperature ratio

$$\frac{T_f}{T_y} = \frac{5}{6} \frac{\gamma_* - \Delta_1}{\gamma_* - 1} \frac{1 + \Delta_1}{2}. \tag{7.31}$$

Formula (7.31) permits considerable simplification for small instances of Q*, if small second-order values with respect to unity are neglected. Substituting $\Delta_1$ from (7.17), we obtain simply

$$\frac{T_f}{T_y} = \frac{5}{6}(1 - Q^*_{dis}); \qquad \frac{T_2}{T_y} = \frac{5}{6}(1 - Q^*_{eq}). \tag{7.32}$$

The error of formula (7.32) for $Q^* \leq 0.4$ is less than 5 percent.

---

[1] In place of $5/2c_v$ it is possible to substitute the value, equal to it, of $\mu/R_0$, where $R_0$ is a universal gas constant, $\mu$ is the molecular weight of air before the front.

Table 8 contains (for various $p_1$ and a range of meteoric velocities) the values of $T_f$, $T_2$ and $T_y$ (for comparison). Figure 11 shows the dependence of temperature $T_2$ on parameters $v_1$ and $p_1$ for the meteoric range of velocities and densities.

As may be seen from Table 8, the influence of dissociation on the "peak" temperature is particularly great at small shock-wave amplitudes, and is less considerable at large amplitudes. The influence of ionization, on the other hand, increases with the amplitude, this being connected with the change of the relative contribution of these phenomena to heat capacity.

Table 8

Temperature Behind the Shock-Wave Front

| $v_1$ | $p_1 = 1$ atm | | | $p_1 = 10^{-1}$ atm | | |
|---|---|---|---|---|---|---|
| | $T_y$ | $T_f$ | $T_2$ | $T_y$ | $T_f$ | $T_2$ |
| 12 | 54 000 | 27 800 | 20 700 | 43 800 | 21 600 | 16 800 |
| 20 | 161 000 | 114 500 | 41 000 | 139 000 | 99 000 | 32 000 |
| 30 | 386 000 | 301 000 | 68 400 | 338 000 | 264 000 | 55 000 |
| 40 | 689 000 | 553 000 | 97 600 | 624 000 | 501 000 | 79 000 |
| 50 | 1 100 000 | 897 000 | 129 000 | 974 000 | 792 000 | 106 000 |
| 60 | 1 590 000 | 1 300 000 | 162 000 | 1 450 000 | 1 190 000 | 133 000 |
| 72 | 2 350 000 | 1 940 000 | 203 000 | 2 100 000 | 1 730 000 | 169 000 |
| $v_1$ | $p_1 = 10^{-2}$ atm | | | $p_1 = 10^{-3}$ atm | | |
| | $T_y$ | $T_f$ | $T_2$ | $T_y$ | $T_f$ | $T_2$ |
| 12 | 41 400 | 21 200 | 14 500 | 37 200 | 18 250 | 13 000 |
| 20 | 127 000 | 90 500 | 27 100 | 115 500 | 82 500 | 24 600 |
| 30 | 300 000 | 234 000 | 46 600 | 274 000 | 213 000 | 42 100 |
| 40 | 556 000 | 447 000 | 66 400 | 487 000 | 392 000 | 57 900 |
| 50 | 870 000 | 708 000 | 87 000 | 760 000 | 619 000 | 75 800 |
| 60 | 1 250 000 | 1 030 000 | 111 000 | 1 090 000 | 898 000 | 94 200 |
| 72 | 1 880 000 | 1 553 000 | 143 000 | 1 730 000 | 1 430 000 | 129 000 |
| $v_1$ | $p_1 = 10^{-4}$ atm | | | $p_1 = 10^{-5}$ atm | | |
| | $T_y$ | $T_f$ | $T_2$ | $T_y$ | $T_f$ | $T_2$ |
| 12 | 34 800 | 17 400 | 11 600 | 32 400 | 16 100 | 10 700 |
| 20 | 109 000 | 78 000 | 21 800 | 103 000 | 73 000 | 20 800 |
| 30 | 232 000 | 181 000 | 35 900 | 217 000 | 169 500 | 30 200 |
| 40 | 439 000 | 353 000 | 50 000 | 412 000 | 332 000 | 44 700 |
| 50 | 645 000 | 525 000 | 66 700 | 665 000 | 541 000 | 62 400 |
| 60 | 985 000 | 809 000 | 81 100 | 985 000 | 809 000 | 76 300 |
| 72 | 1 580 000 | 1 308 000 | 111 000 | 2 290 000 | 1 890 000 | 148 000 |

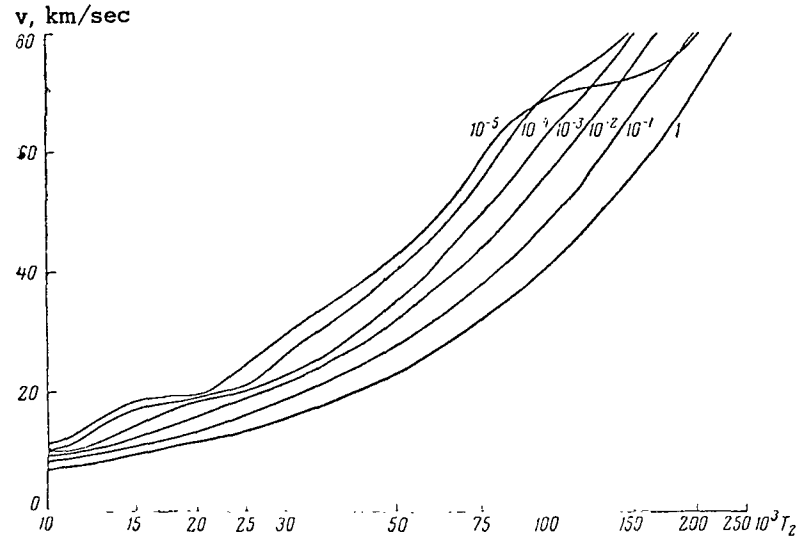


Figure 11. The function $T_2$ ($v_1$, $p_1$).

An increase in the influence of ionization at high altitudes (the ratio $T_f/T_2$ is larger there). This is to be explained by a rise in the degree of equilibrium ionization in rarefied gas (see Section 6).

The last of the processes that must be discussed, occurring behind the front of a shock wave, is *adiabatic compression and heating of the gas between the front and the body*. If $p_2$ and $T_2$ are the pressure and temperature behind the wave front, while $p_3$ and $T_3$ are the pressure and temperature in the point of full deceleration, we have the pressure ratio (Ref. 49) in the case of strong shock waves:

$$\frac{p_3}{p_2} = \left[1 + \frac{(\gamma-1)^2}{4\gamma}\right]^{\frac{\gamma}{\gamma-1}}, \tag{7.33}$$

and for the temperature ratio

$$\frac{T_3}{T_2} = \left(\frac{p_3}{p_2}\right)^{\frac{\gamma-1}{\gamma}} = 1 + \frac{(\gamma-1)^2}{4\gamma}. \tag{7.34}$$

For various instances of $\gamma$ these ratios have the following values:

| $\gamma$ | 1.40 | 1.30 | 1.25 | 1.20 | 1.15 | 1.10 |
|---|---|---|---|---|---|---|
| $p_3/p_2$ | 1.105 | 1.075 | 1.062 | 1.048 | 1.038 | 1.022 |
| $T_3/T_2$ | 1.029 | 1.017 | 1.012 | 1.008 | 1.005 | 1.002 |

Obviously, the adiabatic compression is not great and it is possible generally to disregard adiabatic heating, and subsequently to assume $T_3 = T_2$.

## Section 8. The Influence of Radiation on the Structure of a Shock Wave in the Presence of Ionization

As has already been said before, radiation exerts a substantial effect on the structure of a shock wave and on the temperature distribution both in front of and behind the front. A brief review of the basic literature in which this problem has been studied is provided in Section 6. Our task is to apply the theory developed in these reports to the case of strong ionization.

It is generally possible to consider two basic cases of strong shock waves with radiation:

Case I. The radiation formed behind the front of the shock wave is entirely absorbed directly before the front (in the so-called heating region), without passing outside (deexcitation is absent).

Case II. The radiation to a considerable extent passes outside; in other words, the radiation flux through the front differs from zero (deexcitation of the shock wave occurs).

The first case has been investigated in detail by Ya. B. Zel'dovich (Ref. 46) and Yu. P. Rayzer (Ref. 47). The qualitative pattern of the temperature change in this case has the following form (Figure 12).

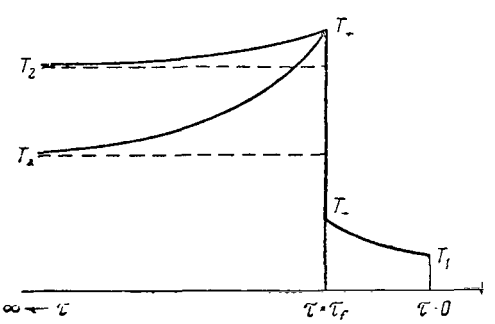


Figure 12. Change of T in passage across the front of a shock wave in the "subcritical" case (according to Zel'dovich and Rayzer).

Before the front, in the heating region the temperature constantly rises from the initial value $T_1$ to some $T_- > T_1$. Subsequently, at the front there occurs a temperature jump to the value $T_+$, and then a gradual lowering to the equilibrium value $T_2$.

In the presence of a radiation flux, the basic shock relationships (7.1) will assume the form:

$$\left.\begin{aligned} \rho v &= \rho_1 v_1, \\ p + \rho v^2 &= p_1 + \rho_1 v_1^2, \\ \rho v\left(\varepsilon + \frac{p}{\rho} + \frac{v^2}{2}\right) + F &= \rho_1 v_1\left(\varepsilon_1 + \frac{p_1}{\rho_1} + \frac{v_1^2}{2}\right) + F_1. \end{aligned}\right\} \tag{8.1}$$

For strong waves, in finding the solution of equations (8.1) behind the wave front, the values $\epsilon_1$ and $p_1$ are disregarded. Under these conditions the third equation of (8.1) takes the form:

$$\varepsilon + \frac{p}{\rho} + \frac{v^2}{2} + \frac{F}{\rho v} = \frac{v_1^2}{2} + \frac{F_1}{\rho_1 v_1}. \tag{8.2}$$

It should be remembered that since the radiation flux and the hydrodynamical energy flux are directionally opposed, the magnitudes $F/\rho v$ and $F_1/\rho_1 v_1$ are negative. Henceforth, where necessary, we shall use the absolute values of these magnitudes.

Let us consider Case I (deexcitation is absent, $F_1 = 0$). Under the assumption of constant heat capacity, the temperature and the radiation flux are expressed in terms of inverse compression, $\eta = \rho_1/\rho$, in this point, and in terms of inverse compression behind the front, in the following manner (Refs. 45, 47):

$$T = T_2 \frac{\eta(1-\eta)}{\eta_2(1-\eta_2)}, \tag{8.3}$$

$$F = \rho_1 v_1 R T_2 \frac{(1-\eta)(\eta-\eta_2)}{2\eta_2^2(1-\eta_2)}. \tag{8.4}$$

Considering that the radiation flux does not undergo discontinuity at the wave front (Ref. 46), under the assumptions indicated above, Yu. P. Rayzer obtained the following expressions for temperatures $T_+$ and $T_-$:

$$\frac{T_+ - T_2}{T_{cr}} = \frac{3-\gamma}{2(\gamma+1)}\left(\frac{T_2}{T_{cr}}\right)^4, \tag{8.5}$$

$$\frac{T_-}{T_{cr}} = \frac{1}{2}\left(\frac{T_2}{T_{cr}}\right)^4. \tag{8.6}$$

Here, $T_{cr}$ is the critical temperature at which the radiation flux is equalized with the hydrodynamic thermal flux; according to Yu. P. Rayzer (Ref. 47), $T_{cr}$ is determined by the formula

$$T_{cr}^3 = \frac{\sqrt{3}}{4} \frac{\rho_1 v_1 R_0}{\sigma(\gamma - 1)\mu}. \tag{8.7}$$

Expressions (8.5) and (8.6) are valid for the case of $T_2 < T_{cr}$. If, on the other hand, $T_2 > T_{cr}$, the relationships

$$\begin{aligned} T_- &\approx T_2, \\ T_+ &= T_2(3 - \gamma) \end{aligned} \tag{8.8}$$

will be in effect.

This is the case of an "isothermal jump," in which, with the exception of the region with a narrow temperature peak, $T_+$, the temperature in the heating region before the wave front smoothly passes into the temperature behind the front (Figure 13). It is precisely such a pattern (but without a peak) that is obtained in the approximation of radiant thermal conductivity. As we shall see latter, this case ($T_2 > T_{cr}$) takes effect in the movement of meteorites at high altitudes with high velocities.

A disadvantage of formulas (8.5)–(8.8) is that they are derived under the assumption of constant heat capacity and molecular weight of the gas. Meanwhile, under actual conditions, as we have already seen, the exponent $\gamma$, as well as the mean molecular weight of air, $\mu$, are variable. In practice, $T_{cr}$, $T_-$, and $T_+$ are determined on the basis of tables of the thermodynamic properties of air at high temperatures (Refs. 30, 32).

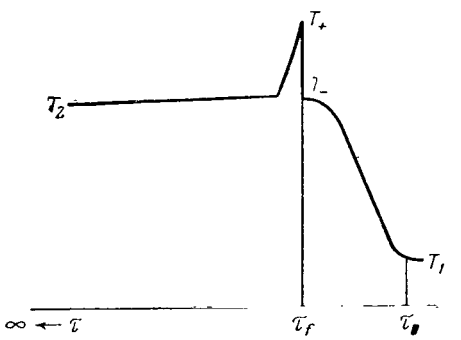


Figure 13. Change of T in passage across the front of a shock wave in the "supercritical" case (according to Rayzer).

For given values of $\rho_1$ and $T_2$, the intrinsic energy of the gas prior to breakaway, $\epsilon(T_-)$, is determined, according to Yu. P. Rayzer (Ref. 47), from the condition that the radiation energy absorbed in the heating zone goes entirely to increase the intrinsic energy of the gas:

$$\sigma T_2^4 = D\rho_1\epsilon(T_-), \tag{8.9}$$

where D is the velocity of the wave front corresponding to the given instances of $\rho_1$ and $T_2$ (specifically, for a meteorite $D = v_1$). The temperature $T_-$ is found from $\epsilon(T_-)$ on the basis of the tables in Refs. 30, 32. The critical temperature $T_{cr}$ is found from the condition $T_- = T_2 = T_{cr}$.

For normal pressure (at sea level) Yu. P. Rayzer in Ref. 121 obtained $T_{cr} = 285{,}000°$ and a series of values of $T_-$ for various given instances of $T_2$. We performed similar calculations for various altitudes and pressures. The results are shown in Table 9.

Table 9

Temperatures $T_-$ and $T_{cr}$ (thousands of degrees)

| $T_2$ | 6 | 8 | 10 | 12 | 20 | 30 | 50 | 75 | 100 | 150 | 250 | $T_{cr}$ |
|---|---|---|---|---|---|---|---|---|---|---|---|---|
| $p_1 = 1$ | — | — | — | — | 0.6 | 1.8 | 7.6 | 14.3 | 25 | 60 | 178 | 285 |
| $p_1 = 10^{-1}$ | — | — | — | 0.6 | 3.8 | 8.3 | 19 | 47 | 83 | — | — | 117 |
| $p_1 = 10^{-2}$ | 0.9 | 1.9 | 3.6 | 7.0 | 11.9 | 23.5 | — | — | — | — | — | 38 |
| $p_1 = 10^{-3}$ | 4.7 | 6.8 | — | — | — | — | — | — | — | — | — | 9.3 |

From Table 9 it can be seen that with a reduction in the pressure of unperturbed gas, i.e., with an increased altitude, the value $T_{cr}$ rapidly diminishes. The dependence of the temperature conditions on the altitude and velocity of the meteorite can be seen graphically from the following table, where the values of the "initial velocities" corresponding to given instances of $p_1$ and $T_{cr}$ are shown.

| | | | | |
|---|---|---|---|---|
| $p_1$, atm | 1 | $10^{-1}$ | $10^{-2}$ | $10^{-3}$ |
| H, km | 0 | 14 | 32 | 49 |
| $T_{cr}$, thousands of degrees | 285 | 117 | 38 | 9.3 |
| $v_{cr}$, km/sec | >72 | 55 | 26 | 10 |

It follows from this that at lower than 10 km the conditions for meteorites will always be subcritical, and at higher than 45 km the conditions will always be supercritical; at altitudes of 10–45 km the conditions are determined by the velocity of the meteorite.

Let us now consider Case II, in which deexcitation takes place, i.e., the radiation flux through the front $F_1 > 0$. The temperatures behind the front will then be lower than in the preceding

case, and its equilibrium value $T_* < T_2$. The value of $T_*$ is determined in the function of $T_2$, and $F_1$ by the following expression, obtained by S. A. Kaplan and I. A. Klimashin (Ref. 33):

$$T_* = \frac{1}{2} T_2 \left[ 1 + \sqrt{1 + \frac{2(\gamma^2 - 1)}{v_1^2} \left| \frac{F_1}{\rho_1 v_1} \right|} - \frac{2(\gamma + 1)}{v_1^2} \left| \frac{F_1}{\rho_1 v_1} \right| \right]. \tag{8.10}$$

Obviously when $F_1 = 0$, $T_* = T_2$.

A complete solution of the equation system (8.1) has been given by Kogure and Osaki (Ref. 41), who obtained expressions for the temperature, the radiation flux, and the pressure and density at any point both before and behind the wave front.

Let us cite these expressions here. The temperatures $T_a$ before the front and $T_b$ behind the front are determined in terms of the radiation fluxes $F_a$ and $F_b$ in the following manner:

$$T_a(\tau) = T_1 + \frac{2}{\rho_1 v_1 R} \frac{\eta_2}{1 - \eta_2} (F_a - F_1), \tag{8.11}$$

$$T_b(\tau) = T_2 + \frac{2}{\rho_1 v_1 R} \frac{\eta_2 (1 - 2\eta_2)}{1 - \eta_2} (F_b - F_1). \tag{8.12}$$

An independent variable is the optical thickness $\tau$, read off from the point with a temperature of $T_1$ towards the front. At the wavefront, $\tau = \tau_f$. The radiation fluxes $F_a$ and $F_b$ are determined by the formulas:

$$F_a = \frac{2}{\sqrt{3}} \left( e^{\sqrt{3}\tau} - \frac{2 - \sqrt{3}}{2 + \sqrt{3}} e^{-\sqrt{3}\tau} \right) \left\{ b_* - b_0 - \left( \tau_f + \frac{1}{\sqrt{3}} \right) b_1 \right\} e^{-\sqrt{3}\tau_f} + \\ + \frac{4}{2 + \sqrt{3}} e^{-\sqrt{3}\tau} b_0 + \frac{4}{3} b_1 \left( 1 - \frac{2}{2 + \sqrt{3}} e^{-\sqrt{3}\tau} \right), \tag{8.13}$$

$$F_b = \frac{2}{\sqrt{3}} e^{-\sqrt{3}\tau} \left[ \frac{2\sqrt{3}}{2 + \sqrt{3}} \left( b_0 - \frac{2}{3} b_1 \right) + (b_* - b_0 - \tau_f b_1) \times \right. \\ \left. \times \left( e^{\sqrt{3}\tau_f} - \frac{2 - \sqrt{3}}{2 + \sqrt{3}} e^{-\sqrt{3}\tau_f} \right) + \frac{b_1}{\sqrt{3}} \left( e^{\sqrt{3}\tau_f} + \frac{2 - \sqrt{3}}{2 + \sqrt{3}} e^{-\sqrt{3}\tau_f} \right) \right]. \tag{8.14}$$

In these formulas the value $\tau_f$ is a parameter, and the coefficients $b_0$, $b_1$ and $b_*$ have the following sense:

$$b_0 = \sigma T_1^4; \quad b_1 = \frac{\sigma}{\tau_f} (T_-^4 - T_1^4); \quad b_* = \sigma T_*^4. \tag{8.15}$$

The temperatures $T_-$ and $T_+$ are found from (8.11) and (8.12), if we assume in them that $F_a = F_b = F_f$. Then

$$T_+ - T_- = (T_2 - T_1) - 2\eta_2 (T_- - T_1) = (T_*^{\cdot} - T_-) + \\ + (1 - 2\eta_2)(T_- - T_1) + \frac{2F_1}{\rho_1 v_1 R} \frac{\eta_2 (1 - 2\eta_2)}{1 - \eta_2}. \tag{8.16}$$

The qualitative pattern of temperature change in the function of optical thickness $\tau$ is represented in Figure 12 for two cases: $F_1 = 0$ and $F_1 > 0$.

For us these solutions are of interest because two processes that appear to be completely different exert qualitatively a completely identical influence on the thermodynamic functions behind the front of the shock wave (temperature, density, pressure). Actually, expressions (7.20) and (8.10) will be identical if in (8.10) $|F_1/\rho_1 v_1|$ is replaced by Q (the specific energy of ionization), and equation (7.17) is used. The same refers to formulas (7.18)–(7.19) for pressure, density, and steam velocity.

It is readily apparent that this is true in that both processes may be regarded as an energy sink. Therefore, the qualitative pattern of temperature distribution within a shock wave in the presence of radiation and ionization may be represented analogously to the pattern for Case II (with deexcitation).

At high altitudes it is also possible to encounter a case where both ionization and deexcitation will take place. In this case, formula (8.2) will take the form:

$$\varepsilon_{\text{forw}} + \frac{p}{\rho} + \frac{v^2}{2} - \left| \frac{F}{\rho v} \right| + \left[ \left| \frac{F_1}{\rho_1 v_1} \right| + Q \right] = \frac{v_1^2}{2}. \tag{8.17}$$

It would be tempting to use the solution of Kogure-Osaki for calculating the temperature distribution in a shock wave with simultaneous consideration of ionization and radiation. This is, however, difficult in practice for two reasons. First, in this solution, as in the solution of Yu. P. Rayzer, it is assumed that $\gamma = \text{const}$, although for various conditions of the problem the values of $\gamma$ are taken in accordance with the condition (7.12). Second, for each point it is necessary to know the value Q and, consequently, the degree of ionization x. It is, however, possible to determine the latter in each point of the nonequilibrium zone only by solving the equation system of ionization kinetics. Such a system, the derivation of which will be given in Section 9, cannot be solved analytically because of its complexity. It is solved by numerical methods. As a result, there is found not only the degree of ionization at any point behind the wave front, but also the distribution of the ion and electron temperatures, as well as the value of the equilibrium temperature $T_2$. Examples of such a solution will be given in Section 12.

In solving the equation system of ionization kinetics, however, it is very difficult to take into account the effect of radiation. Therefore, it is unavoidably necessary to proceed according to the method of successive approximations, that is, first to solve the equation system of

ionization kinetics without taking account of radiation, and thereafter, by means of the method of Zel'dovich-Rayzer or that of Kogure-Osaki, to take into account this influence of radiation on temperature distribution.

The question of the effect of shock-wave radiation on this meteorite body will be considered in Section 14.

# CHAPTER 2. DISTRIBUTION OF TEMPERATURE AND IONIZATION IN THE SHOCK WAVE

## Section 9. The Equations of Ionization Kinetics and Energy Exchange

We shall now consider the region of nonequilibrium ionization behind the shock-wave front. Here we first encounter a discontinuity between the ion temperature and the electron temperature, originating directly behind the front. Because of the small mass of electrons in comparison to ions, the electron temperature $T_e$ makes almost no jump at the wave front, and is found to be considerably lower than the ion temperature $T_i$ (Refs. 42, 52). The difference between them gradually diminishes due to the transfer of energy from ions to electrons. The value of the transferred energy (per one ion and electron), according to L. O. Landau (Ref. 53) is equal (in erg · cm$^3$/sec) to:

$$E_{ie} = \frac{2\sqrt{2\pi}z^2e^4L}{m_e^{1/2}}\frac{m_e}{m_i}\frac{k(T_i - T_e)}{(kT_e)^{3/2}}, \tag{9.1}$$

where $m_e$ and $m_i$ is the electron and ion mass; e is the electron charge; z is the ion charge in terms of units of electron charge; k is Boltzmann's constant; L is a logarithmic multiplier, the significance of which will be explained below. Expressions similar to (9.1) have also been used by Petschek and Byron (Ref. 54), who studied the establishment of equilibrium ionization behind strong shock waves in argon, and by Bhatnagar, et al., (Ref. 55) and S. B. Pikel'ner (Ref. 56), who studied the passage of shock waves in the formative stages of plasma.

Denoting the concentration of electrons and ions by $n_e$ and $n_i$, and taking into account that $z = r$ (ionization multiple), and introducing the designation

$$A_1 = \frac{4\sqrt{2\pi}e^4m_e^{1/2}}{3k^{3/2}m_i} = 1{,}35\cdot10^{-4}, \tag{9.2}$$

we obtain the following expression for the rise in electron temperature as a result of energy obtained from ions:

$$\frac{3}{2}kn_e\left(\frac{dT_e}{dt}\right)_1 = \frac{3}{2}kn_eA_1\sum_r n_r r^2\frac{T_i - T_e}{T_e^{3/2}}L. \tag{9.3}$$

Energy obtained from collisions with ions is used by electrons for the further ionization of atoms and ions. The estimate of energy expended on ionization depends on the adoption of one of the following two schemes.

Scheme I. It is assumed that under the influence of electron impact there occurs "stepwise ionization," that is the passage of electrons from the basic level to excited levels, and then ionization from the excited levels. Therefore, the total ionization level is considered to be equal to the potential of ionization from the basic level $I_r$.

Scheme II. It is assumed that a Boltzmann distribution by levels is always in effect when temperature rises, with excitation occurring due to radiation. In this case the ionization energy is considered equal to the binding energy of the $\Delta I_{r,n}$.

As will be shown below, Scheme I does not reflect the actual course of the phenomena, and Scheme II will have to be taken as the basis. However, Scheme I is convenient for calculations, and the transition from it to Scheme II affords no difficulty. Therefore, we shall consider both schemes and shall compare expenditures on ionization in one and in the other.

In Scheme I the energy loss on the r-th ionization, and consequently, the reduction of electron temperature comprise,

$$\frac{3}{2}kn_e\left(\frac{dT_e}{dt}\right)_{2,r} = -n_e n_{r-1}\left(I_r + \frac{3}{2}kT_e\right)Z_r, \tag{9.4}$$

where $I_r$ is the potential, and $Z_r$ is the coefficient of the r-th ionization, i.e., the quantity of acts of ionization for one ion and electron per second. Summing along all stages of ionization, we have for the loss of energy on ionization:

$$\frac{3}{2}kn_e\left(\frac{dT_e}{dt}\right)_2 = -n_e\sum_r n_{r-1}\left(I_r + \frac{3}{2}kT_e\right)Z_r. \tag{9.5}$$

In formulas (9.4) and (9.5), the second parenthesized term expresses the energy communicated to an electron knocked out in the course of ionization (under the assumption of a Maxwell distribution of the velocities of an electron gas).

Let us now consider Scheme II. If we consider the atom levels to be hydrogen-like, i.e., if we assume that $\Delta I_r = I_r/n^2$, where n is the main quantum number, the energy of the r-th ionization from the level of n will be equal to

$$\frac{3}{2}kn_e\left(\frac{dT_e}{dt}\right)_{2,r,n} = -n_e n_{r-1,n} Z_{r,n}\left(\frac{I_r}{n^2} + \frac{3}{2}kT_e\right). \tag{9.6}$$

Summing level by level, with account taken of the Boltzmann distribution, we obtain

$$\frac{3}{2}kn_e\left(\frac{dT_e}{dt}\right)_{2,r} = -n_e n_{r-1}\left[I_r \frac{e^{-u_1}}{U_{r-1}}\sum_n g_n e^{u_n}\frac{Z_{r,n}}{n^2} + \frac{3}{2}kT_e Z_r\right], \tag{9.7}$$

where $g_n$ is a statistical weight; $U_{r-1}$ is the sum with respect to the states of the atom or the $(r-1)$ ion; $u_1 = I_r/kT_e$, $u_n = u_1/n^2$. In the hydrogen-likeness approximation, it may be assumed that $g_n/U_{r-1} = n^2$.

Let us simplify formula (9.7) by substituting in it the expression for the ionization coefficient $Z_{r,n}$ obtained in Ref. 64 (see below, Section 10):

$$Z_{r,n} = A_2 T_e^{-1/2} n \,\mathrm{Ei}_1(u_n), \tag{9.8}$$

where $A_2 = 1.1 \cdot 10^{-5}$. The summation in formula (9.7) may be replaced by integration along n from 0 to some limit level, $n_0$, determined by reduction of the ionization potential due to Coulomb interactions (Refs. 64, 69). Then the first parenthesized term in (9.7) will be equal to

$$\begin{aligned} K_1 &= A_2 T_e^{-1/2} I_r e^{-u_1}\int_0^{n_0} n e^{u_n}\,\mathrm{Ei}_1(u_n)\,dn = \\ &= A_2 T_e^{-1/2} I_r e^{-u_1}\frac{u_1}{2}\int_{u_0}^{\infty}\frac{e^{u_n}}{u_n^2}\,\mathrm{Ei}_1(u_n)\,du_n, \end{aligned} \tag{9.9}$$

where it is designated that

$$u_0 = \frac{I_r}{kT_e n_0^2} = \frac{u_1}{n_0^2};\quad \mathrm{Ei}_1(u_n) = \int_{u_n}^{\infty} e^{-u}\frac{du}{u}. \tag{9.10}$$

The integral

$$J(u_0) = \int_{u_0}^{\infty}\frac{e^{u_n}}{u_n^2}\,\mathrm{Ei}_1(u_n)\,du_n \tag{9.11}$$

is computed numerically, or graphically. In the interval $10^{-2} < u_0 < 5$, it may be approximated by the expression

$$\log J(u_0) = -0.11(\log u_0)^2 - 1.71 \log u_0 - 0.475. \tag{9.12}$$

The energy expenditure on the r-th ionization will now be equal to

$$\frac{3}{2} k n_e \left(\frac{dT_e}{dt}\right)_{2,\,r} = - n_e n_{r-1} \left[ A_2 T_e^{-1/2} I_r e^{-u_1} \frac{u_1}{2} J(u_0) + \frac{3}{2} k T_e Z_r \right], \tag{9.13}$$

and the total energy expenditure on ionization is obtained by the summation of (9.13)[1] along the stages of ionization r.

In order to compare the energy expenditure on ionization in both schemes, we form the ratio $K_1/I_r Z_r$. In doing so, we take into account the fact that, according to Ref. 64,

$$Z_r = \frac{A_2}{5} T_e^{-1/2} e^{-u_1} \frac{u_1^2}{u_0^{2.5}}. \tag{9.14}$$

Then

$$\frac{K_1}{I_r Z_r} = 2.5 \frac{u_0^{2.5}}{u_1} J(u_0). \tag{9.15}$$

Hence, the ratio of the energies expressed by formulas (9.13) and (9.4) is equal to

$$\tilde{E} = \frac{E_{II}}{E_I} = \frac{1 + \frac{5}{3} u_0^{2.5} J(u_0)}{1 + \frac{2}{3} u_1}. \tag{9.16}$$

For convenience in making calculations according to Scheme II, it is necessary that it be possible to calculate the numerator in formula (9.16).

Therefore, in Table 10 are shown the values of $J(u_0)$, of $u_0^{2.5}$, and of their products. Obviously, the energy expenditures in the two schemes would be equal with fulfillment of the following condition

$$u_0^{2.5} J(u_0) = \frac{2}{3} u_1. \tag{9.17}$$

But since usually $u_1 > 1$ and even $u_1 > 2.5$, the condition (9.17) is never fulfilled, and $E_{II} < E_I$ and $\tilde{E} < 1$ will always be the case (Figure 14). This is also clear from the general considerations,

[1] As will be seen in Section 10, for complex atoms when summing $Z_{r,n}$ within the limits of the Boltzmann distribution, the sum should be multiplied by the multiplier $\Gamma_r$, which takes multiplicity into account.

Table 10

| $u_0$ | $u_0^{2.5}$ | $J(u_0)$ | $u_0^{2.5}J(u_0)$ | $u_0$ | $u_0^{2.5}$ | $J(u_0)$ | $u_0^{2.5}J(u_0)$ |
|---|---|---|---|---|---|---|---|
| 0,010 | $1.00\cdot10^{-5}$ | 321,0 | $3.21\cdot10^{-3}$ | 0,30 | $4,94\cdot10^{-2}$ | 2,562 | $1,27\cdot10^{-1}$ |
| 0,015 | $2,76\cdot10^{-5}$ | 187,0 | $5,16\cdot10^{-3}$ | 0,40 | $1,01\cdot10^{-1}$ | 1,616 | $1,63\cdot10^{-1}$ |
| 0.020 | $5.66\cdot10^{-5}$ | 128,5 | $7.27\cdot10^{-3}$ | 0,50 | $1,77\cdot10^{-1}$ | 1;125 | $1,99\cdot10^{-1}$ |
| 0,025 | $9,87\cdot10^{-5}$ | 95,4 | $9,41\cdot10^{-3}$ | 0,60 | $2,79\cdot10^{-1}$ | $8.28\cdot10^{-1}$ | $2,31\cdot10^{-1}$ |
| 0,030 | $1.56\cdot10^{-4}$ | 74,4 | $1,16\cdot10^{-2}$ | 0,70 | $4,11\cdot10^{-1}$ | $6.42\cdot10^{-1}$ | $2,64\cdot10^{-1}$ |
| 0,04 | $3,20\cdot10^{-4}$ | 50,00 | $1.60\cdot10^{-2}$ | 0,80 | $5,73\cdot10^{-1}$ | $5,00\cdot10^{-1}$ | $2.86\cdot10^{-1}$ |
| 0,05 | $5,60\cdot10^{-4}$ | 36,75 | $2,06\cdot10^{-2}$ | 0,90 | $7,70\cdot10^{-1}$ | $4.08\cdot10^{-1}$ | $3,14\cdot10^{-1}$ |
| 0.06 | $8,83\cdot10^{-4}$ | 28,35 | $2,50\cdot10^{-2}$ | 1,00 | 1,00 | $3.38\cdot10^{-1}$ | $3.38\cdot10^{-1}$ |
| 0,07 | $1,30\cdot10^{-3}$ | 22.69 | $2,95\cdot10^{-2}$ | 1,5 | 2,76 | $1,68\cdot10^{-1}$ | $4,64\cdot10^{-1}$ |
| 0,08 | $1,81\cdot10^{-3}$ | 18,67 | $3,38\cdot10^{-2}$ | 2,0 | 5,66 | $9.88\cdot10^{-2}$ | $5,59\cdot10^{-1}$ |
| 0,09 | $2,43\cdot10^{-3}$ | 15,69 | $3,82\cdot10^{-2}$ | 2,5 | 9,87 | $6,53\cdot10^{-2}$ | $6,44\cdot10^{-1}$ |
| 0,10 | $3.16\cdot10^{-3}$ | 13,40 | $4,24\cdot10^{-2}$ | 3.0 | 15,6 | $4,72\cdot10^{-2}$ | $7,36\cdot10^{-1}$ |
| 0,15 | $8,74\cdot10^{-3}$ | 7,50 | $6.55\cdot10^{-2}$ | 4,0 | 32.0 | $2,70\cdot10^{-2}$ | $8,64\cdot10^{-1}$ |
| 0.20 | $1,79\cdot10^{-2}$ | 4,857 | $8,70\cdot10^{-2}$ | 5.0 | 56.0 | $1,78\cdot10^{-2}$ | $9,97\cdot10^{-1}$ |

since the binding energy of the excited levels is always less than that of the basic level; therefore, the energy expenditure on ionization in Scheme II will be less.

In addition to ionization, there will take place in a gas the process of recombination with triple collisions, in the course of which an electron recombines with an ion, giving part of the energy to the third particle, which will almost always be another electron. As a result of recombination by triple collisions, the energy of an electron gas will receive an increment equal to

$$\frac{3}{2}kn_e\left(\frac{dT_e}{dt}\right)_s = n_e\sum_r n_r\left[\frac{3}{2}kT_eC_r^{(3)} + I_r\sum_n C_{r,n}^{(3)}\frac{1}{n^2}\right], \tag{9.18}$$

where $C_{r,n}^{(3)}$ is the coefficient of triple recombination of an electron to the n-th level of an ion of the r-th multiplicity, and $C_r^{(3)}$ is the coefficient of recombination to all levels. The parenthesized expression in formula (9.18) is obtained in the following manner. In recombination to the n-th level, the following energy is released:

$$\frac{3}{2}kn_e\left(\frac{dT_e}{dt}\right)_{3,r,n} = n_en_rC_{r,n}^{(3)}\left(\Delta I_{r,n} + \frac{3}{2}kT_e\right), \tag{9.19}$$

where $\Delta I_{r,n} = I_r - I_{r,n}$ is the binding energy of level n. Summing within the limits of n and r, we obtain

$$\frac{3}{2}kn_e\left(\frac{dT_e}{dt}\right)_3 = n_e\sum_r n_r\left[C_r^{(3)}\left(I_r + \frac{3}{2}kT_e\right) - \sum_n C_{r,n}^{(3)}I_{r,n}\right]. \tag{9.20}$$

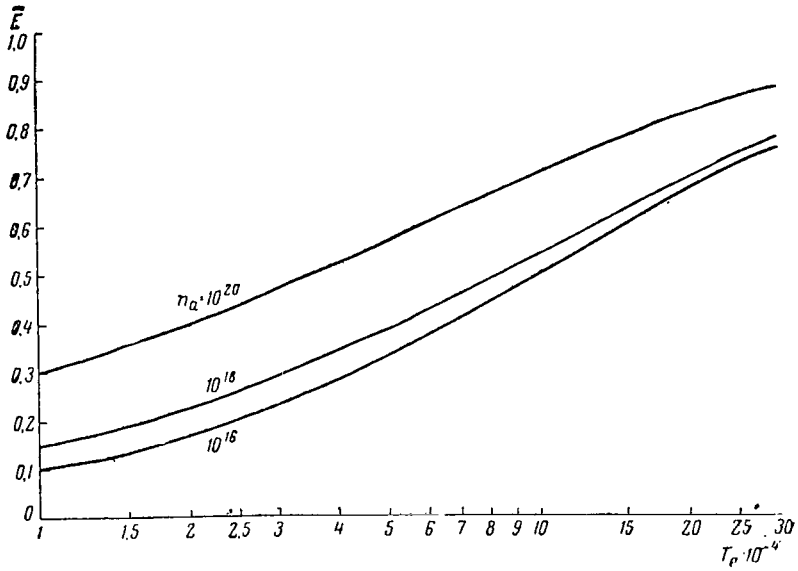


Figure 14. Ratio of ionization energies $\tilde{E} = E_{II}/E_I$.

Formula (9.20) may be simplified, adopting the approximation of hydrogen-likeness, i.e., assuming $\Delta I_{r,n} = I_r/n^2$. Substituting this expression for $\Delta I_{r,n}$ into formula (9.19) and summing, we obtain formula (9.18).

The expressions for the coefficients $C^{(3)}_{r,n}$ and $C^{(3)}_r$ will be presented in Section 10.

On the basis of formulas (9.3), (9.13) and (9.18), we write the equation for the overall balance of electron energy in Scheme II):

$$\frac{3}{2} k n_e \frac{dT_e}{dt} = n_e n_i E_{ie} - n_e \sum_r n_{r-1} \left[ \frac{A_2}{2} \Gamma_r k T_e^{1/2} u_1^2 e^{-u_1} J(u_0) + \right.$$
$$\left. + \frac{3}{2} k T_e Z_r \right] + n_e \sum_r n_r \left[ \frac{3}{2} k T_e C_r^{(3)} + I_r \sum_n C^{(3)}_{r,n} \frac{1}{n^2} \right]. \tag{9.21}$$

For the change of the ion temperature (and ion energy), we shall have the more simple expression:

$$\frac{3}{2} k n_a \frac{dT_i}{dt} = - n_e n_i E_{ie}, \tag{9.22}$$

where $n_a$ is the total number of neutral atoms and ions (their temperatures may be considered equal because of the rapid establishment of thermodynamic equilibrium among them).

The change in electron concentration $n_e$ as a result of the processes of ionization and recombination will be expressed by the formula:

$$\frac{dn_e}{dt} = n_e \sum_r n_{r-1} Z_r - n_e \sum_r n_r C_r, \tag{9.23}$$

where $C_r$ is the coefficient of recombination from the r-th state, including, in distinction from $C_r^{(3)}$, all forms of recombination. The change of concentration $n_r$ of ions that are in the r-th state is, generally speaking, determined by the following four processes (Figure 15):

process I – ionization to the r + 1-th state,
process II – ionization from the r – 1-th state into the r-th state,
process III – recombination from the r + 1-th state into the r-th state,
process IV – recombination from the r-th state into the r – 1-th state.

Processes III and IV are inverse in nature to processes I and II. Obviously, processes II and III bring about an increase in $n_r$, while processes I and II bring about its diminution. Thus,

$$\begin{aligned}\frac{dn_r}{dt} = &- n_e n_r Z_{r+1} + n_e n_{r-1} Z_r + \\ &+ n_e^2 n_{r+1} C_{r+1} - n_e n_r C_r.\end{aligned} \tag{9.24}$$

For convenience in subsequent calculations, we introduce the degree of ionization $x = n_e/n_a$ and the specific ion concentrations $y_r = n_r/n_a$. We divide the two parts of formula (9.21) by $n_a n_e$, and those of formulas (9.22), (9.23) and (9.24), by $n_a^2$. We also introduce the designations:

$$\Phi_r = \frac{A_2}{3} \Gamma_r T_e^{1/2} u_1^2 e^{-u_1} J(u_0) + T_e Z_r, \tag{9.25}$$

$$\Psi_r = T_e C_r^{(3)} + \frac{2I_r}{3k} \sum_n C_{r,n}^{(3)} \frac{1}{n^2}. \tag{9.26}$$

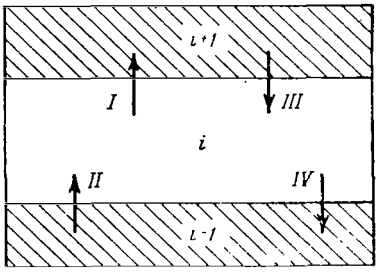


Figure 15. The processes of ionization and recombination.

Also taking into account that the value z (the relative ion charge) entering into formula (9.1) is identically equal to r (ionization multiple), we obtain the final system of equations

$$\left.\begin{aligned}
\frac{dT_e}{n_a\,dt} &= A_1 \sum_r y_r r^2 \frac{T_i - T_e}{T_e^{3/2}} L - \sum_r y_{r-1}\Phi_r + \sum_r y_r \Psi_r,\\
\frac{dT_i}{n_a\,dt} &= -A_1 x \sum_r y_r r^2 \frac{T_i - T_e}{T_e^{3/2}} L,\\
\frac{dx}{n_a\,dt} &= x\sum_r y_{r-1} Z_r - x\sum_r y_r C_r,\\
\frac{dy_r}{n_a\,dt} &= -xy_r Z_{r+1} + xy_{r-1}Z_r + xy_{r+1}C_{r+1} - xy_r C_r.
\end{aligned}\right\} \qquad (9.27)$$

In all the formulas cited above, summation within the limits of r must be understood in the following sense:

$$\sum_r y_r = \sum_{r=1}^{5} y_r + 0.22 y_6, \qquad (9.28)$$

which indicates summation from the first to the fifth ionization for air on the whole, and to the sixth ionization for oxygen alone. In practice, ions with two, or at most three, multiples of ionization will be simultaneously present in ionized gas, but for the sake of generality system (9.27) should be regarded as a system of 10 conventional differential equations with 10 unknowns: $T_e$, $T_i$, $x$, $y_0$, $y_1, \ldots y_6$ (by $y_0$ we designate the specific concentration of neutral atoms). Obviously $\sum_r n_r = n_a$ and $\sum_r y_r = 1$. The form of equations (9.27) is convenient in that the concentration of initial atoms $n_a$ determines only the time scale and does not enter directly into the right-hand parts of the equations. However, unfortunately, more detailed analysis (see Section 10) shows that the electronic concentration $n_e$ enters into the calculations in a complex manner[1] in terms of the coefficients $Z_r$, $C_r$ and the value L. Therefore, for a given shock-wave amplitude it is impossible to make only one calculation, as has been done by S. B. Pikel'ner (Ref. 56); rather it is necessary to carry out a series of calculations for various instances of $n_e$.

Let us now consider the sense of the logarithmic multiplier L. Most authors (Refs. 53, 56–58) cite it in the form of

$$L = 2\ln\Lambda, \qquad (9.29)$$

where

[1]This follows, in particular, from formula (9.30), as well as from the formulas of Section 10; in that Section it will be shown that the electron concentration influences the course of ionization due to reduction of the ionization potential.

$$\Lambda = \frac{3kT_e^{3/2}}{2\sqrt{\pi n_e^{1/2} e^3 z_1 z_2}}, \tag{9.30}$$

$z_1$ and $z_2$ being the charges of electrons and ions (in units of proton charge). The value of $\Lambda$ has been tabulated by Spitzer (Ref. 57); however, for large instances of $n_e$ and small instances of $T_e$, the values of $\Lambda$ are not given, since the theory of the diffusion of particles in ionized gas developed by Spitzer then becomes inconsistent. Since the values of $\Lambda$ absent in Ref. 57 are in the region of densities and temperatures that is of interest to us, we shall try to introduce some refinements into this theory.

From the general theory of the diffusion of charged particles in ionized gas (Refs. 57, 58), it follows that

$$L = 2\int_0^{p_m/p_0} \frac{x\,dx}{1+x^2}, \tag{9.31}$$

where $p_0$ is the parameter of particle collision corresponding to deflection of the lighter particle by 90°; $p_m$ is the "cutoff parameter," equal to the distance at which close interaction of the particles ceases. As has been shown by Cohen, Spitzer and Routly (Ref. 59), this distance in most cases exceeds the mean distance between particles $n_i^{-1/3}$, and may be taken as equal to the Debye radius $h_D$, where

$$h_D = \left[\frac{kT_e}{4\pi e^2 (n_e + \sum n_r r^2)}\right]^{1/2}. \tag{9.32}$$

Designating that $\Lambda = p_m/p_0$, we obtain

$$L = \ln(1 + \Lambda^2). \tag{9.33}$$

Since usually $\Lambda \gg 1$, it is from this that formula (9.29) is obtained. However, in the first place, at large instances of $n_e$ and small instances of $T_e$, the value of $\Lambda$ increases rapidly, and unity may not be disregarded in formula (9.33). In the second place, in this case the Debye radius diminishes and, finally, when the condition,

$$\lambda = \frac{n_i^{-1/3}}{h_D} = 0.145\, n_i^{-1/3} T_e^{-1/2} \left(n_e + \sum n_r r^2\right)^{1/2} > 1 \tag{9.34}$$

is observed, the Debye radius becomes less than the mean distance between particles, and, therefore, may not be taken for the "cutoff parameter." We shall, in this connection, stipulate to take $h_D$ as the "cutoff parameter" when $\lambda < 1$, and $n_i^{-1/3}$ when $\lambda > 1$. The values of L determined in

Table 11
Values of L

| $T_e$ | $n_e$ | | | | | | | | | |
|---|---|---|---|---|---|---|---|---|---|---|
| | $10^{12}$ | $10^{13}$ | $10^{14}$ | $10^{15}$ | $10^{16}$ | $10^{17}$ | $10^{18}$ | $10^{19}$ | $10^{20}$ | $10^{21}$ |
| $1\cdot10^4$ | 18,86 | 16.55 | 14.25 | 11,94 | 9,64 | 7,34 | 5.78 | 4,26 | 2,78 | 1.45 |
| $2\cdot10^4$ | 20.88 | 18.59 | 16.30 | 14,02 | 11,74 | 9,42 | 7,16 | 5.62 | 4.12 | 2.16 |
| $3\cdot10^4$ | 22,07 | 19.80 | 17.53 | 15.27 | 13,01 | 10.75 | 8.33 | 6.45 | 4,93 | 3.42 |
| $4\cdot10^4$ | 22,90 | 20,63 | 18.36 | 16,09 | 13.82 | 11.55 | 9.19 | 7,00 | 5,48 | 3,97 |
| $5\cdot10^4$ | 23.57 | 21,31 | 19.05 | 16,78 | 14.51 | 12.24 | 9.97 | 7.57 | 5.93 | 4.42 |
| $6\cdot10^4$ | 24,11 | 21,85 | 19.59 | 17,33 | 15.07 | 12,81 | 10,55 | 8.12 | 6.30 | 4.77 |
| $7\cdot10^4$ | 24,56 | 22,30 | 20,04 | 17.78 | 15.52 | 13,26 | 11,00 | 8,57 | 6.59 | 5,08 |
| $8\cdot10^4$ | 24,96 | 22,71 | 20,46 | 18.20 | 15.94 | 12,68 | 11,42 | 8.97 | 6,88 | 5,34 |
| $9\cdot10^4$ | 25,30 | 23,05 | 20,80 | 18,54 | 16,28 | 14,02 | 11.76 | 9,33 | 7,12 | 5,59 |
| $1\cdot10^5$ | 26,60 | 23.35 | 21,10 | 18,86 | 16,55 | 14.25 | 11,94 | 9.64 | 7,32 | 5,80 |
| $1.5\cdot10^5$ | 26,76 | 24,52 | 22.28 | 20,05 | 17.76 | 15.48 | 13,16 | 10,90 | 8,55 | 6,61 |
| $2\cdot10^5$ | 27,55 | 25.33 | 23,11 | 20.88 | 18,59 | 16.30 | 14,02 | 11,74 | 9.42 | 7.20 |
| $2,5\cdot10^5$ | 28.16 | 25,96 | 23.76 | 21,56 | 19.27 | 16.99 | 14,71 | 12.44 | 10.09 | 7,78 |
| $3\cdot10^5$ | 28,60 | 26,42 | 24.24 | 22.07 | 19,80 | 17.53 | 15.27 | 13,01 | 10,75 | 8,33 |

this manner are shown in Table 11. From this table it follows that for hot air, L has an order of 10, and for the range of $n_e = 10^{16}$–$10^{20}$ and $T_e = (1–30) \cdot 10^4$, the value of L is contained within the fairly narrow limits of L = 3–20.

## Section 10. Coefficients of Ionization and Recombination

In order to calculate the processes of ionization and recombination behind the wave front in hot air that is in a state of plasma, it is necessary to know the coefficients of ionization $Z_r$, and the coefficients of recombination $C_r$. In order to obtain these coefficients, it is necessary to evaluate the comparative role of the various elementary processes; in contemporary scientific literature this is by no means done unambiguously.

The basic mechanism of ionization in hot air is electron impact (Ref. 42). The general expression for the coefficient of ionization by electron impact, as cited in astrophysics courses (Refs. 60, 61), has the form

$$Z_{r,n} = 4\pi \left(\frac{m_e}{2\pi k T_e}\right)^{3/2} \int_{v_0}^{\infty} \sigma_{r,n}(v)\, e^{-\frac{m_e v^2}{2kT_e}}\, dv. \tag{10.1}$$

Here v is the velocity of the striking electron; $v_0$ is the minimum velocity leading to ionization; and $\sigma_{r,n}(v)$ is the effective cross section of the r-th ionization from the n-th level at a velocity of

v. It is usually assumed here that ionization takes place mainly from the basic level, since the population of excited levels is infinitesimal in the case of a Boltzmann distribution.

In calculating the passage of a shock wave in the formative stages of plasma, S. B. Pikel'ner (Ref. 56) found that in this case the energy expanded on electron excitation is two orders greater than energy going for ionization. Such a relationship must actually occur for rarefied formative stages of plasma, where the energy expanded on electron excitation passes into radiation, i.e., when deexcitation occurs. In hot air an entirely different pattern will take place. At high temperatures air is almost opaque to radiation, in other words, the energy of electron excitation passing into radiation will again excite another atom or ion, an equilibrium (Boltzmann) distribution will be established in the gas with respect to the levels, and there will be little deexcitation. Therefore, in our case it is not necessary to take into account the expenditure of energy on excitation (without subsequent ionization).

We find the coefficient of ionization $Z_{r,1}$ from the basic level. In computing the integral entering into expression (10.1), it is customary (Refs. 60, 61) to use the concept of the mean effective cross section of ionization $\overline{\sigma}_{r,v}$, carrying it out beyond the integral sign. Then

$$Z_{r,1} = 2\sqrt{\frac{2}{\pi}}\,\overline{\sigma}_{r,v}\left(\frac{kT_e}{m_e}\right)^{1/2} e^{-\frac{I_r}{kT_e}}\left(1+\frac{I_r}{kT_e}\right). \tag{10.2}$$

Here it is taken into account that $I_r = M_e v_0^2/2$. However, the value $\sigma_{r,v}$ depends on the temperature $T_e$, and on the ionization potential $I_r$, i.e., on $v_0$. Therefore, it is convenient, as has been done in Ref. 56, to make use of the circumstance that in the energy range of interest to us, the value $\sigma_{r,v}$ increases linearly in the function $v^2$ (Figure 16). In this case

$$\sigma_{r,v} = \sigma_0 \frac{v^2 - v_0^2}{v_0^2}, \tag{10.3}$$

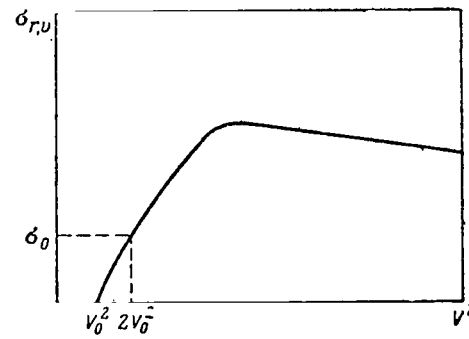


Figure 16. Dependence of the cross section of ionization on electron velocity.

where $\sigma_0$ is the effective cross section of ionization at an energy of $2I_r$, i.e., at a velocity of $v_0\sqrt{2}$. Substituting (10.3) into (10.1) and computing the integral, we find the following expression for the coefficient of ionization:[1]

$$Z_{r,1} = 2\sqrt{\frac{2}{\pi}}\sigma_0\left(\frac{kT_e}{m_e}\right)^{1/2} e^{-I_r/kT_e}\left(1+\frac{2kT_e}{I_r}\right). \tag{10.4}$$

From a comparison of (10.2) and (10.4) it immediately follows that

$$\bar{\sigma}_{r,v} = \sigma_0\frac{1+\frac{2kT_e}{I_r}}{1+\frac{I_r}{kT_e}} = \sigma_0\frac{kT_e}{I_r}\frac{I_r+2kT_e}{I_r+kT_e}. \tag{10.5}$$

Assuming that $\sigma_0 = 8.8\cdot 10^{-17}$ cm$^2$ and substituting the numerical values of the constants into formula (10.4), we reduce it to a form that is convenient for calculations:

$$Z_{r,1} = 5.5\cdot 10^{-11}T_e^{1/2}\left(1+\frac{2kT_e}{I_r}\right)e^{-I_r/kT_e}. \tag{10.4a}$$

The values of the coefficients of ionization from the basic level, computed for air according to formula (10.4a), are shown in Table 12 and in Figure 17.

However, ionization from the basic level far from determines the overall course of ionization. As has been shown in the work of G. S. Ivanov-Kholodnyy, G. M. Nikol'skiy and R. A. Gulyayev (Refs. 62, 63), as well as in that of L. M. Biberman, Yu. N. Toropkin and K. N. Ul'yanov (Refs. 64, 65), the greatest contribution to ionization is made by the upper levels. Actually, despite their low population in comparison to the basic level, the coefficient of ionization from the upper levels increases sharply because of the reduction of the binding energy of the levels.

The ionization coefficient of hydrogen from the level n is equal (Ref. 64) to:

$$Z_n = 1.1\cdot 10^{-5}T^{-1/2}n\,\mathrm{Ei}_1(u_n), \tag{10.6}$$

where $u_n = I_r/kTn^2$, and $\mathrm{Ei}_1(u_n)$ is an integral index function. The course of the product $n\cdot \mathrm{Ei}_1(u_n)$ with the level number n for various values of $u_1 = I_r/kT$ is shown in Figure 18.

---

[1] In Ref. 56 in place of the multiplier $[1 + (2kT_e/I_r)]$ there stands simply $kT_e/I_r$; this is apparently an error. Therefore, the coefficients $Z_r$ there are excessively low by one-half an order of magnitude; this, however, is of little importance to the results of this work because of the predominating role of electron excitation in the formative stages of plasma.

Table 12

Coefficients of Ionization from the Basic Level

| $T_e$ | $Z_1$ | $Z_2$ | $Z_3$ | $Z_4$ | $Z_5$ | $Z_6$ |
|---|---|---|---|---|---|---|
| $1\cdot10^4$ | $3{,}94\cdot10^{-16}$ | — | — | — | — | — |
| $2\cdot10^4$ | $2{.}46\cdot10^{-12}$ | $1{.}90\cdot10^{-16}$ | — | — | — | — |
| $3\cdot10^4$ | $5{,}15\cdot10^{-11}$ | $7{,}57\cdot10^{-14}$ | — | — | — | — |
| $4\cdot10^4$ | $2{,}59\cdot10^{-10}$ | $1{.}91\cdot10^{-12}$ | $8{.}60\cdot10^{-15}$ | — | — | — |
| $5\cdot10^4$ | $7{,}22\cdot10^{-10}$ | $1{.}32\cdot10^{-11}$ | $1{,}72\cdot10^{-13}$ | $2{,}29\cdot10^{-16}$ | — | — |
| $6\cdot10^4$ | $1{.}47\cdot10^{-9}$ | $4{,}47\cdot10^{-11}$ | $1{,}27\cdot10^{-12}$ | $4{,}98\cdot10^{-15}$ | — | — |
| $7\cdot10^4$ | $2{.}54\cdot10^{-9}$ | $1{,}27\cdot10^{-10}$ | $5{,}56\cdot10^{-12}$ | $4{,}61\cdot10^{-14}$ | $9{.}58\cdot10^{-16}$ | — |
| $8\cdot10^4$ | $3{,}85\cdot10^{-9}$ | $2{,}67\cdot10^{-10}$ | $1{.}66\cdot10^{-11}$ | $2{,}47\cdot10^{-13}$ | $8{.}20\cdot10^{-15}$ | — |
| $9\cdot10^4$ | $5{.}50\cdot10^{-9}$ | $4{,}79\cdot10^{-10}$ | $3{.}99\cdot10^{-11}$ | $9{.}34\cdot10^{-13}$ | $4{.}49\cdot10^{-14}$ | — |
| $1\cdot10^5$ | $7{.}38\cdot10^{-9}$ | $7{,}81\cdot10^{-10}$ | $8{,}06\cdot10^{-11}$ | $2{.}71\cdot10^{-12}$ | $1{,}80\cdot10^{-13}$ | $2{.}52\cdot10^{-16}$ |
| $1.5\cdot10^5$ | $1{.}99\cdot10^{-8}$ | $3{,}66\cdot10^{-9}$ | $7{.}26\cdot10^{-10}$ | $7{,}29\cdot10^{-11}$ | $1{.}24\cdot10^{-11}$ | $6{,}25\cdot10^{-13}$ |
| $2\cdot10^5$ | $3{.}67\cdot10^{-8}$ | $8{.}80\cdot10^{-9}$ | $2{.}45\cdot10^{-9}$ | $4{,}03\cdot10^{-10}$ | $1{.}10\cdot10^{-10}$ | $1{.}04\cdot10^{-11}$ |
| $2.5\cdot10^5$ | $5{,}72\cdot10^{-8}$ | $1{,}60\cdot10^{-8}$ | $5{.}31\cdot10^{-9}$ | $1{.}19\cdot10^{-9}$ | $3{.}62\cdot10^{-10}$ | $6{,}29\cdot10^{-11}$ |
| $3\cdot10^5$ | $8{.}00\cdot10^{-8}$ | $2{,}48\cdot10^{-8}$ | $9{.}37\cdot10^{-9}$ | $2{.}55\cdot10^{-9}$ | $1{.}16\cdot10^{-9}$ | $2{.}08\cdot10^{-10}$ |

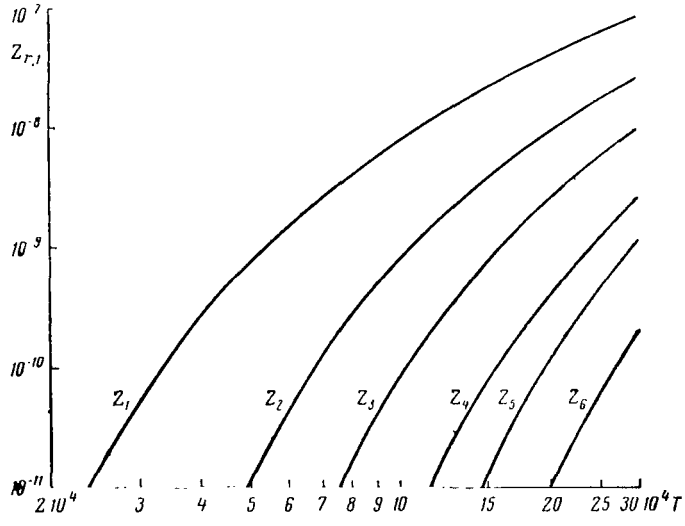


Figure 17. Coefficients of ionization from the basic level.

In order to determine the overall ionization coefficient of hydrogen (from all levels), $Z_n$ is summed taking account of the Boltzmann distribution level by level:

$$Z = \frac{e^{-u_1}}{U} \sum_n g_n e^{u_n} Z_n, \tag{10.7}$$

where $g_n$ are statistical weights, and U is the sum, by states, of the given atom or ion. The sum (10.7) diverges if we do not take into consideration the distribution by levels from the Boltzmann,

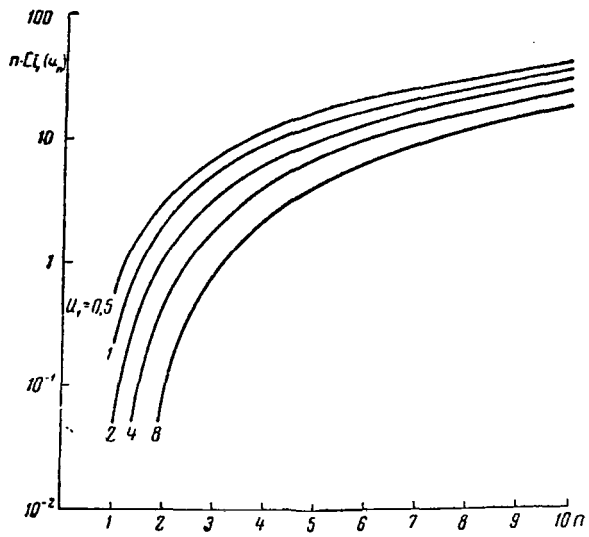


Figure 18. The product $n \cdot Ei_1(u_n)$.

which is the consequence of reciprocal ion perturbation (Coulomb interaction). This phenomenon has been considered in the classical Thompson approximation by G. S. Ivanov-Kholodnyy, et al. (Ref. 62), and in the Bethe-Born approximation by L. M. Biberman, Yu. N. Toropkin and K. N. Ul'yanov (Ref. 64). The qualitative results of the two works coincide, and are reduced to the fact that levels above some $n_0$ in an actual gas are not realized. However, the evaluation of $n_0$ for hydrogen in Ref. 62 is somewhat too low (i.e., the effect of charge exchange is exaggerated), as is shown by comparison with experimental data (Ref. 64).

For evaluating $n_0$ in Ref. 62, there is proposed the formula (close to the analogous formula of Wiesold):

$$\log(n_0 + 1) = \frac{1}{6}(21.65 - \log n_e), \tag{10.8}$$

where $n_e$ is the electronic concentration. For various forms of plasma in Ref. 62, the following values of $n_0$ are found, to which we have added the values for hot air (Table 13):

Table 13

| Form of plasma | $n_e$ | $T$ | $n_0$ |
|---|---|---|---|
| Formative stages of plasma..... | $10^4$ | $10^4$ | 870 |
| Ionosphere ..... | $10^6$ | $10^3$ | 420 |
| Solar corona..... | $10^8$ | $10^6$ | 190 |
| Chromosphere..... | $10^{11}$ | $5 \cdot 10^3$ | 58 |
| Prominences..... | $10^{12}$ | $7.5 \cdot 10^3$ | 40 |
| Hot air..... | $10^{16}$ | $10^5$ | 8—10 |
| Hot air..... | $10^{20}$ | $10^5$ | 1—2 |

It can be seen that in hot air there can actually be effectuated a comparatively small number of levels. On the one hand, this circumstance facilitates summation and makes it possible to proceed entirely without integrating formula (10.7) along the upper levels, as is usually done. However, a small number of levels involves exacting requirements for a correct evaluation of $n_0$.

L. M. Biberman, Yu. N. Toropkin and K. N. Ul'yanov (Ref. 64) have obtained, as a result of the integration of formula (10.6) within the limits of the Boltzmann distribution ($0 < n < n_0$), the following approximate expression for $Z_r$ in the range of $0.01 < u_0 < 5$, where $u_0$ is determined by formula (9.10):

$$Z_r = 2{,}2 \cdot 10^{-6}\, T^{-1/2} e^{-u_1} \frac{u_1^2}{u_0^{2,5}}, \tag{10.9}$$

which may be reduced to the form

$$Z_r = 2.2 \cdot 10^{-6}\, T^{-1/2} e^{-I_r/kT} \left(\frac{I_r}{kT}\right)^{-1/2} n_0^5. \tag{10.10}$$

In the astrophysical examples collected in Table 13, an error of 2–3 units in the evaluation of $n_0$ will have little effect upon the result, since $n_0$ is large. In our example, however, when $n_0$ is small, an error even of one unit will bring about a change of $Z_r$ by an entire order of magnitude, since $n_0$ enters into the formula in the fifth power. At the same time, in an actual gas the $n_0$ levels of all the atoms of the gas will never be effectuated simultaneously. These will be in effect some statistical distribution of the atoms with respect to $n_0$, and, generally speaking, the effective value of $n_0$ will be expressed by a fraction.

In order to determine $n_0$ we use the expression for reducing the ionization potential cited by Brunner (Ref. 66):

$$\Delta E_i \doteqdot 0.121 \left(\frac{n_e}{10^{16}}\right)^{1/3} + 0.025 \left(\frac{n_e}{T_e \cdot 10^{12}}\right)^{1/3}. \tag{10.11}$$

The first term expresses the reduction of the binding energy, and the second term expresses the polarization effects originating with the movement of charges with a variable mean distance. An analogous expression with somewhat difficult coefficients is given by Eckert and Weizel (Ref. 67), but we shall use Brunner's formula, since it is based on newer data.

Further, in accordance with Ref. 65, it may be assumed that

$$n_0 = \sqrt{\frac{I_r}{\Delta E_i}}. \tag{10.12}$$

It is this expression that gives us the value of $n_0$.

Let us now consider the phenomenon of recombination. This phenomenon can proceed along two courses, with the release of a radiation quantum and as a result of triple collisions, in which case the third particle to which the energy surplus is transmitted will almost always be an electron.

As a coefficient of recombination with radiation, in the hydrogen-like approximation it is possible to use Menzel's well-known formula (Ref. 57):[1]

$$C_r' = 2zA_r \left(\frac{2kT_e}{\pi m_e}\right)^{1/2} u_1 \varphi(u_1), \tag{10.13}$$

where z is the ion charge (in terms of units of proton charge); $A_r$ is the capture constant, equal to

$$A_r = \frac{16}{3\sqrt{3}} \frac{he^2}{m_e^2 c^3} = 2.11 \cdot 10^{-22} \text{ cm};$$

$\phi(u_1)$ is a function tabulated by Spitzer (Ref. 57), and equal[2] to

$$\varphi(u_1) = \sum_{n=1}^{\infty} \frac{u_1}{n^3} e^{u_n} \mathrm{Ei}_1(u_n). \tag{10.14}$$

The value $\phi(u_1)$ for the required interval $T_e$, is of the order of unity, as can be seen from Figure 19.

The comparative role of the various levels is determined by the temperature. When the temperature rises, the relative quantity of recombinations to the basic level will rise (Ref. 62). Therefore, the restriction of the number of levels, noted above, will have little effect on recombinations with radiation. The values of the recombination coefficients $C_r'$ are shown in Figure 20 in the function $T_e$.

For triple recombination (or for recombination with three collisions), a formula is derived in Ref. 64 that determines the coefficient of recombination to the level n:

$$C_{r,n}^{(3)} = 8.8 \cdot 10^{-21} T^{-2} n^3 e^{u_n} \mathrm{Ei}_1(u_n). \tag{10.15}$$

---

[1] In the work of Seaton (Ref. 68), this formula has a somewhat different form, but is easily reduced to the form of (10.13). However, this formula is applicable only to the isoelectronic hydrogen series.

[2] Spitzer designates $u_1$ by $\beta$, and in place of $u_n$ uses the expression (equal to it), $\beta/n^2$. These designations have been also retained in the article by the present author (Ref. 69).

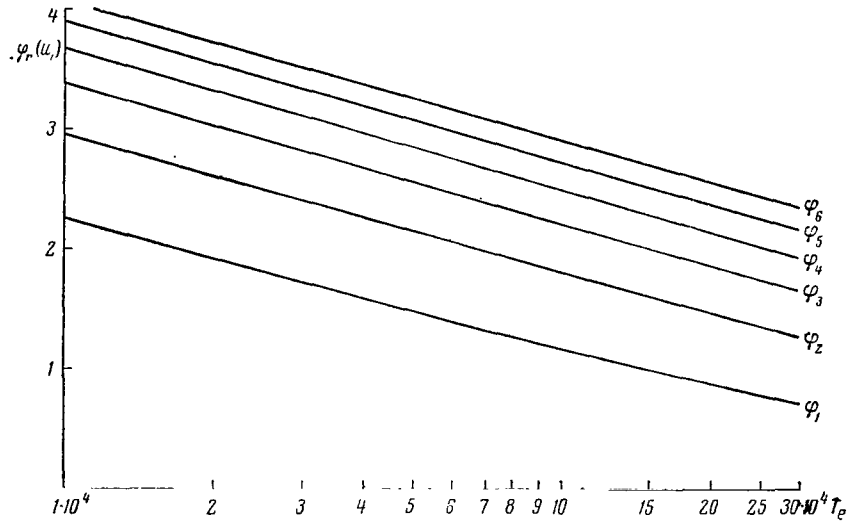


Figure 19. The functions $\phi_r(u_1)$.

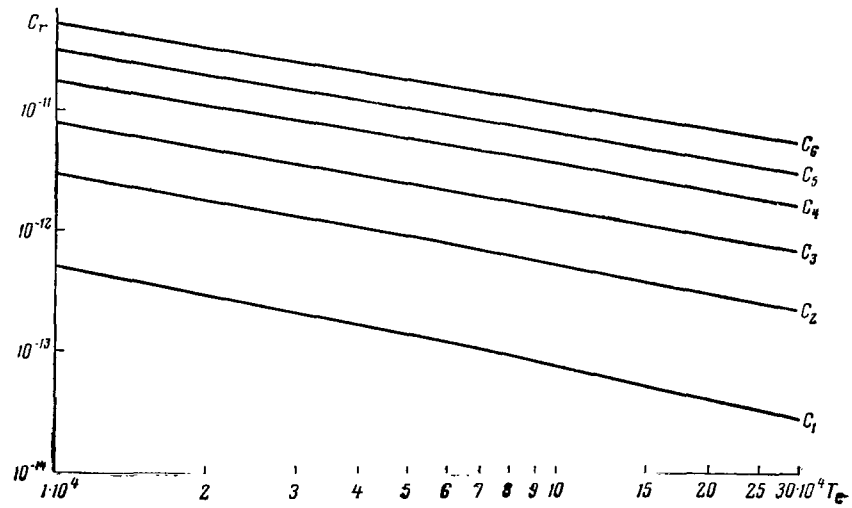


Figure 20. Coefficients of recombination with radiation.

After integrating with respect to the levels, we obtain

$$C_r^{(3)} = 4.15 \cdot 10^{-16} e^{u_1} T^{-3/2} Z_r, \tag{10.16}$$

or, after substituting (10.10) into (10.16),

$$C_r^{(3)} = 9.13 \cdot 10^{-22} T^{-2} \left( \frac{I_r}{kT} \right)^{-1/2} n_0^5. \tag{10.17}$$

It is, however, necessary here to take into account that part of the upper levels is in practice not effectuated because of so-called counter ionization, when the probability of ionization from a given level exceeds the probability of spontaneous transition to lower levels. Therefore, the effective coefficient of triple recombination has the form

$$C_r^{(3)*} = \sum_n \frac{C_{r,n}^{(3)}}{1 + \frac{Z_{r,n} n_e}{A_n}}, \tag{10.18}$$

where $A_n$ is the probability of spontaneous transition from the level n ($A_n = 1.1 \cdot 10^{10} n^{-4.5}\ \text{sec}^{-1}$).

The authors of Ref. 64 propose to introduce summation to some level, $n_1 < n_0$, starting from which the terms in the sum (10.18) diminish sharply, its being possible, from this point, to disregard the 1 in the denominator. The remainder is determined by means of integration from $n_1$ to $n_0$.

For our problem, however, this approach cannot be used, since the number of $n_0$ levels is small (Table 13). Therefore, we shall make use of the concept of an effective boundary level with the quantum number $n_{eff}$, which we shall define as the value which, after substitution into formula (10.17), yields in place of $n_0$ the precise value of $C_r^{(3)*}$ computed by direct summation according to formula (10.18). An example of such summation and determination of $n_{eff}$ is given in Ref. 69.

The influence of counter ionization, which leads to stripping of the upper levels, is particularly strong in the case of large instances of n. The maximum value of $C_{r,n}^{(3)*}$, when $n_e$ increases, passes from the third level to the second, and then to the basic level. The value of $n_{eff}$ when $n_e \geq 10^{20}$ is close to unity, in other words, the "life-time" of the upper levels, is rather low.

In considering the course of the product $C'' = C^{(3)*} n_e$, which determines the coefficient of recombination for one ion and electron, the following pattern is obtained (Figure 21). At not very great concentrations the value C'' grows slowly, since a gradual transition of the maximum number of recombinations from the upper levels downward to the basic level, is taking place. Then begins a rapid growth of C'', since, despite continued weakening of the role of the upper levels, counter ionization from the basic level does not yet have a particular role, and $C^{(3)*}$ remains almost constant with the growth of $n_e$. Finally, with a further increase in $n_e$ the sector of saturation arrives, the cause of which is counter ionization. On the same Figure 21, dotted lines show the course of $n_{eff}$, which tends toward unity. With a reduction of T, $n_{eff}$ increases approximately as $T^{-1/2}$.

The comparative role of recombination with radiation and triple recombination depends on the values of $n_e$, $T_e$ and the ionization multiplicity factor. When $n_e = 10^{20}$, triple recombination with radiation prevails, when $n_e = 10^{16}$, recombination with radiation prevails. With an increase of $T_e$,

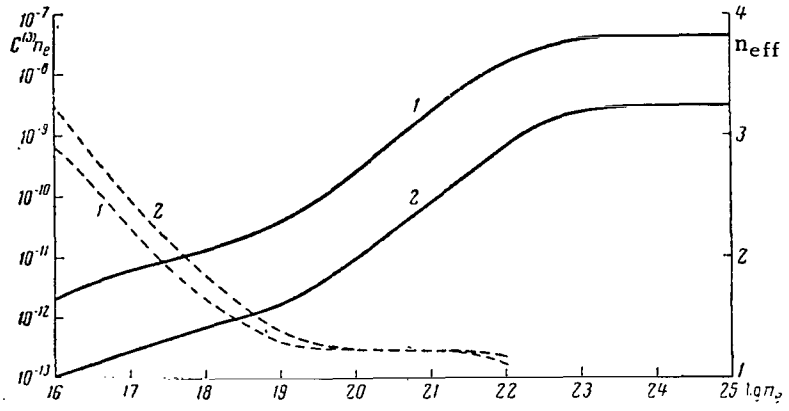


Figure 21. Course of the product $C^{(3)*}n_e$ (solid lines), and of $n_{eff}$ (dotted lines). 1 – hydrogen ($T_e$ = 17,500°); 2 – air ($T_e$ = 100,000°, r = 4)

and with transition to higher ions, the role of the latter increases. The overall coefficient of recombination entering into the equations of Section 9 will be equal to

$$C_r = C_r' + C_r''. \tag{10.19}$$

To now we have considered all of the levels in atoms and ions to be hydrogen-like, although this is actually far from being true. In order to make a more precise computation for complex atoms and ions, it is possible to make use of the concept of the effective quantum number n*, determined from the condition (Refs. 68, 70):

$$I_{nl} = I_H \frac{z^2}{n^{*2}}. \tag{10.20}$$

where $I_{nl}$ is the binding energy of the level determined by the quantum numbers n, l; $I_H$ = 13.56 ev is the ionization potential of a hydrogen atom; and, z = r + 1 is the charge of the atomic remainder (z = 1 for neutral atoms, z = 2 for singly charged ions, etc.). The difference $n - n^* = \mu$, called the quantum defect, tends toward zero as the levels rise, the upper levels becoming hydrogen-like.[1]

In the works of L. M. Biberman and associates (Refs. 64, 65, 71, 72), formulas are derived which take into account the quantum defect of actual levels of complex atoms, and which make it possible for the coefficients of recombination and ionization to be found. In the work of Burgess

[1]Therefore, in particular, for nitrogen and oxygen, in the case of which to the main level there corresponds the quantum number n = 2, summation in formula (10.18), and in those similar to it, is actually carried out not along n, but along n*, starting with n* = 1.

and Seaton (Ref. 70), the general formula of the photoionization cross sections of complex atoms, as well as numerous examples of its application is cited.

The formula of the coefficient of recombination with ionization for complex atoms has the form of

$$C_r' = 1.04 \cdot 10^{-11} \cdot T^{-3/2} \int_0^\infty \frac{\xi(\nu, T)}{\nu} e^{-u} (e^{u'} - 1)\, d\nu, \tag{10.21}$$

where the frequency $\nu$ is determined by the energy of the recombining electron ($h\nu = mv^2/2$), $u' = h\nu'/kT$, $\nu' = \nu$, if $\nu \leq \nu_g$ and $\nu' = \nu_g$; if $\nu \geq \nu_g$; where $\nu_g$ is the frequency corresponding to the lowest excited state $n_g$, from which integration commences (concerning the selection of $n_g$ and $\nu_g$, see Ref. 71).

The distinction from hydrogen-likeness is expressed by the function $\xi(\nu, T)$, which has a varying course for various atoms and ions (Ref. 71). For oxygen and nitrogen atoms $\xi(\nu, T) < 1$ does not depend on temperature and diminishes almost linearly with $\nu$ (when $\nu \leq 10^{15}$ sec$^{-1}$). But for various oxygen ions the course of $\xi(\nu)$ varies considerably, it being possible for this value to be greater or less than unity (Ref. 72). However, with an increase in ion multiplicity, the course of $\xi(\nu)$ becomes smoother, approaching the straight line $\xi = 1$; this is explained by the fact that the levels of ions of high multiplicity approach those of hydrogen-like ones even more.

At the high temperatures in air that occur in shock waves in front of a flying meteorite ($T = (5–20) \cdot 10^4$°K), the first ionizations take place fairly rapidly, and do not make much of a contribution to heat capacity; and the recombination of ions of low multiplicity is negligibly small. Therefore, in the problem at hand the use of a precise formula (10.21) is not justified by necessity, and it is possible everywhere to assume $\xi = 1$. Possible errors for ions OI–OIII partially compensate for each other, since the difference $\xi - 1$ for these ions has the opposite sign.

Therefore, for computing recombination with radiation we shall make use of formulas (10.13) and (10.14).

With regard to ionization and triple recombination, the application of formulas (10.10), (10.15) and (10.18) to complex atoms should also not lead to great errors (Ref. 64). However, into formula (10.10) it is necessary to introduce the multiplier $\Gamma_r$, taking into account the multiplicity of atoms:

$$\Gamma_r = \frac{2U_r}{U_{r-1}}, \tag{10.22}$$

where $U_r$ is the sum with respect to the states.[1]

[1]The necessity for introducing the multiplier $\Gamma_r$ into formula (10.10), as well as into some formulas in Section 9, stems from the fact that into these formulas enter the statistical weights of the terms corresponding to the given levels. For complex terms these weights must be multiplied by $\Gamma_r$.

Figures 22 and 23 show the values of the coefficients of ionization (from all levels) and triple recombination, calculated for the $T_e = (1-30) \cdot 10^4$ degrees range of electron temperatures.

Study of Figure 22 shows that $Z_r$ strongly depends not only on $T_e$, but also on $n_e$, whereas the coefficients of ionization from the basic level (Table 12, Figure 18) do not depend on $n_e$. Here once again the role of the upper levels is demonstrated; and, since their number is determined by electron density, the dependence of the coefficients $Z_r$ and $n_e$ must manifest itself.

Also of interest is the dependence of $Z_r$ on the ionization multiplicity r for large instances of T. Whereas, for small instances of T the coefficients $Z_r$ diminish in a regular manner as the ionization multiplicity increases, when $T_e \sim 3 \cdot 10^5$ a characteristic maximum of $Z_r$ becomes apparent for which r = 3. Formally, this is explained by the fact that the product $u_1^2 e^{-u_1}$ has a maximum when $u_1 = 2$, i.e., when $I_r = 2kT_e$, this being effectuated only for large instances of $T_e$ (usually $u_1 > 2$). The physical sense of this phenomenon is clear from Figure 16, since the ionization cross section has a maximum at some value of v.

For some values of $T_e$, $n_e$ (for instance, when $T_e = 3 \cdot 10^5$, $n_e = 10^{20}$), the value of $Z_1$ determined according to formula (10.10) is found to be less than the coefficient of ionization $Z_{1.1}$ from

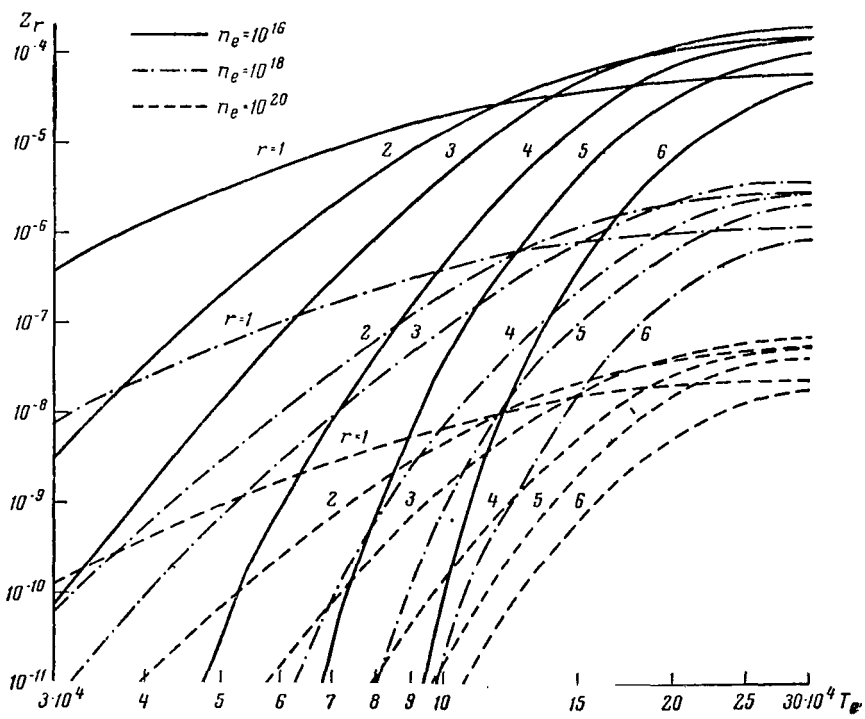


Figure 22. Coefficients of ionization from all levels.

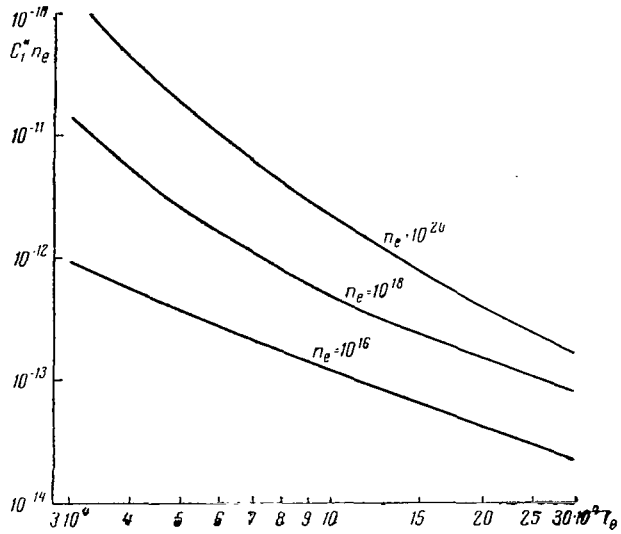


Figure 23. Coefficients of triple recombination for single-charge ions.

the basic level found from formula (10.4). Here the effect is felt of the difference in the approximations used, since (10.4) has as its basis the approximation of Thompson, whereas the approximation of Bethe-Born serves as the basis for (10.10). However, the divergence between them is not great.

With regard to photoionization, it should be recalled that photoionization is determined not by the external radiation field, but by the radiation originating precisely on the spot, within the shock wave, due to acts of photorecombination. When $n_e > 10^{18}$, its role is infinitesimally small in comparison to ionization by electron impact. When $10^{16} < n_e < 10^{18}$, it may be assumed that the number of acts of photoionization and recombination with radiation per unit of time per unit of volume are equal to one another. For $n_e < 10^{16}$ more complete investigation is necessary (see, for instance, Ref. 124).

The coefficients $Z_r$, $C_r'$, and $C_r''$, found according to the formulas of this section, have been used in the solution of the basic system of equations of ionization kinetics (9.27).

## Section 11. Ionization Relaxation Time

Let us now consider the sequence and time of the various relaxation processes in the ionization stage. This is first a process of energy exchange between ion and electron gas, bringing about an equalization of their temperatures (we designate the relaxation time by $\tau_{ei}$). Furthermore,

since the second ionization starts in practice after the first ionization is completed, etc. (Ref. 42), it is possible to consider separately the times of completion of each stage of ionization ($\tau_1$, $\tau_2$, ..., $\tau_6$); and, finally, the overall time for the attainment of ionization equilibrium $\tau_i$. Depending on the value of the equilibrium stage of ionization $x_{eq} = \alpha_{el}/2$, the time $\tau_1$ may assume different values, in particular

$$\begin{aligned} &\text{when } x_{eq} = 1 \qquad && \tau_i = \tau_1, \\ &\text{when } x_{eq} = 2 \qquad && \tau_i = \tau_1 + \tau_2, \\ &\text{when } x_{eq} = 3 \qquad && \tau_i = \tau_1 + \tau_2 + \tau_3, \text{ etc.} \end{aligned}$$

Obviously, when $x_{eq} < r$, the r-th ionization does not proceed to the end.

In order to obtain the values of $\tau_r$ ($r = 1, 2, \ldots, 6$), we use the equation of ionization kinetics obtained from (9.23):

$$\frac{dn_e}{dt} = n_e n_{r-1} Z_r - n_e n_r C_r = n_e \frac{1}{\tau_r}. \tag{11.1}$$

The coefficients of ionization $Z_r$ and of recombination $C_r$ are determined according to the formulas of Section 10. For a given concentration of atoms, $n_a$, in accordance with what has been said above, $n_a \cong n_{r-1} + n_r$. It is expedient to select the relationship between $n_{r-1}$ and $n_r$ on the basis of the following considerations.

A graph of the concentration change of each ion component, $n_r$, can be well represented by a Gaussian curve. The greatest rate of ionization is attained when $n_{r-1} = n_r = n_a/2$, and the curve has an inflection point. The rate of ionization at this point is equal to

$$\frac{dn_e}{dt} = n_e \frac{n_a}{2} (Z_r - C_r). \tag{11.2}$$

Let us replace $dn_e/dt$ by the value $dn_r/dt$, which is almost equal to it, and divide both parts of equation (11.2) by $n_a$. We obtain

$$\frac{dy_r}{dt} = \frac{n_e}{2} (Z_r - C_r). \tag{11.3}$$

This value is equal to the tangent of the angle of inclination of the curve at the inflection point. Using the known properties of a Gaussian curve, from (11.1) and (11.3) we obtain

$$\frac{1}{\tau_r} = \frac{\sqrt{e}}{4} n_a (Z_r - C_r), \tag{11.4}$$

where the values of $Z_r$ and $C_r$ are taken for $T_e$ corresponding to $y_r = y_{r-1} = 0.5$.

For determination of the time $\tau_{ei}$, we use an expression obtained by Spitzer (Ref. 57),

$$\tau_{ei} = \frac{3\sqrt{m_e} m_i k^{3/2}}{8\sqrt{2\pi}\, n_i z_e^2 z_i^2 e^4 \ln\Lambda}\left(\frac{T_e}{m_e} + \frac{T_i}{m_i}\right)^{3/2}. \tag{11.5}$$

This expression has been derived for any two groups of particles ("field" and "test"). In our case, for electrons $z_e = 1$, for ions $z_i \sum_r r y_r$. Considering that on the average for air $m_i = 2.6 \cdot 10^4 m_e$, we may disregard the second term in the brackets. Besides, we make the substitution $L = 2\ln\Lambda$. After this, formula (11.5) takes the form

$$\tau_{ei} = \frac{3 m_i (kT_e)^{3/2}}{4\sqrt{2\pi n_e^{1/2}} n_i e^4 z_i^2 L}. \tag{11.6}$$

The time for the establishment of a Maxwell distribution in each group of particles is, according to Spitzer, equal to

$$\tau_c = \frac{m^{1/2}(3kT)^{3/2}}{2\sqrt{2\pi} n e^4 z^4 \ln\Lambda}. \tag{11.7}$$

If the times $\tau_c$ are designated $\tau_{ii}$ and $\tau_{ee}$ for ions and electrons, respectively, it follows from formulas (11.6) and (11.7) that in air

$$\tau_{ei} \approx 84\, \tau_{ii} \text{ (ions)},$$
$$\tau_{ei} \approx 1.36 \cdot 10^4\, \tau_{ee} \text{ (electrons)}.$$

We now compare the times $\tau_r$ and $\tau_{ei}$. It is first necessary to make one remark. All the relaxation times considered here do not generally constitute the finite completion times of a given process, but are merely characteristic times determined by the state of ion-electron gas at a given moment. The sense of $\tau_r$ is determined by formula (11.1), while the sense of $\tau_{ei}$ is determined by the analogous expression (Ref. 57):

$$\frac{dT_e}{dt} = \frac{T_i - T_e}{\tau_{ei}}. \tag{11.8}$$

The basic parameter determining the times $\tau_r$ and $\tau_{ei}$ is the electron temperature $T_e$. Tables 14 and 15 show the values of $\tau_{ei}$ and of the products $n_a\tau_r$ for various instances of $T_e$, the second argument in Table 14 being $n_i z_i^2$, while in Table 15 the second argument is $n_e$ (for $r = 1.2$).

In order to obtain the direct values of $\tau_r$ from Table 15, it is necessary to divide the numbers cited in it by $n_a$. It is not difficult to become convinced that the values of $\tau_r$ for high temperature depend weakly on r and $T_e$, and that $\tau_r$ and $\tau_{ei}$ are values of the same order of magnitude.

Table 14

Relaxation Time $\tau_{ei}$, sec

| $n_i z_i^2$ | $T_e \cdot 10^{-3}$ | | | | | |
|---|---|---|---|---|---|---|
| | 5 | 10 | 20 | 40 | 80 | 160 |
| $10^{16}$ | $5.5 \cdot 10^{-8}$ | $1.2 \cdot 10^{-7}$ | $2.8 \cdot 10^{-7}$ | $6.9 \cdot 10^{-7}$ | $1.6 \cdot 10^{-6}$ | $4.2 \cdot 10^{-6}$ |
| $10^{17}$ | $8.0 \cdot 10^{-9}$ | $1.6 \cdot 10^{-8}$ | $3.5 \cdot 10^{-8}$ | $8.1 \cdot 10^{-8}$ | $2.0 \cdot 10^{-7}$ | $4.8 \cdot 10^{-7}$ |
| $10^{18}$ | $1.4 \cdot 10^{-9}$ | $2.4 \cdot 10^{-9}$ | $4.7 \cdot 10^{-9}$ | $1.0 \cdot 10^{-8}$ | $2.4 \cdot 10^{-8}$ | $5.5 \cdot 10^{-8}$ |
| $10^{19}$ | — | $4.4 \cdot 10^{-10}$ | $6.6 \cdot 10^{-10}$ | $1.3 \cdot 10^{-9}$ | $2.9 \cdot 10^{-9}$ | $6.9 \cdot 10^{-9}$ |
| $10^{20}$ | — | — | $1.4 \cdot 10^{-10}$ | $2.0 \cdot 10^{-10}$ | $3.9 \cdot 10^{-10}$ | $8.7 \cdot 10^{-10}$ |
| $10^{21}$ | — | — | — | $4.4 \cdot 10^{-10}$ | $6.0 \cdot 10^{-11}$ | $1.2 \cdot 10^{-1}$ |
| $10^{22}$ | — | — | — | — | $1.3 \cdot 10^{-11}$ | $1.8 \cdot 10^{-1}$ |

Table 15

The Product $n_a \tau_r$

| $n_e$ | $r$ | $T_e \cdot 10^{-3}$ | | | | | |
|---|---|---|---|---|---|---|---|
| | | 10 | 20 | 40 | 80 | 160 | 320 |
| $10^{14}$ | 1 | $2.1 \cdot 10^{9}$ | $5.1 \cdot 10^{5}$ | $7.8 \cdot 10^{3}$ | $9.7 \cdot 10^{2}$ | $3.4 \cdot 10^{2}$ | $2.0 \cdot 10^{2}$ |
| | 2 | — | $2.6 \cdot 10^{9}$ | $3.5 \cdot 10^{5}$ | $4.1 \cdot 10^{3}$ | $4.4 \cdot 10^{2}$ | $1.4 \cdot 10^{2}$ |
| $10^{16}$ | 1 | $1.6 \cdot 10^{11}$ | $2.6 \cdot 10^{7}$ | $3.9 \cdot 10^{5}$ | $4.7 \cdot 10^{4}$ | $1.6 \cdot 10^{4}$ | $9.6 \cdot 10^{3}$ |
| | 2 | — | $1.5 \cdot 10^{11}$ | $1.8 \cdot 10^{7}$ | $2.0 \cdot 10^{5}$ | $2.1 \cdot 10^{4}$ | $6.9 \cdot 10^{3}$ |
| $10^{18}$ | 1 | — | $1.0 \cdot 10^{9}$ | $1.6 \cdot 10^{7}$ | $2.0 \cdot 10^{6}$ | $7.2 \cdot 10^{5}$ | $4.3 \cdot 10^{5}$ |
| | 2 | — | — | $7.4 \cdot 10^{8}$ | $8.7 \cdot 10^{6}$ | $9.4 \cdot 10^{5}$ | $3.1 \cdot 10^{5}$ |
| $10^{20}$ | 1 | — | — | $8.0 \cdot 10^{8}$ | $9.7 \cdot 10^{7}$ | $3.4 \cdot 10^{7}$ | $2.0 \cdot 10^{7}$ |
| | 2 | — | — | $2.5 \cdot 10^{11}$ | $4.1 \cdot 10^{8}$ | $4.4 \cdot 10^{7}$ | $1.4 \cdot 10^{7}$ |

## Section 12. Results of Calculations of Ionization Kinetics and Energy Exchange within the Shock-Wave Front

Calculations based on the solution of a system of ionization kinetics equations, which yield a distribution of the degrees of ionization and of the temperatures $T_e$ and $T_i$ in a shock wave, are very few in number.

In 1954, S. B. Pikel'ner (Ref. 56) published a series of such calculations for the formative stages of plasma consisting of hydrogen with an admixture of 20 percent helium. In this case energy expenditures were important for the excitation of atoms with subsequent deexcitation. However, the obtained qualitative pattern was a very characteristic one (Figure 24).

In 1957, J. Bond (Ref. 107) calculated the structure of a shock wave in argon for velocities of 5–6 km/sec, and an initial pressure of 59.3 cm Hg. In his work are given graphs of $T_i$, x, $\rho_2^*$,

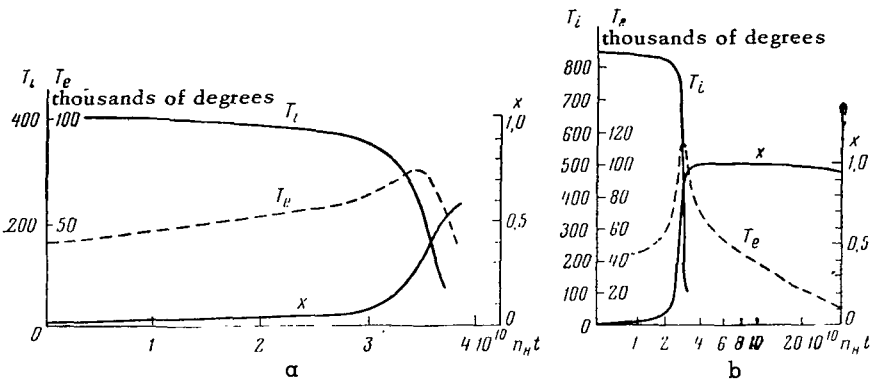


Figure 24. Variation of $T_i$, $T_e$, x behind the front of a shock wave in formative stages of plasma (according to S. B. Pikel'ner).

a – temperature $T_{i0} = 400{,}000°$; b – $T_{i0} = 850{,}000°$

$p_2^*$, u in a function of the distance from the wave front (Figure 25). His calculations were based on the principle of detailed balancing.

At almost the same time, Petschek and Bryon (1957, Ref. 54) carried out analogous calculations for argon, on the basis of a balance between the energy obtained by electrons from ions, and the energy expended on ionization and the increase of electron temperature (they disregarded recombination).

Their results are represented in a form less convenient for survey, but they yield almost all the data of interest to us. The basic argument is enthalpy corresponding to the velocity of the shock wave (Figure 26). On the graph are plotted lines of constant enthalpy (from left to right) and isolines of the degree of ionization (from the top downward). From each initial value of the ion temperature $T_{i0}$, it is possible to trace the change of $T_e$ and x in the function $T_i$ (or of $T_e$ and $T_i$ in the function x), preceding along the line of equal enthalpy. However, the graph of Petschek and Byron does not permit these processes to be traced in time (although this may be done without difficulty, according to the formulas of their work).

Finally, a series of calculations for air based upon the calculations of Section 9 has been carried out recently by the author of this book (Figures 27–29).

The overall course of the three principal variables, $T_i$, $T_e$, and x, may be provisionally divided into three sectors. In the first sector $T_i$ diminishes slowly, and $T_e$ and x increase equally as slow. In the second sector comes the so-called "avalanche ionization," i.e., $T_e$ and x increase rapidly, $T_i$ falls (Figures 24, 25, 27–29).

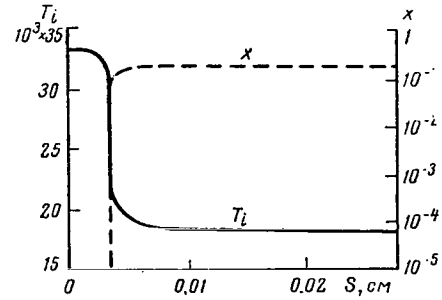


Figure 25. The course of $T_i$ and x behind the front of a shock wave in argon (according to Bond).

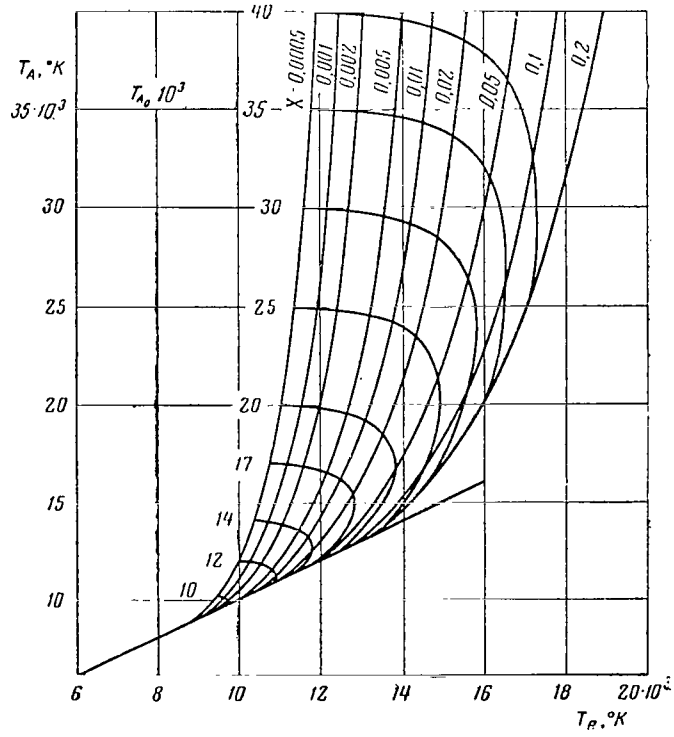


Figure 26. Diagram of change of $T_e$ and x in the function $T_i$ for various values of $T_{i_0}$ (according to Petschek and Byron).

Lines of constant enthalpy, corresponding to the indicated values of $T_{i_0}$, yield the pattern of change of $T_e$ and x in the movement of a particle behind the shock wave.

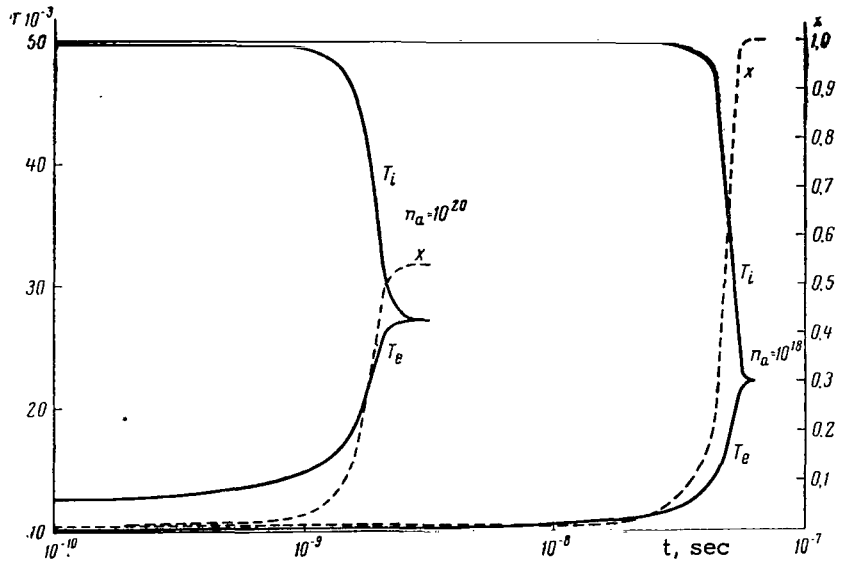


Figure 27. Change of $T_i$, $T_e$ and x in air when $T_{i0} = 50{,}000°$, $x_0 = 10^{-2}$.

The third sector of temperature and ionization change corresponds to a comparatively slow evening off of $T_e$ and $T_i$, and to the approach of the degree of ionization to the equilibrium value.

Let us examine in greater detail the change in the electron temperature $T_e$. In the first sector, $T_e$ increases because of the transfer of ion energy to electrons. If the amplitude of the shock wave (and, consequently, the initial $T_e$ as well) is small, ionization efficiency is at first small and $T_e$ increases slowly, until the increase of x, i.e., of the number of ions, accelerates the process of energy transfer to electrons, this effecting a rapid growth of $T_e$. But the energy expenditure for ionization is intensified with the growth of $T_e$, which, passing through a maximum, begins to diminish together with $T_i$. Such a pattern was obtained by S. B. Pikel'ner for the hydrogen-helium formative stages of plasma (Figure 24); the same pattern was obtained by Petschek and Byron for argon when $T_{i0} \leq 35{,}000°$ (the lines of constant enthalpy in Figure 26 have a maximum with respect to the argument $T_e$).

As the amplitude of the shock wave increases, the difference between the ion and electron temperatures becomes so great that despite the energy expenditures for ionization, the electrons continue to acquire sufficient energy from the ions for the continuation of the growth of $T_e$. In this case $T_e$ does not have a maximum. Such a pattern for argon has been registered by Petschek and Byron when $T_{i0} \geq 40{,}000°$. Unfortunately, Bond does not cite data concerning $T_e$, but the nature of the change of $T_i$ and x is the same as in the other works.

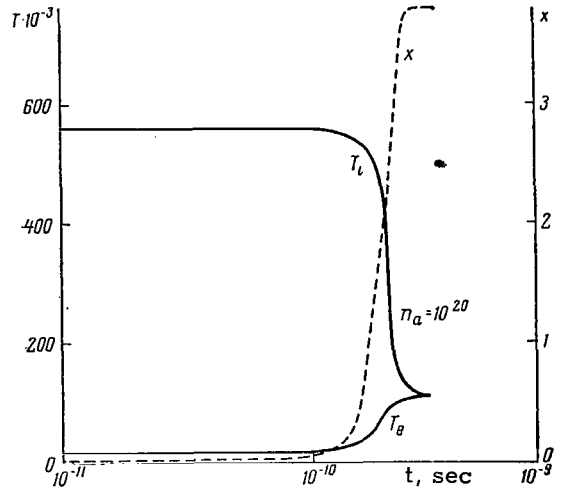


Figure 28. Change of $T_i$, $T_e$ and x in air when $T_{i0} = 580{,}000°$, $x_0 = 10^{-2}$.

Let us consider the results of our calculations for air. The calculations were made on the "Strela-3" electronic computer of the Computer Center of the Academy of Sciences, USSR. The programs were compiled by A. N. Chigorin, to whom the author expresses deep gratitude for this work, as well as for carrying out the calculations themselves.

First, the calculations showed that of the two schemes considered in Section 9, only Scheme II leads to correct results. The expenditure of energy for ionization in Scheme I is so great that the electron temperature scarcely rises. It is also important to take into account the differences of complex atoms from hydrogen-likeness (for hydrogen-like atoms the course of $T_e$ and $T_i$ is steeper).

Henceforth, all calculations were carried out in accordance with Scheme II (Boltzmann distribution, level by level). We took $10^{20}$ and $10^{18}$ $cm^{-3}$ as the initial values of $n_a$; this corresponds to altitudes of approximately 15 and 45 km (we assume here that compression in the shock wave is equal to 10; refinement of this value will have little effect on altitude values).

The initial ion temperatures were taken as 50,000°, 580,000° and 2,000,000°. In their physical sense they correspond to the temperatures $T_f$ from Section 7, i.e., to the temperatures at the wave front after completion of dissociation. As can be seen from Table 8, these values of $T_f$ correspond to meteorite velocities, respectively, of 18 km/sec, 47–57 km/sec, and over 72 km/sec (larger numbers correspond to an altitude of 45 km, smaller ones correspond to 15 km). The initial degree of ionization x was always assumed equal to 0.01. This value is to a certain extent an

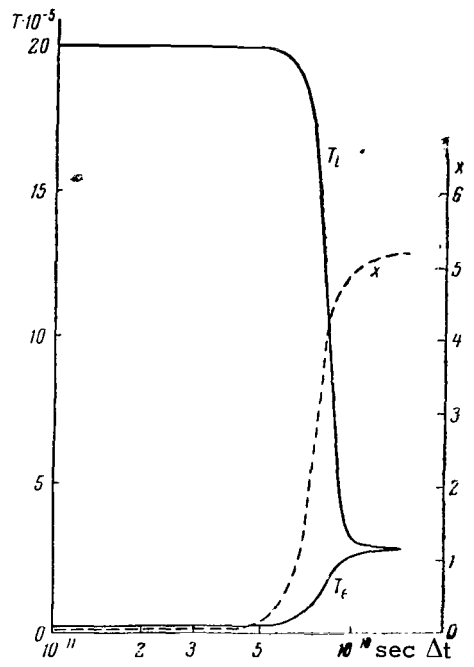


Figure 29. Change of $T_i$, $T_e$ in air when $T_{i0} = 2{,}000{,}000°$, $x_0 = 10^{-2}$, $n_a = 10^{20}$.

arbitrary one, due to the indeterminacy of the mechanism of the initial stage of ionization. The initial value of the electron temperature $T_{e0}$ was found from a condition based on the principle of detailed balancing:

$$\frac{dT_e}{n_a\, dt} = 0. \tag{12.1}$$

Imprecision in the evaluation of the initial value $T_{e0}$ has almost no effect on the results, since already in the first stages of calculation, $T_e$ assumes correct values that correspond to the principle of detailed balancing.

As can be seen from Figure 27, the establishment of an equilibrium state behind the front of a shock wave at low altitude ($\sim$15 km) is attained somewhat rapidly—over a time of the order of $3 \cdot 10^{-9}$ sec—even at comparatively small shock-wave amplitude ($v_1 = 16$ km/sec, $T_{i0} = 50{,}000°$, $T_{e0} = 12{,}400°$). For high amplitude waves, $v_1 = 47$ km/sec, $T_{i0} = 580{,}000°$, $T_{e0} = 15{,}400°$) equilibrium is established even more rapidly—over a time of the order of $5 \cdot 10^{-10}$ sec. Taking into account the flow velocity behind the front $v_2$, we obtain a wave-front width, or more precisely, the width of the sector of the establishment of equilibrium for the considered examples, of $5 \cdot 10^{-4}$

and $2 \cdot 10^{-4}$ cm. These values are in good agreement with the calculations of Bond (Ref. 107) for the smaller initial velocities and amplitudes. Thus, the front of the shock wave is very thin, and the gas in the compressed layer may be considered as being in equilibrium.

At high altitudes ($\sim$45 km), as can be seen from Figure 27, the duration of the establishment of equilibrium conditions increases by an order of magnitude and more (when $v_1 = 17$ km/sec, $T_{i0} = 50{,}000°$, and $T_{e0} = 10{,}100°$, this time amounts to $6 \cdot 10^{-8}$ sec). Nevertheless, the width of the shock-wave front here is measured in fractions of a millimeter.

At even higher altitudes ($\sim$80 km), under conditions of highly rarefied air, the rate of ionization is considerably lower and the width of the shock front is much greater, and (considering the action of radiation) may be measured in centimeters. In the movement of not very large bodies in the atmosphere, the nonequilibrium region may extend to the very body of the meteorite.

## Section 13. Temperature Distribution within the Shock Wave

To now we have been considering the change of ionization and temperature along the axis of a shock wave originating in the flow of a hypersonic stream of gas about a body. Considering the shapes of the body and wave to be axially symmetrical, let us consider the distribution of the same values, as well as of pressure and density, at the intersection of the wave by a plane passing through its axis.

On the basis of the theory of oblique shock waves (Ref. 49), far from the axis, where the oncoming stream meets the wave front at an angle $\phi$, a stream line forms with the front the angle $\omega$, bound to $\phi$ by the relationship

$$\tan\omega = \tan\varphi\left(\frac{\gamma-1}{\gamma+1} + \frac{2}{(\gamma+1)\,\mathrm{Ma}^2\sin^2\varphi}\right). \tag{13.1}$$

Designating by u the velocity component v which is normal to the front, we shall have the following relationships:

$$\begin{gathered}\rho_1 u_1 = \rho_2 u_2;\ u_2 = v_2 \sin\omega;\\ u_1 = v_1 \sin\phi.\end{gathered} \tag{13.2}$$

Hence the density ratio

$$\frac{1}{\tilde{\rho}} \equiv \frac{\rho_1}{\rho_2} = \frac{\tan\omega}{\tan\varphi} = \frac{1}{\gamma+1}\left[\gamma - 1 + \frac{2}{\mathrm{Ma}^2\sin^2\varphi}\right]. \tag{13.3}$$

On the basis of (7.2) and (13.3), the density ratio is equal to

$$\tilde{p} \equiv \frac{p_2}{p_1} = 1 + \frac{2\gamma}{\gamma+1}(\mathrm{Ma}^2 \sin^2\varphi - 1). \tag{13.4}$$

And, finally, the ratio of the temperatures at the front of a shock wave are equal to the product of the ratios expressed by formulas (13.3) and (13.4):

$$\tilde{T} \equiv \frac{T_y}{T_1} = \frac{1}{\gamma+1}\left[\gamma - 1 + \frac{2}{\mathrm{Ma}^2 \sin^2\varphi}\right]\left[1 + \frac{2\gamma}{\gamma+1}(\mathrm{Ma}^2 \sin^2\varphi - 1)\right]. \tag{13.5}$$

We introduce the designation

$$\mathrm{M} = \mathrm{Ma} \sin \phi. \tag{13.6}$$

Then

$$\tilde{T} \approx \frac{1}{\gamma+1}\left[\gamma - 1 + \frac{2}{M^2}\right]\left[1 + \frac{2\gamma}{\gamma+1}(M^2 - 1)\right]. \tag{13.5a}$$

If $\mathrm{M}^2 \gg 1$, formula (13.5a) assumes the simple form of

$$\tilde{T} = \frac{\gamma-1}{2} M^2. \tag{13.7}$$

Formula (13.7) is applicable when $\mathrm{M} \geq 10$. However, in such strong waves dissociation and ionization begin to have a substantial influence, and in place of $T_y$ in formula (13.5), there should stand $T_f$ or $T_2$. On the basis of (7.30),

$$\frac{T_f}{T_1} = \frac{5}{12}(\gamma - 1)(1 - Q^*_{\mathrm{dis}}) M^2; \quad \frac{T_2}{T_1} = \frac{5}{12}(\gamma - 1)(1 - Q^*_{\mathrm{p}}) M^2. \tag{13.8}$$

The values of M in the function Ma and $\phi$ are shown in Table 16. Table 17 shows the ratios of temperatures, pressures and densities in the function M for $\gamma = 1.25$. A transition to other instances of $\gamma$ has little effect on $\tilde{p}$ and more on $\tilde{\rho}$ and $\tilde{T}$.

Thus, on the "flanks" of a shock wave the intensity of the temperature and pressure jump diminishes, first slowly and then ever more rapidly. In this connection the initial conditions of the ionization kinetics equations (Section 9) also change, as does the time scale entering into these equations.

Table 16

| Ma \ φ | 90° | 80° | 70° | 60° | 50° | 40° | 30° | 20° | 10° | 5° |
|---|---|---|---|---|---|---|---|---|---|---|
| 30 | 30,0 | 29,5 | 28,2 | 26,0 | 23,0 | 19,3 | 15,0 | 10,25 | 5,21 | 2,61 |
| 50 | 50,0 | 49,2 | 46,9 | 43,0 | 38,3 | 32,0 | 25,0 | 17,1 | 8,69 | 4,36 |
| 75 | 75,0 | 73,8 | 70,4 | 64,9 | 57,4 | 48,2 | 37,5 | 25,6 | 13,0 | 6,54 |
| 100 | 100,0 | 98,7 | 93,8 | 86,5 | 76,6 | 64,3 | 50,0 | 31,2 | 17,4 | 8,71 |
| 125 | 125,0 | 123,0 | 117,2 | 108,2 | 95,7 | 80,3 | 62,5 | 42,7 | 21,7 | 10,9 |
| 150 | 150,0 | 147,6 | 140,7 | 129,8 | 115,0 | 96,5 | 75,0 | 51,3 | 26,2 | 13,1 |
| 175 | 175,0 | 172,2 | 164,1 | 151,4 | 134,0 | 112,5 | 87,5 | 59,8 | 30,4 | 15,2 |
| 200 | 200,0 | 196,8 | 187,6 | 173,0 | 153,2 | 128,5 | 100,0 | 68,4 | 34,7 | 17,4 |
| 225 | 225,0 | 221,4 | 211,0 | 194,6 | 172,4 | 144,5 | 112,5 | 77,0 | 39,1 | 19,6 |

Table 17

| $M$ | 1 | 2 | 3 | 4 | 5 | 10 | 20 | 50 | 100 | 200 |
|---|---|---|---|---|---|---|---|---|---|---|
| $\tilde{\rho}$ | 1,00 | 3,00 | 4,8 | 6,0 | 6,8 | 8.3 | 8,8 | 9,0 | 9,0 | 9.0 |
| $\tilde{p}$ | 1,00 | 4,33 | 9,89 | 17,7 | 27,7 | 111 | 444 | $2.78 \cdot 10^3$ | $1.11 \cdot 10^4$ | $4.44 \cdot 10^4$ |
| $\tilde{T}$ | 1,00 | 1,44 | 2.07 | 2,94 | 4,06 | 13,3 | 50,1 | $3.09 \cdot 10^2$ | $1.24 \cdot 10^3$ | $4.93 \cdot 10^3$ |

The flow velocity of various relaxation processes is a function of the number of particle collisions. The latter is, in its turn, proportional to $\rho v dt = \rho dx'$, where $dx'$ is read off along the path of movement of the particles of the flow behind the shock-wave front.

On the basis of (13.2) and (13.3)

$$dx' = v_1 \frac{\cos \varphi}{\cos \omega} dt. \tag{13.9}$$

Using these stream line relationships and equations (Section 5), it is possible to find the surfaces connecting points with equal ionization and temperature. As the distance from the point of full deceleration increases, these surfaces will press ever more closely to the surface of the body.

The qualitative pattern of the distribution of ion temperature $T_i$ in a shock wave will be as follows (Figure 30a). The hottest region adjoins a point on the wave axis, and isothermal surfaces surround it, these surfaces being second-order curves in cross section. Further, the shape of the isotherms changes sharply: they have their origin at the front of the shock wave, and then they bend along the stream. In some point on the wave front the temperature becomes insufficient

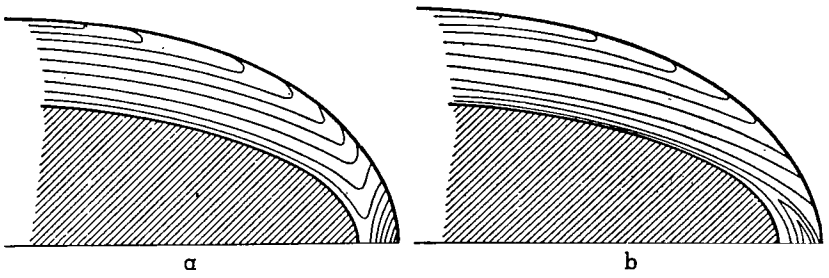


Figure 30. Shock wave temperature distribution.

a — ion; b — electron temperature

for the onset of ionization (and subsequently, of dissociation as well), although ions may get into these "cold" regions due to diffusion.

The distribution of $T_e$ (Figure 30b) at the "nose" of the shock wave at high altitudes (in rarefied air) is of a somewhat different nature, since in this case $T_e$ increases somewhat slowly along the stream, either attaining a maximum or leveling from $T_i$. Therefore, the value $T_{e\,max}$ will be reached somewhere on the wave axis between the front and the point of full deceleration. The isotherms of $T_e$ in cross section have here the shape of lunes. In denser air strata these lunes flatten out in the narrow region of the front itself. Further along the wave front there is a transition to the very lowest instances of $T_e$, and further still, the difference between $T_e$ and $T_i$ loses its sense, since the temperature there is insufficient to maintain ionization.

Thus, in the head part of a shock wave it is possible to distinguish three regions of change of the ion temperature: a hot region immediately behind the wave front, a region of rapid temperature fall (avalanche ionization), and a region of established equilibrium.

But since the shock-wave separation distance depends mainly on the dimensions of the body, whereas the time for the establishment of ionization equilibrium and the corresponding distance depend (at a given height) only on the amplitude of the shock wave, in the shock waves of large meteorites there is time for equilibrium to be established, whereas it will not be attained in the case of smaller bodies. In addition, at high altitudes equilibrium ionization in a shock wave is usually not attained because of low air density and the small number of particle collisions.

Determination of the pattern of distribution of gasdynamic and thermodynamic parameters in a shock wave (including ionization) makes it possible to approach the solution of the problem of thermal action of the shock wave on the meteorite body. This problem will be considered in Chapter III. The processes taking place in the flow field at a distance from the head portion of the

wave (including the formation of secondary waves of compression and rarefication, ion recombination and trail formation), are not considered here since they have almost no influence on heat exchange.

# CHAPTER III. HEAT TRANSFER TO THE METEORITE BODY

## Section 14. Radiation Flux

If we are given a temperature and density distribution in a compressed layer, it is possible to calculate the radiation flux for any elementary area on the body of the meteorite. However, before deriving the equations for the radiation flux, we shall make some general remarks.

The conditions in a shock wave formed in front of a flying meteorite are comparable with the conditions in stellar photospheres. Actually, the density of the photosphere at the edge of the sun has an order of magnitude of $10^{-8}$ g/cm$^3$ and increases toward the center, attaining at a depth of 120,000 km values of $10^{-2}$ g/cm$^3$, which corresponds to the density in the compressed layer of a shock wave in air at the surface of the earth. The temperature of the sun at the same depth interval increases from 6,000° to 500,000°, which again corresponds closely to the temperature interval in shock waves.

However, in considering the radiant transfer in a shock wave, a number of substantial differences from celestial photospheres should also be taken into account. Thus, in celestial photospheres the temperature increases toward the center and radiant heat transfer is directed outwards. In a shock wave the temperature distribution is of a more complex nature, the hottest regions being adjacent to the wave front. The radiant heat transfer of interest to us is directed inward toward the meteorite body.[1]

The nature of radiation in a shock wave is the same as in stellar photospheres, i.e., it includes recombination radiation (free-bound transitions) and bremsstrahlung (free-free transitions). The absorption of radiation is brought about by inverse processes. The role of radiation and absorption in lines (bound-bound transitions) is negligibly small due to the small width of the lines. However, the relative role of linear radiation increases at relatively low temperatures ($T \leq 10{,}000°$),

[1]It is reasonable that there will also be a radiation flux outwards, bringing about deexcitation of the shock wave. This question has been studied in detail by Ya. B. Zel'dovich, A. S. Kompaneyets and Yu. P. Rayzer (Ref. 73), and will not be considered by us.

as can be seen from general consideration and the detailed analysis of theoretical and experimental data carried out by Mayerott (Ref. 74).

It is of interest to make a general comparison of the conditions in a shock wave and in the photosphere, as well as in the solar corona and in the formative stages of plasma (Table 18).

Table 18
Comparison of the Conditions in Formative Stages of Plasma, the Solar Corona, the Photosphere, and a Shock Wave in Air

| Formative stage of plasma | Corona | Photosphere | Shock wave |
|---|---|---|---|
| 1. Radiation forms outside the formative stage of plasma | 1. Radiation forms outside the corona | 1. Radiation forms within the photosphere itself | 1. Radiation forms within the wave itself |
| 2. The dilution factor is infinitesimal | 2. The dilution factor is the order of 0.1–0.5 | 2. The dilution factor is equal to 0.5–1 | 2. The dilution factor is equal to 1 |
| 3. The radiation temperature $T_0$ is high ($\sim 10^5$) | 3. The radiation temperature is low ($\sim 5 \cdot 10^3$) | 3. The radiation temperature is low ($\sim 5 \cdot 10^3$) | 3. The radiation temperature is of the order of $10^4$–$10^5$ |
| 4. The electron temperature is high, but is lower than $T_0$ ($\sim n \cdot 10^4$) | 4. The electron temperature is very high ($\sim 106^\circ$) | 4. The electron temperature is low ($\sim 5 \cdot 10^3$) | 4. The electron temperature is medium ($\sim 10^4$–$10^5$) |
| 5. Electron and ion temperatures equal | 5. Electron and ion temperatures of the same order | 5. Electron and ion temperatures equal | 5. Electron and ion temperatures not equal ($T_e < T_i$) |
| 6. Given $T_0$, $n_e$, find $T_e$ | 6. Given $T_0$, $n_e$, find $T_e$ | 6. $T_0$, $n_e$, $T_e$ are determined independently | 6. Given $T_e$, $T_i$, $n_e$, find $T_0$ |
| 7. $T_e$ can be checked on the basis of spectrum (state of ionization, ion composition) | 7. $T_e$ can be checked by various methods (spectrum, radio emission) | 7. See No. 6 | 7. $T_0$ cannot be reliably checked on the basis of spectrum, method has not been worked out |

Table 18 (Continued)

| Formative stage of plasma | Corona | Photosphere | Shock Wave |
|---|---|---|---|
| 8. Ionization effected by radiation | 8. Ionization effected both by radiation and electron collision (heavy elements) | 8. Ionization effected primarily by radiation | 8. Ionization effected primarily by electron collision |
| 9. Recombination proceeds primarily with radiation | 9. Recombination proceeds primarily with radiation | 9. Recombination proceeds primarily with radiation, influence of triple collisions is small | 9. Recombination proceeds primarily with triple collisions (when $n_e > 10^{16}$) |
| 10. Deexcitation great (fluorescence, radiation in forbidden lines) | 10. Deexcitation great (radiation in forbidden lines) | 10. Deexcitation great at surface and rapidly diminishes with depth | 10. Radiation suppressed, deexcitation low (when $n_e > 10^{18}$ |

In calculations of the radiation flux in stellar photospheres, there frequently enters into the equations the radiation temperature $T_0$, not equal to any of the kinetic temperatures $T_i$, $T_e$. In determining $T_0$ it is usually assumed that the spectral density of radiation $u_\nu$ is usually described by Planck's formula (Ref. 60, 61, 108). However, the radiation in a shock wave is generally not Planck radiation.

In order to solve the question of whether $u_\nu$ is subject to Planck's law or not, it is necessary to know the relationship between the path length of the radiation of frequency $\nu$—$l_\nu$, and the characteristic dimension of the region under consideration, D. In those frequencies where $l_\nu \ll D$, there is established a Planck distribution of the radiation density with respect to frequency, and if this condition is valid for the basic frequency range, the radiation may be considered to be Planck radiation. If, on the other hand, $l_\nu \gg D$, we shall be dealing with volume radiation, the spectral distribution of which will depend on the radiant emissivity of the gas in the corresponding frequencies.

In order to determine whether the condition $l_\nu \ll D$ is satisfied for the basic frequency range, it is necessary to find $\nu_g$, the threshold frequency of recombination determined by the condition

$$h\nu_g = \Delta I_{r,n} \tag{14.1}$$

($\Delta I_{r,n}$ is the binding energy of the level at which the recombination takes place). We introduce the mean threshold frequency $\bar{\nu}_g$; in order to do this we average level by level, taking into account the recombination coefficients for each level and assuming the levels to be hydrogen-like. We obtain

$$\bar{\nu}_g = \frac{I_r}{h} \frac{\sum_n C'_{r,n}/n^2}{C'_r}, \tag{14.2}$$

where $C'_r$ is the overall coefficient of recombination with radiation, yielded by formula (10.13), and $C'_{r,n}$ are the corresponding coefficients for the levels. Taking their expressions according to Seaton (Ref. 68), we obtain

$$\bar{\nu}_g = \frac{I_r}{h} \frac{e^{u_1}(u_1 - 1) + 1}{u_1(e^{u_1} - 1)}. \tag{14.3}$$

For $u_1 \geq 4$ a sufficient approximation is yielded by the expression

$$\bar{\nu}_g = \frac{I_r}{h} \frac{u_1 - 1}{u_1}. \tag{14.4}$$

The values of the correction multiplier in the right-hand parts of (14.3) and (14.4) are shown below:

| $u_1$ | 0.5 | 1 | 2 | 3 | 4 | 5 | 10 | 15 |
|---|---|---|---|---|---|---|---|---|
| Correction multiplier | 0.538 | 0.581 | 0.665 | 0.719 | 0.767 | 0.804 | 0.900 | 0.933 |

Thus, for instance, for $T_e$ = 23,000° the boundary wavelength corresponding to $\bar{\nu}_g$ is equal to 1,000 Å.

As has been shown in Table 18 (No. 7), it was heretofore impossible to rely on the direct determination even of the form of the function $T_0(\nu)$ on the basis of the spectra of bright meteors and bodies. The fact of the matter is that the luminescence directly registered by instruments is not the luminescence of the shock wave, the radiation of which is usually suppressed, but constitutes the luminescence of the heated zone before the front of the shock wave (Ref. 106). The spectral composition of this luminescence is entirely different than in a shock wave.

As far as the electron temperature $T_e$ is concerned, in subsequent calculations it must be recalled that the energy of recombination radiation is determined by the mean velocity of electrons

with respect to ions. But since $T_i$ and $T_e$ are of one order of magnitude, while $m_i \gg m_e$, it follows that $v_i \ll v_e$; ions may be considered immobile, and the "electron-ion" temperature, $T_{ei} = T_e$.

In order to gain a general conception of the conditions of radiant transfer in a shock wave, it is necessary to compute the value of the mean radiation path. A simple method of computing mean radiation paths and absorption coefficients in ionized gases at high temperatures has been developed by Yu. P. Rayzer (Ref. 75).

The mean absorption coefficient per unit of volume $\varkappa_1$ and the effective mean radiation path $l_1$ corresponding to it (characterizing the radiant emissivity) are determined by the expression

$$\varkappa_1 = \frac{1}{l_1} = \int_0^\infty \varkappa_\nu (1 - e^u)\, G_1(u)\, du, \tag{14.5}$$

where

$$G_1(u) = \frac{15}{\pi^4} \frac{u^3}{e^u - 1}, \qquad u = \frac{h\nu}{kT_e}. \tag{14.6}$$

Integrating, and then summing within the limits of the various degrees of ionization, r, Yu. P. Rayzer obtained the following approximate expression:

$$l_1 = \frac{1.1 \cdot 10^{23} T_e^{7/2}}{n_a^2 x (x+1)^2 \bar{u}_1}, \tag{14.7}$$

where $n_a$ is the overall concentration of atoms and ions, $x = n_e/n_a$.

$$\bar{u}_1 = \ln\left(\frac{AT_e^{3/2}}{n_a x}\right),$$
$$A = 2\left(\frac{2\pi m_e k}{h^2}\right)^{3/2} = 4.8 \cdot 10^{15}\ \text{cm}^{-3} \cdot \text{deg}^{-3/2}. \tag{14.8}$$

The approximate dependence of $l_1$ on $T_e$ and $n_a$ has the form

$$l_1 \sim T_e^{1.35} n_a^{-1.68}. \tag{14.9}$$

On the basis of data cited in Ref. 75, we compile the following table for the values of $l_1$ for various densities and temperatures (Table 19).

The method of Yu. P. Rayzer is sufficiently precise for approximate evaluations, although it cannot be recommended for precise calculations in application to complex atoms. In the latter

Table 19
Values of $l_1$, cm

| $T_e$ | $n_a$ | | |
|---|---|---|---|
| | $10^{16}$ | $10^{18}$ | $10^{20}$ |
| 25 000° | $1{,}3\cdot10^4$ | 5,0 | $2{,}5\cdot10^{-3}$ |
| 50 000 | $3{,}1\cdot10^4$ | 12,5 | $6{,}3\cdot10^{-3}$ |
| 100 000 | $7{,}9\cdot10^4$ | 32 | $1{,}6\cdot10^{-2}$ |
| 200 000 | $2{,}0\cdot10^5$ | 79 | $4{,}0\cdot10^{-2}$ |

case it is necessary to use the calculation method worked out by L. M. Biberman, G. E. Norman and K. N. Ul'yanov (Refs. 71, 72), based on the quantum-defect method developed by Seaton and Burgess (Refs. 68, 70). This absorption coefficient, calculated for one atom, is equal to

$$\varkappa(\nu, T) = C_1 \Gamma T_e e^{-u_1} (e^{u'} - 1)\, z^2 \xi(\nu, T_e)\, \nu^{-3}, \tag{14.10}$$

where

$$\left.\begin{aligned} C_1 &= \frac{16\pi^2}{3\sqrt{3}} \frac{e^6 k}{ch^4} = 0{,}89\cdot10^{24}\ \text{cm}^2/\text{sec}^3 \cdot \text{deg}, \\ \Gamma &= \frac{2U_1}{U_0}, \qquad \begin{aligned} u' &= u \quad \text{for} \quad \nu \leqslant \nu_g, \\ u' &= u_g \quad \text{for} \quad \nu > \nu_g. \end{aligned} \end{aligned}\right\} \tag{14.11}$$

Entering into the expression (14.10) are the already familiar multipliers $\Gamma$ and $\xi$, the multiplier $\Gamma$ determining the correction for the multiplicity and shifted terms of complex atoms, while $\xi(\nu, T_e)$ determines the correction for the quantum defect (see Section 10). The introduction of these multipliers increases the values of $\varkappa_\nu$ almost in all cases (only for the ion OIII is $\Gamma\xi < 1$), but not more than by a factor of 2 or 3. The values of $l_1$ cited in Table 19 are diminished by the same factor.

The question of radiation paths in hot air is also considered in the work of V. N. Zhigulev, Ye. A. Romishevskiy and V. K. Vertushkin (Ref. 76). In calculating the absorption coefficient of atoms in the fundamental state, they use the precise formula of Seaton (Ref. 68), while for excited states, Kramers' formula is used with the introduction of correction multipliers that take into account the difference of the energy level and their statistical weights from the hydrogen-like levels corresponding to them. For the 10,000–20,000°K temperature range, values have been obtained in Ref. 76 that are close in their order of magnitude to those cited in Table 19.

Because the introduction of multipliers $\Gamma$ and $\xi$ does not change the order of magnitude of the radiation-path lengths, we may use the data of Table 19 for general analysis. It becomes

clear from an examination of this table that generally there can be three cases of the relationship between the radiation-path length $l_1$ and the characteristic length, which we shall represent by the shock wave separation distance $\delta$. Designating $\omega = \delta/l_1$, we shall have:

$$\begin{aligned} &\text{for } n_a = 10^{16} && \omega \ll 1, \\ &\text{for } n_a = 10^{18} && \omega \sim 1, \\ &\text{for } n_a = 10^{20} && \omega \gg 1. \end{aligned}$$

It is reasonable that these relationships depend on the dimensions of the meteorite body, but in principle this does not alter the situation.

Ref. 76 deals with the influence of radiation on hypersonic flow about bodies when $\omega \ll 1$ and $\omega \gg 1$. First, there is obtained a reduction of temperature and pressure, and an increase of density in accordance with the shift along the surface of the body about which the flow takes place. Second, there is obtained the conventional diffusion scheme (diffusion approximation), the energy transfer having the nature of radiant heat transfer. This case is investigated in greater detail in Ref. 116.

Let us now consider the more general case of $\omega \sim 1$ for the critical point, and try to find an approximate solution for it. Let us imagine (Figure 31) the cross section of the front of a shock wave by a plane passing through the axis of the wave (assuming the body and the surface of the front to be axially symmetrical). From the center of curvature of the body at the critical point we draw a sphere with the radius $R_s = R_b + \delta$ ($R_b$ is the radius of the curvature of the body at the same point, $\delta$ is the shock wave separation distance); we shall call this the reference sphere. Our approximation consists of replacing the true surface of the shock-wave front with the reference sphere. In this manner we at the same time disregard the radiation of the regions located on the

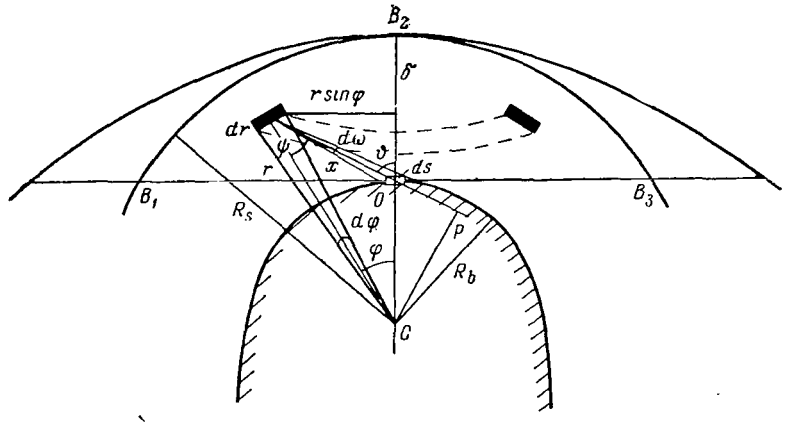


Figure 31. Determination of the thermal flux at the critical point.

"wings" of the shock wave between said shock wave and the reference sphere. However, as has been shown in Section 13, the temperature of the air at the wings and, consequently the radiation flux as well, diminishes sharply, and failure to take it into account will have little effect on the result.

It is necessary for us to find the radiation flux q on the elementary area ds, with the critical point in the center. We draw the "horizon line" of this area $B_1B_3$. Obviously, we are interested in the radiation arriving from all of the directions for which the position angle $\Theta$ is confined within the limits $0 < \Theta < \pi/2$. We shall henceforth assume the distribution of the radiation temperature $T(x, \Theta) \equiv T(r, \phi)$ to be given, shall assume that the radiation does not alter this distribution, and shall disregard the temperature of the body and the distribution from its surface, as well as the effect of radiation scattering and reflection. The solution of the problem may be obtained by the following two methods.

First method. We consider an element of air, volume dV, with a mass of $dm = \rho dV$, confined between two spherical surfaces and two planes passing through the wave axis. Since the problem is axially symmetrical, we may immediately assume the angle between the surfaces to be equal to $2\pi$, i.e., we assume that the volume dV has the form of a hoop with a cross section of $rdrd\phi$. Therefore, integration is performed along the azimuth, and the azimuth angle will no longer be of influence. The volume dV will be equal to

$$dV = 2\pi r^2 \sin \phi d\phi dr. \tag{14.12}$$

The quantity of energy $dQ_\nu$, radiated by the volume dV per unit of time in an elementary frequency interval, will be equal (Ref. 61) to

$$dQ_\nu = j_\nu dm d\omega, \tag{14.13}$$

and, furthermore,

$$j_\nu = \varkappa'_\nu B_\nu(T). \tag{14.14}$$

Here $j_\nu$ is the coefficient of radiation; $\varkappa'_\nu$ is the absorption coefficient per unit of mass; $B_\nu(T)$ is the intensity of radiation of an absolutely black body at a temperature of T and a frequency of $\nu$. The use of formula (14.14) is equivalent to the introduction of a hypothesis of local thermodynamic equilibrium for gas on the shock wave. Further, the solid angle $d\omega$, at which the area ds can be seen from the volume dV, is equal to

$$d\omega = \frac{ds \cos \vartheta}{x^2}, \tag{14.15}$$

where x is the distance between them. Substituting (14.12), (14.14) and (14.15) into (14.13), we obtain

$$dQ_\nu = \varkappa'_\nu B_\nu \rho \cdot 2\pi r^2 \sin\varphi \, d\varphi \, dr \frac{ds \cos\vartheta}{x^2}. \tag{14.16}$$

Integrating with respect to frequencies and using the averaged absorption coefficient $\bar{\varkappa}$, we find the radiation flux dq from the volume dV per unit of volume of the area ds, with account taken of absorption on the way from dV to ds:

$$dq = \frac{dQ}{ds} = \bar{\varkappa}\pi B\,(x, \vartheta)\,\rho \cdot 2\,\frac{r^2}{x^2} \sin\varphi \cos\vartheta \, dr \, d\varphi \cdot e^{-\int_0^x \bar{\varkappa}\rho \, dx} \tag{14.17}$$

As can easily be deduced from Figure 31, r sin $\phi$ = x sin$\Theta$, from which it follows that

$$dq = \bar{\varkappa}\pi B\,(x, \vartheta)\,\rho \cdot e^{-\int_0^x \bar{\varkappa}\rho \, dx} \sin 2\vartheta \, dx \, d\vartheta. \tag{14.18}$$

In order to obtain the full flux q, the expression (14.18) must be integrated with respect to the half-segment $B_1OB_2$:

$$q = \int_{\Delta} \pi B\,(x, \vartheta)\, e^{-\int_0^x \bar{\varkappa}\rho \, dx} \bar{\varkappa}\rho dx \sin 2\vartheta \, d\vartheta. \tag{14.19}$$

We introduce the optical thickness $\tau$, assuming that

$$d\tau = -\bar{\varkappa}\rho \, dx; \quad \tau_b - \tau = \int_0^x \bar{\varkappa}\rho \, dx' \tag{14.20}$$

($\tau$ = 0 at the wave front, $\tau = \tau_b$ at the body). Then, instead of (14.19), we shall finally have

$$q = \int_{\Delta} \pi B\,(\tau, \vartheta)\, e^{-(\tau_b - \tau)} \sin 2\vartheta \, d\vartheta \, d\tau. \tag{14.21}$$

The described method is, in particular (with insignificant alterations) presented by Koh (Ref. 123), where, in addition, calculation formulas are given for computing the expression (14.21).

Second method. We use radiant-transfer equations for an imaginary "star" with a radius of $R_s$, within which there is a hollow in the form of a sphere with a radius of $R_b$. Let us consider the radiation flux onto the area ds on the surface of this sphere, taking into account the fact that

radiation within the hollow is equal to zero. The equation of radiant transfer for the spherical-symmetrical problem is written down in the following manner (Ref. 122):

$$\cos\vartheta\frac{dI}{dr}-\frac{\sin\vartheta}{r}\frac{dI}{d\vartheta}=-\bar{\varkappa}\rho\,[I\,(r,\vartheta)-B\,(r,\vartheta)]. \tag{14.22}$$

The solution of this equation, according to Chandrasekar (Ref. 122) has the form:

$$I\,(r,\vartheta)=p\int_{\vartheta}^{\pi}B\,(p\,\operatorname{cosec}\psi,\psi)\,e^{-p\int_{\vartheta}^{\psi}\bar{\varkappa}\rho\,\operatorname{cosec}^2\psi\,d\psi}\bar{\varkappa}\rho\,\operatorname{cosec}^2\psi\,d\psi, \tag{14.23}$$

where p is the shortest distance of a ray from the center of curvature, $\psi$ is the angle between the ray and the radius vector at the point (p cosec $\psi$, $\psi$). Since

$$\mathrm{dx}=\mathrm{p}\,\operatorname{cosec}^2\psi\mathrm{d}\psi, \tag{14.24}$$

we can, using (14.20), simplify (14.23), reducing it to the form of

$$I\,(\vartheta)=\int_{0}^{\tau_b}B\,(x,\vartheta)\,e^{-\int_{\tau}^{\tau_b}d\tau'}d\tau. \tag{14.25}$$

Since the radiation flux from the hemisphere per unit of area is equal to

$$q=2\pi\int_{0}^{\pi/2}I\,(\vartheta)\cos\vartheta\sin\vartheta\,d\vartheta, \tag{14.26}$$

we obtain as a result

$$q=\int_{0}^{\pi/2}\int_{0}^{\tau_b}\pi B\,(x,\vartheta)\,e^{-(\tau_b-\tau)}\sin 2\vartheta\,d\vartheta\,d\tau, \tag{14.27}$$

which is entirely analogous to the expression (14.21) obtained by the first method.

On the basis of the above proposals

$$\pi\mathrm{B}(\mathrm{x},\Theta)=\sigma[\mathrm{T}(\mathrm{x},\Theta)]^4. \tag{14.28}$$

The local radiation temperature T(x, $\Theta$), which should be substituted into formula (14.28), is not equal to $T_e$. Discussion of the relationship between them is found in a number of works and

monographs (Refs. 60, 61, 109), and is usually reduced to the assertion that this relationship is of a rather complex nature, but under conditions of stellar photospheres, as well, apparently, as in a gas discharge, T must be very close to $T_e$. Under our conditions it must also be assumed that $T \approx T_e$.

Let us now consider the case of $\omega \ll 1$ (volume radiation). In this case we consider the gas to be transparent, and, disregarding the exponential multiplier, obtain from (14.27) and (14.28)

$$q = \sigma \int_0^{\pi/2} \int_0^{\delta \sec \vartheta} \bar{\varkappa} \rho T^4 \sin 2\vartheta \, d\vartheta \, dx, \tag{14.29}$$

it being always possible to substitute $1/l_1$ for $\bar{\varkappa}\rho = \bar{\varkappa}_1$. In the case of volume radiation it is convenient to consider the recoil of radiation of unit volume in all directions, which is equal to

$$E = 4\pi \varkappa_1 J = uc\varkappa_1 = \frac{4\sigma T^4}{l_1}, \tag{14.30}$$

where J is the mean intensity of equilibrium radiation at a given point, u is the radiation density.

In Ref. 76 expressions have been derived separately for the energy of recombination radiation of an elementary volume for nitrogen and oxygen that are applicable for $\omega \ll 1$, and in the $10{,}000° \leq T \leq 20{,}000°$ range. Averaging the coefficients for air, we obtain the following expression for E, which, taking (14.30) into account, may be substituted into formulas (14.27) and (14.29):

$$E = 2.90 \cdot 10^{-22} T^{-1/3} + 7.22 \cdot 10^{-27} T^{1/3} + 7.21 \cdot 10^{-32} T^{3/3}. \tag{14.31}$$

Finally, let us go into the third case of $\omega \gg 1$. This case has also been considered by V. N. Zhigulev, Ye. A. Romishevskiy and V. K. Vertushkin (Ref. 76). As a result of integrating the transfer equation, they obtained a formula analogous to (14.25) for radiation intensity at a frequency of $\nu$:

$$I_\nu = \int_0^R e^{-\int_x^R \varkappa_\nu dx'} B_\nu \varkappa_\nu \, dx. \tag{14.32}$$

Expanding $\varkappa_1$ and $\varkappa_1 B$ into Taylor series and effecting a number of simplifications, the authors of Ref. 76 obtained the following expression for I:

$$I = B - \frac{\partial B}{\partial r}\Big|_R \frac{1}{\varkappa_1(R)} + \frac{1}{\varkappa_1(R)} \frac{\partial}{\partial r}\left(\frac{1}{\varkappa_1} \frac{\partial B}{\partial r}\right)\Big|_R + O\left(\frac{B}{\omega^3}\right), \tag{14.33}$$

where R is the thickness of the layer whose radiation reaches the body.

Considering I to depend neither on the frequency nor, in the given instance, on the direction (since at small paths $l_1$ radiation reaches the body only from the region immediately adjacent to it), we obtain

$$q = \pi I. \tag{14.34}$$

Of great significance is the question as to just what temperature should be substituted into formula (14.33). According to Ref. 76, this should be the temperature at the distance of R, which has the same order of magnitude as the radiation path length $l_1$. We designate this temperature by $T_{eff}$ and shall try to evaluate it.

Let the temperature of the gas at the surface of the body be equal to $T_w$, and at the margin of the thermal boundary layer–to $T_2$ (Figure 32). We shall find the effective temperature from the condition that the thermal flux to the wall from the isothermal gas layer at this temperature is equal to the actual thermal flux:

$$\sigma T_{eff}^4 = \frac{1}{\Delta}\int_0^{\Delta} \sigma T^4 e^{-\varkappa_1 x}\, dx. \tag{14.35}$$

We introduce the dimensionless variables:

$$\xi = \frac{x}{\Delta}; \qquad \eta = \frac{T - T_w}{T_2 - T_w}, \tag{14.36}$$

where $\Delta$ is the thickness of the thermal boundary layer. We approximate the course of the temperature by a branch of the Gaussian curve, assuming

$$\eta = e^{-4\pi(1-\xi)^2}. \tag{14.37}$$

Then, taking (14.36) and (14.37) into account, we obtain

$$T_{eff} = T_w + (T_2 - T_w)\int_0^1 e^{-K(\xi)}\, d\xi, \tag{14.38}$$

where it is designated that

$$K(\xi) = 4\pi(1 - \xi)^2 + \frac{\Delta}{4l_1}\xi. \tag{14.39}$$

Thus, the only parameter determining $T_{eff}$ is the value $\Delta/4\, l_1$, proportional to the ratio of the thickness of the thermal boundary layer and the radiation path length. Table 20 shows the values

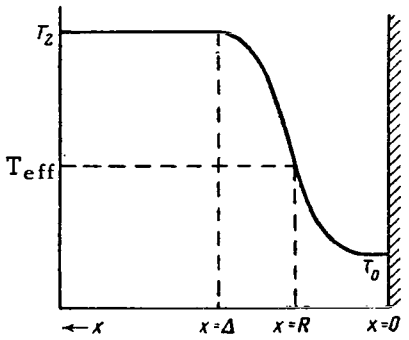


Figure 32. Temperature distribution near the body.

Table 20

Effective Temperature $T_{eff}$ ($T_2 = 10^5$; $T_w = 3 \cdot 10^3$)

| $\frac{\Delta}{4l_1}$ | 0 | 0.25 | 0.5 | 1 | 2 | 5 | 10 |
|---|---|---|---|---|---|---|---|
| Integral | 0,25 | 0,21 | 0,16 | 0,11 | 0,048 | $4{,}6 \cdot 10^{-3}$ | $1{,}6 \cdot 10^{-4}$ |
| $T_{eff} \cdot 10^{-3}$ | 27.2 | 23,1 | 18,9 | 13,7 | 7,6 | 3,4 | 3.0 |

of the integral from formula (14.38) for several values of this parameter, as well as $T_{eff}$ for the case of $T_w = 3{,}000°$, $T_2 = 100{,}000°$.

Obviously, when $\Delta > 20\ l_1$, it may be assumed that $T_{eff} = T_w$. Evaluations of $\Delta$ for specific cases of flow about bodies by a hypersonic stream are available in the work of Ye. A. Romishevskiy (Ref. 116). In the case of $\omega \gg 1$

$$\Delta = \frac{D}{\sqrt{\mathrm{Re}}\sqrt{\mathrm{Pr}}}, \tag{14.40}$$

where D is the characteristic dimension of the body, Re and Pr are Reynolds and Prandtl numbers (see Sections 3 and 16). Analysis of formula (14.40) shows that $\Delta$ increases somewhat slowly with altitude, and diminishes with the velocity of the body; therefore, the course of the ratio $\Delta/l_1$ (or of $\Delta/4\ l_1$) is determined by radiation path length $l_1$. In particular, for a body with D = 100 cm, according to the data of Ref. 116, we shall have:

when v = 10 km/sec, H = 30 km; $\Delta$ = 5.9 cm, $l_1$ = 10 cm, $\Delta/4\ l_1 = 0.15$,
when v = 15 km/sec, H = 30 km; $\Delta$ = 3.16 cm, $l_1$ = 0.2 cm, $\Delta/4\ l_1 = 3.95$,
when v = 15 km/sec, H = 50 km; $\Delta$ = 18.2 cm, $l_1$ = 10 cm, $\Delta/4\ l_1 = 0.45$.

Thus, for instance, $\Delta/4\ l_1$ becomes sufficiently large at high velocities, at low velocities, and also for large bodies.

Now we may return to evaluation of the radiation flux for the case under consideration. We introduce the value $\Theta = \sigma T_{eff}^4$. Then taking (14.28) into account, we finally obtain from (14.33) and (14.34) the expression for the radiation flux

$$q = \Theta - \frac{\partial \Theta}{\partial r}\Big|_R \frac{1}{\varkappa_1(R)} + \frac{1}{\varkappa_1(R)} \frac{\partial}{\partial r}\left(\frac{1}{\varkappa_1} \frac{\partial \Theta}{\partial r}\right)\Big|_R + O\left(\frac{\Theta}{\omega^3}\right), \tag{14.41}$$

and this yields the solution of the problem for $\omega \gg 1$.

## Section 15. Electron Heat Conduction

At a considerable degree of ionization behind the shock-wave front, air acquires the properties of plasma. One of the consequences of this is heat transfer by electrons (electron heat conduction). It is known (Refs. 42, 47, 52) that electron heat conduction considerably exceeds ion heat conduction, since at comparable temperatures $T_e$ and $T_i$ the thermal velocity of electrons is $\sqrt{m_i/m_e}$ times greater than that of ions.

The flux of electron heat conduction is equal to

$$q_e = -\varkappa_e \nabla T_e, \tag{15.1}$$

where $\varkappa_e$ is the coefficient of electron heat conduction. Determination of $\varkappa_e$ (as well as of other electron transfer coefficients) is based upon a solution of the Boltzmann equation, which expresses the distribution of gas particles in a phase space of coordinates and impulses. The general theory and solution of the Boltzmann equation by the method of successive approximations belongs to Enskog. An exposition of Enskog's method and calculations to the second approximation for inhomogeneous gases is contained in the book of Chapman and Cowling (Ref. 78), calculations for completely ionized plasma to the fourth approximation have been made by Landshoff (Ref. 79). Further refinements, connected in particular with the transition from a Lorentz gas to an actual gas, have been made by Spitzer and Härm (Ref. 80), and the results of the analysis are cited in Spitzer's book (Ref. 57). Formulas determining $\varkappa_e$ in the absence of a magnetic field have also been obtained by V. D. Shafranov (Ref. 52). According to Spitzer, for a Lorentz gas[1]

[1]A Lorentz gas is here called a mixture in which particles of one kind (for example, electrons) have a negligibly small mass in comparison to particles of another kind (for example, ions), it

$$\varkappa_e = 40\left(\frac{2}{\pi}\right)^{3/2}\frac{k(kT_e)^{5/2}}{m_e^{1/2}e^4 zL}, \tag{15.2}$$

where L is the Coulomb logarithm that was defined in Section 9.

In the works of Schirmer and Friedrich (Ref. 81) there is given a detailed derivation of precise formulas of $\varkappa_e$ for the case of multiple ionization in various approximations. Investigation of the convergence of these approximations has shown that if plasma is regarded as a Lorentz (specifically, a pure ion) gas, the second, and sometimes even the first approximations yield good results. For a completely (singly) ionized gas, Spitzer and Härm have obtained a formula differing from (15.2) only by the multiplier $\delta_T$, which takes into account the difference between the first approximation and the precise value. This multiplier is equal to:

| z | 1 | 2 | 3 | 4 | 5 | 6 |
|---|---|---|---|---|---|---|
| $\delta_T$ | 0.225 | 0.356 | 0.446 | 0.513 | 0.567 | 0.608 |

Substituting all the values of the constants into formula (15.2), we obtain

$$\varkappa_e = 9.34\cdot 10^{-12}\frac{T_e^{5/2}}{zL}\ \text{cal/sec}\cdot\text{deg}\cdot\text{cm}. \tag{15.3}$$

Analogously to (15.2), for ion heat conduction we shall have

$$\varkappa_i = 40\left(\frac{2}{\pi}\right)^{3/2}\frac{k\,(kT_i)^{5/2}}{e^4 z^4 m_i^{1/2}L}, \tag{15.4}$$

and for their ratio we shall have

$$\frac{\varkappa_e}{\varkappa_i} = \left(\frac{m_i}{m_e}\right)^{1/2}\left(\frac{T_e}{T_i}\right)^{5/2} z^3. \tag{15.5}$$

Since for air $(m_i/m_e)^{1/2} \approx 163$, electron heat conduction exceeds ion heat conduction if $T_i < 7.7\,T_e$ (when z = 1). Since $T_e$ behind the wave front increases rapidly and z increases simultaneously, whereas $T_i$ diminishes, it follows that the condition $\varkappa_e \gg \varkappa_i$ is satisfied rather quickly. The electron-temperature gradient in the compressed layer is directed toward the wave front, this effecting electron diffusion in the same direction and heating of the gas before the front. The

---

being possible to disregard mutual collisions of the light particles. The second condition is fulfilled if either the number of light particles, or the radius of activity of their force field, is much smaller than in the case of heavy particles.

size of the diffusion stream, with account taken of the temperature, density and pressure gradients, has been computed by Bond (Ref. 29).

In the boundary layer a considerable temperature gradient directed toward the meteorite body is formed. Therefore, electron heat conduction is an additional factor effecting heating of the meteorite.

Experimental determinations of $\varkappa_e$, carried out by Goldstein, Sekiguchi and Herndon (Ref. 82) for xenon, neon and helium, are in good agreement with the theory of Spitzer and Härm (Ref. 80). The only noted divergence is that the dependence of $\varkappa_e$ on $n_e$ is stronger than follows from formula (15.2), where this dependence is manifested through the value L. In Ref. 82 an almost linear dependence of $\varkappa_e$ on $n_e$ was obtained. However, the authors of Ref. 82 note that this effect may be a consequence of incompleteness of the experiment (unaccounted–for variations of $T_e$), and besides, all this was observed at very low instances of $T_e$ (300–500°K). Therefore, it may be assumed that the formulas cited above are applicable for calculating the part played by electron heat conduction in the heating of a meteorite.

However, one significant circumstance must be taken into account here. As has been pointed out by G. I. Pokrovskiy (Ref. 11), if the meteorite body is an insulator (this is valid for stone meteorites), the flow of electrons to the body will bring about the formation on its surface of an electron layer blocking off subsequent electron current and reducing the thermal flux carried by the electron heat conduction. If the meteorite material is a conductor (in the case of iron meteors), electrons will penetrate the body and, in addition, catalytic recombination of electrons with ions will take place on the surface (see Section 16).

Analogous ideas have been expressed by Bond (Ref. 29), who also drew attention to the possible appearance of negative potential in the boundary layer, and to the necessity for taking into account the action of a reacting wall (the surface of the body). Bond notes that despite the research carried out, it is to now impossible to foresee what will be the influence of the wall on a given heat-exchange mechanism. The experiments of P. K. Kabkov (Ref. 11) indicate that the thermal erosion (ablation) of bodies situated in a stream of plasma at comparatively high temperatures (6,000–10,000°) proceeds considerably more rapidly in bodies which are conductors, and less intensively in bodies which are insulators, although more resistant in the thermal sense. In the recently published works of Yu. V. Makarov and Yu. A. Polyakov (Ref. 120), there is described the experimentally observed formation of a negative surface charge on brass models in an air stream at Ma = 12. Grounding of the model resulted in the adhesion of ions to the model and the formation of a positive charge.

It is possible to take this into account by introducing into formula (15.1) the correction coefficient $\eta$, which we shall conditionally call the coefficient of electron blocking. Then, from (15.1) and (15.3), we finally obtain

$$q_e = 9.34 \cdot 10^{-12} \frac{T_e^{5/2}}{zL} \eta \nabla T_e. \tag{15.6}$$

The determination of $\eta$ for various materials requires special experimental research.

## Section 16. Convective Heat Exchange

Convective heat exchange is the basic mechanism of heat transfer to a body situated in a stream of oncoming air, even at not very high velocities. The question of the quantity of heat transferred convectively has been worked out in detail by Lees (Ref. 83) and Sibulkin (Ref. 84), who gave approximate solutions based on the extrapolation of previously obtained formulas for low velocities. The expression for the thermal flux at the critical point $q_s$ has been given by Sibulkin in the form:[1]

$$q_s = 0.763 \, \mathrm{Pr}^{-0.6} (h_{se} - h_{sw}) \sqrt{\overline{\rho_{se}\mu_{se} \left( \frac{dv_e}{dx} \right)_s}}, \tag{16.1}$$

where Pr is the Prandtl number, h is enthalpy, $\mu$ is viscosity, $\rho$ is gas density, the subscript s pertains to the critical point, the subscript e pertains to the external stream, the subscript w pertains to the wall. The enthalpy difference

$$h_{se} - h_{sw} = c_p(T_{se} - T_{sw})$$

is introduced in place of the temperature difference to account for dissociation.

Critical analysis of these and other similar solutions (Refs. 85, 86) has been carried out by Fay, Riddell and Kemp (Refs. 87–89), who gave a precise solution taking into account dissociation and diffusion in the boundary layer. Also investigated were various properties of the boundary layer (establishment of equilibrium, rate of recombination) and their influence on the results. The final solution of Fay and Riddell has the form (in the case of equilibrium dissociation):

$$q_{sE} = 0.763 \mathrm{Pr}^{-0.6} (h_{se} - h_{sw}) \left( \frac{\rho_w \mu_w}{\rho_{se} \mu_{se}} \right)^{0,1} \times$$
$$\times \sqrt{\overline{\rho_{se}\mu_{se} \left( \frac{dv_e}{dx} \right)_s}} \left[ 1 + (\mathrm{Le}^{0.52} - 1) \frac{h_{De}}{h_{se}} \right] \tag{16.2}$$

[1] In Lees' formula enthalpy is neglected, and in place of 0.763 $\mathrm{Pr}^{-0.6}$ there stands 0.71 $\mathrm{Pr}^{-2/3}$, which is almost the same.

(in the case of "frozen" dissociation, the exponent in the case of the Lewis number, Le, is equal to 0.63). In both cases the second term in the brackets takes heat transfer by diffusion into account. The "dissociation enthalpy" of a unit of mass of the air of the external stream, i.e., the dissociation energy per unit of mass, averaged with respect to the mass concentrations of air components, is $h_{D_e}$.

The ratio of the quantities of heat transferred by diffusion and heat conduction is expressed by the Lewis number

$$\mathrm{Le} = \frac{\rho D_{12} c_p}{\varkappa}, \tag{16.3}$$

where $D_{12}$ is the diffusion coefficient. If Le = 1, heat is transferred equally well by heat conduction and by diffusion, and the expressions for equilibrium and "frozen" dissociation become identical. If, however, Le > 1, in the case of a "frozen" boundary layer heat transfer increases somewhat in comparison with the equilibrium layer. The multiplier $(\rho_w \mu_w / \rho_{se} \mu_{se})^{0.1}$ is of the order of unity and increases the value of the flux $q_s$ by 10–20 percent.

Comparison with experiments at velocities to 8 km/sec has demonstrated their good agreement with formula (16.2), particularly at high altitudes. Formula (16.1) and others of its type yield excessively low results.

At meteorite velocities, taking ionization into account is of great importance. A preliminary investigation of this question was conducted by Adams (Ref. 90). He assumes that at temperatures of $T \leq 8{,}000°$, $\varkappa \sim T^{1/2}$, whereas when $T > 8{,}000°$, $\varkappa \sim T^{5/2}$, as for fully ionized gas (see Section 15). Viscosity, when $T \leq 8{,}000°$, increases according to the law of $\mu \sim T^{1/2}$, then diminishes; and when $T = 70{,}000°$, the law of its change approaches the form of $\mu \sim T^{5/2}$. The coefficient of ambipolar diffusion exceeds by a factor of 2 the diffusion coefficient for neutral atoms and molecules, with $D_{12} \sim T^{1/2}$ (at constant density this is true, and under the actual conditions of a shock wave, deviations will be small).

Before passing on to further exposition, we shall make several remarks concerning the role of diffusion in overall heat transfer. In partially dissociated gas the diffusion of atoms with respect to molecules creates a supplementary thermal flux to the body, raising the overall thermal flux, as we have seen, by approximately 20 percent. In the presence of partial ionization there originates the phenomenon of ambipolar diffusion, i.e., of the transfer of ion-electron pairs with respect to molecules, said phenomenon proceeding twice as fast as conventional atom-molecular diffusion (Ref. 90). As a result of the diffusion of atoms and of ion pairs through the boundary layer recombination takes place, with the release of energy either in the boundary layer itself, or at the wall.

If, however, the gas is completely dissociated, but ionization has not yet begun, atom-molecular diffusion is replaced by the process of self-diffusion, which is considered in detail by Chapman and Cowling (Ref. 78) and Lees (Ref. 83). Besides the general diffusion brought about by the density gradient, thermal diffusion, which depends on the temperature gradient, will also take place (Ref. 78).

With the beginning of ionization in a completely diffused gas, diffusion of ions in the gas itself (Ref. 91) and electron diffusion occur. The role of the latter increases with the growth of ionization. In completely ionized gas it is possible to consider the diffusion of electrons with respect to ions, the diffusion effecting heat transfer and charge transfer, i.e., phenomena already considered in Section 15.

Diffusion phenomena on the whole, and particularly in the presence of ionization, are sufficiently complex (see, for instance, Ref. 78). Considering the preceding discussion, however, it is clear that since the complete dissociation of air behind the shock wave is completed rapidly, there is no need to consider atom-molecular diffusion. The gas in the compressed layer will be completely ionized, and, therefore, it is ions and electrons that will be diffusing through the boundary layer. Depending on the electron density, either ambipolar or electron diffusion will take place (Ref. 92).

Lees (Ref. 83) has shown that the relationship between the thermal fluxes transferred due to heat conduction and diffusion is determined by two parameters: the Lewis number, Le (16.3), and the value

$$N = \frac{\Sigma h_{iw}(\alpha_{ie} - \alpha_{iw})}{h_{se} - h_{sw}}, \tag{16.4}$$

determining the ratio of the sums of the enthalpies of all the components of the gas at the wall to the difference of the overall enthalpies at the margin of the boundary layer and at the wall (in parentheses in the numerator stands the difference of concentrations of the i-th component at these boundaries). Lees' analysis pertains to the case of atom-molecular diffusion, and the presence of ions and electrons is not taken into account. In this case

$$\frac{q_D}{q_T} = \frac{\mathrm{Le}^{2/3} N}{1 - N}. \tag{16.5}$$

If Le = 1, the inflow of heat does not depend on the heat-transfer mechanism.

In our case of electron-ion diffusion, the parameter N is determined, as before, by the expression (16.4), with substitution of the values of enthalpy, and electron and ion concentration, but the Lewis number must be determined by the nature of the diffusion. According to Allis and

Rose (Ref. 92), in the case of high electron density, free electron and ion diffusion is replaced by ambipolar diffusion. Here only single ionization was considered. The pattern of diffusion in the case of multiple ionization has not as yet been considered by anyone, and the Lewis number in this case is unknown. But since the coefficient of ambipolar diffusion exceeds the corresponding coefficient for ions by a factor of 2, it is possible as a first approximation to assume that Le = 2, as has been done by Adams (Ref. 90), particularly since the Le number enters into formula (16.2) in a power of 0.5 or 0.6 (usually it is assumed that Le = 1.4).

Let us now consider the introduced correction for ionization.

Let the thermal flux due to convective heat transfer at the critical point comprise, in the absence of ionization

$$q_0 = q_{0,T} + q_{0,D}, \tag{16.6a}$$

and in the presence of ionization

$$q_1 = q_{1.T} + q_{1.D}, \tag{16.6b}$$

where the subscripts T and D denote, respectively, heat conduction and diffusion. We designate

$$\zeta = \frac{q_{1.D}}{q_{0.T}}; \quad \chi = \frac{q_{0.D}}{q_{0.T}}; \quad \psi = \frac{q_{1.T}}{q_{0.T}}. \tag{16.7}$$

Then, for the desired ratio $q_1/q_0$, which determines the correction for ionization, we obtain

$$\frac{q_1}{q_0} = \frac{\psi + \zeta}{1 + \chi}, \tag{16.8}$$

and furthermore, according to Ref. 90,

$$\zeta = \frac{\sum \beta_i \alpha_i Q_i}{c_p (T_e - T_w)}; \qquad \chi = \frac{\sum \alpha_i Q_i}{c_p (T_e - T_w)}, \tag{16.9}$$

where $T_e$ is the temperature that is external with respect to the boundary layer (i.e., the temperature of the gas stream in the compressed layer at the outer surface of the boundary layer); $T_w$ is the temperature of the wall; $Q_i$ is the energy expended on the dissociation and ionization of a unit of mass of the gas supplied by the stream; $\alpha_i$ is the concentration of a given form of ions or atoms; $\beta$ is a coefficient approximately equal to $\sqrt{\text{Le}}$, i.e., $\beta_a = 1$ for atoms, and $\beta_i = \sqrt{2}$ for ions, if it is assumed that Le = 2. For the case of complete ionization it may be assumed that

$$\chi = \frac{Q}{\bar{c}_p (T_e - T_w)}; \quad \zeta = \sqrt{2}\chi \quad (Q = \Sigma \alpha_i Q_i). \tag{16.10}$$

The value $\psi$ is found in the following manner. As a result of the simultaneous solution of the equations of energy conservation and momentum, Adams reduces the equation of conservation of energy to the form of

$$-\frac{\xi}{\theta^{1-2/n}} \frac{d\theta}{d\xi} = \frac{d^2\theta}{d\xi^2}, \tag{16.11}$$

where it is designated that

$$\theta = \left(\frac{T}{T_c}\right)^{n/2}; \quad \xi = \sqrt{2\alpha \frac{\rho_c \bar{c}_p}{\varkappa} \frac{\partial u}{\partial x}}\, \eta. \tag{16.12}$$

Here $T_c = 8{,}000°$ is the critical temperature at which ionization commences and the heat-conduction regime undergoes sharp change, that is, when $T > T_c$, $\varkappa \sim T^{5/2}$, whereas when $T < T_c$, $\varkappa \sim T^{1/2}$. In accordance with this, $n = 1$ when $\theta \leq 1$, and $n = 5$ when $\theta > 1$. $\rho_c$ is the density when $T = T_c$; $\alpha < 1$ is a constant connected with the Pr number; $\partial u/\partial x$ is the gradient of the tangential component velocity in the boundary layer; $\eta$ is the Howard-Dorodnitsyn variable (the y axis is directed along a normal to the surface of the boundary layer):

$$\eta = \int_0^y \frac{\rho}{\rho_c} dy. \tag{16.13}$$

Solving equation (16.11), Adams assumes that in the absence of ionization, $n = 1$, and in the presence of ionization, $n = 5$. Further designating

$$\theta_0 = \left(\frac{T}{T_c}\right)^{1/5}; \quad \theta_1 = \left(\frac{T}{T_c}\right)^{5/5}; \quad \theta' = \frac{d\theta}{d\xi}, \tag{16.14}$$

Adams obtains the following expressions for thermal fluxes:

$$q_{0,T} = 2\theta_0'(0) \sqrt{2\alpha \frac{\rho_e \varkappa_{0.e}}{\bar{c}_p} \frac{\partial u}{\partial x}}\, \bar{c}_p T_e, \tag{16.15}$$

$$q_{1,T} = 2\theta_1'(0) \sqrt{2\alpha \frac{\rho_e \varkappa_{1,e}}{\bar{c}_p} \frac{\partial u}{\partial x}}\, \bar{c}_p T_e \left(\frac{T_c}{T_e}\right)^{7/4}, \tag{16.16}$$

whence the desired ratio

$$\psi = \frac{q_{1,T}}{q_{0,T}} = \frac{\theta_1'(0)}{\theta_0'(0)} \left(\frac{T_c}{T_e}\right)^{7/4} \sqrt{\frac{\varkappa_{1.e}}{\varkappa_{0.e}}}. \tag{16.17}$$

The functions $\theta_0'(0)$ and $\theta_1'(0) \cdot (T_c/T_e)^{7/4}$ have been calculated by Adams (Ref. 90) and are cited in the form of graphs; from these graphs it follows that at high temperatures $\theta_0'(0)$ tends asymptotically toward a value of 0.55, while $\theta_1'(0) \cdot (T_c/T_e)^{7/4}$ tends asymptotically toward a value of 0.2. The value $\sqrt{\varkappa_{1,e}}/\varkappa_{0,e}$ for $T_e < T_c$ is equal to unity, and for $T_e > T_c$

$$\sqrt{\frac{\varkappa_{1.e}}{\varkappa_{0.e}}} = \frac{T_e}{T_c}. \tag{16.18}$$

Since under our conditions it always holds true that $T_e > T_c$, the latter condition (16.18) is valid and thus, approximately,

$$\psi \approx 0.36 \frac{T_e}{T_c}. \tag{16.19}$$

Substituting (16.19) and (16.10) into (16.3), and disregarding the wall temperature $T_w \ll T_e$ in the expression for $\chi$, we obtain the following approximate expression for the correction for ionization:

$$\frac{q_1}{q_0} = \frac{0.36\frac{T_e}{T_c} + \sqrt{2}\frac{Q}{c_p T_e}}{\frac{Q}{c_p T_e} + 1}. \tag{16.20}$$

In calculating the inflow of heat due to convective heat transfer, the Prandtl number Pr is of great value. For air it is usually assumed that Pr = 0.71. However, as has been shown by Marshall (Ref. 93), in plasma the Prandtl number will be much less, since in completely ionized gas the impulse is transferred primarily by ions, while thermal energy is transferred primarily by electrons (heat conduction). For completely ionized atomic hydrogen, according to Chapman (Ref. 94), viscosity and heat conduction are, respectively, equal to $\mu = 0.96\,\mu_i$, $\varkappa = 14\,\varkappa_i$, and, therefore,

$$\mathrm{Pr} = \frac{\mu c_p}{\varkappa} = \frac{0.96}{14}\frac{\mu_i c_p}{\varkappa_i} = 0.07\,\mathrm{Pr}_i \cong 0.05. \tag{16.21}$$

A more precise calculation by Chapman and Cowling (Ref. 78) yields for any singly ionized gas

$$\mathrm{Pr} = 0.065\,A^{-1/2}, \tag{16.22}$$

where A is the atomic weight of ions. For air A = 14.5 and Pr = 0.017.

However, the division of the charges in plasma creates an electrostatic field, which, according to Sen and Guess (Ref. 48) diminishes heat conduction by a factor of 2, thereby increasing the

Pr number. The absence of an equilibrium state, when $T_i > T_e$ and $dT_i/dy > dT_e/dy$, brings about a still greater increase of Pr. It may, therefore, be assumed that Pr = 0.05, and this is, after all, an order of magnitude less than the conventional value.

For calculations of convective heat transfer at the critical point, use should be made of formulas (16.2) and (16.20), with account taken of the remarks that have been made concerning Le and Pr.

Let us now compare the relative part played by all three of the heat-transmission mechanisms: convective thermal flux ($q_{conv}$), radiation flux ($q_{rad}$), and the flux transferred by electron heat conduction ($q_{elec}$). We shall make the comparison for the point of the full deceleration of a body with a spherical nose that has a curvature radius of R = 1 m for two cases:

1) Altitude 80 km, $n_a = 10^{16}$ cm$^{-3}$ (in the shock wave), the case of volume radiation; and,

2) Altitude 15 km, $n_a = 10^{20}$ cm$^{-3}$, the radiation flux is evaluated in a diffusion approximation.

The convective thermal flux is calculated according to formulas (16.2) and (16.20), for $T_e = 10^5$, there being assumed Le = 2, Pr = 0.05. The radiation fluxes were determined according to the formulas of Section 14 for the corresponding cases. The basic parameters obtained in the course of calculation, and which are of interest, are cited in Table 21.

The values of the thermal fluxes, expressed in terms of ergs/cm$^2$, are cited in Table 22.

The principal heat-transmission mechanism in all cases is convective heat transfer. The influence of radiation is relatively great at high velocities and high altitudes. Lower, in the dense strata of the atmosphere, despite the overall increase of the radiation flux, its relative share falls because of the rapid reduction of air transparency and radiation path length.

Table 21

Calculation Parameters

| $n_a$ | $T_e$ | $v_1$, cm/sec | Re | $T_{eff}$ | $\varkappa_e$, erg/sec · deg · cm |
|---|---|---|---|---|---|
| $10^{16}$ | $10^4$ | 11,5 | $1.4 \cdot 10^3$ | $10^4$ | $1.2 \cdot 10^6$ |
| | $10^5$ | 68,5 | $8,4 \cdot 10^3$ | $10^5$ | $1.7 \cdot 10^7$ |
| $10^{20}$ | $10^4$ | 8.7 | $5 \cdot 10^7$ | $3.9 \cdot 10^3$ | $1.7 \cdot 10^7$ |
| | $10^5$ | 48.0 | $2,8 \cdot 10^8$ | $2.44 \cdot 10^4$ | $7.8 \cdot 10^7$ |

Table 22

Thermal Fluxes to the Meteorite Body

| $n_a$ | $T_e$ | $q_{conv}$ | $q_{rad}$ | $q_{elec}$ | $q$ |
|---|---|---|---|---|---|
| $10^{16}$ | $10^4$ | $2.3 \cdot 10^{10}$ | $2.9 \cdot 10^9$ | $1.7 \cdot 10^9$ | $2.8 \cdot 10^{10}$ |
| | $10^5$ | $1.6 \cdot 10^{12}$ | $1.3 \cdot 10^{12}$ | $8.2 \cdot 10^{11}$ | $3.7 \cdot 10^{12}$ |
| $10^{20}$ | $10^4$ | $2.3 \cdot 10^{13}$ | $1.3 \cdot 10^{10}$ | $3.9 \cdot 10^{12}$ | $2.7 \cdot 10^{13}$ |
| | $10^5$ | $1.6 \cdot 10^{15}$ | $2.0 \cdot 10^{13}$ | $5.6 \cdot 10^{14}$ | $2.2 \cdot 10^{15}$ |

In regard to electron heat conduction, although the coefficient $\varkappa_e$, defined according to formula (15.3), depends weakly upon $n_a$ (approximately in the same manner as $n_a^{0.2}$), with the transition to denser strata of the atmosphere, there a sharp increase in the temperature gradient takes place (due to reduction of the boundary layer width), and it is this that leads to an increase in the flux of electron heat conduction almost proportionally to $n_a$. As a result, in the lower strata of the atmosphere the flux of electron heat conduction may exceed the radiation flux.

The approximate dependence of all the thermal fluxes on temperature has the form:

$$q_{conv} \sim T^2, \quad q_{rad} \sim T^3, \quad q_{elec} \sim T^{2.5}.$$

With a change in the characteristic dimension of the body R, the thermal fluxes change in the ratio:

$$q_{conv} \sim R^{-1/2}, \quad q_{rad} \sim R, \quad q_{elec} \sim R^{-1/2},$$

i.e., for large bodies the influence by radiation increases.

All of these evaluations have been made without consideration of meteorite evaporation, which can considerably change the pattern. This question will be considered in Section 17.—

## Section 17. Concerning Meteorite Ablation

The question of the mechanism of meteorite mass removal (ablation) has been discussed more than once in works dealing with the physics of meteorites and with meteorite science. Meteorite specialists, in particular Ye. L. Krinov (Ref. 95), on the basis of analysis of structural singularities of the fusion crust of meteorites comes to the conclusion that the basic mechanism of meteorite ablation is fusion. Actually, on the surface of many meteorites there are noted

perceptible streams and sinters, as well as solidified spatters of molten meteorite substance (Figure 33). These phenomena are quite clearly traced out in iron meteorites, in particular in the Sikhote-Alinskiy (Ref. 95) and the Yardymlinskiy meteorites (Ref. 96). Ye. L. Krinov therefore concluded that a meteorite loses mass as a result of fusion and blowing away of the molten film by the airstream. It is reasonable, however, that this conclusion is based upon analysis of phenomena occurring at the final sector of the flight.

On the other hand, B. Yu. Levin (Ref. 1), considering the ablation process of small meteorite bodies, concluded that for these bodies evaporation is the most significant factor. This conclusion is confirmed by comparison with photographic observations of bright meteors by Jacchia (Ref. 5) and Ceplecha (Ref. 97). Incidentally, as has been shown by an analysis of this question by N. A. Anfimov and M. Ya. Yudelovich (Ref. 98), the conclusion of B. Yu. Levin is insufficiently substantiated, since with some variation of the coefficient of blockage of the meteorite body with air molecules $a\Lambda$ (see Section 2), it is possible to obtain results in favor either of evaporation or fusion. N. A. Anfimov (Ref. 99), using the same data as Jacchia and Ceplecha, demonstrated that apparently in the removal of meteorite mass both processes are important, evaporation predominating at the upper sector and fusion predominating at the lower.

This entire discussion is on small meteorite bodies that engender conventional meteors, i.e., are valid for movement in conditions of flow with slip. But B. Yu. Levin transfers his conclusion

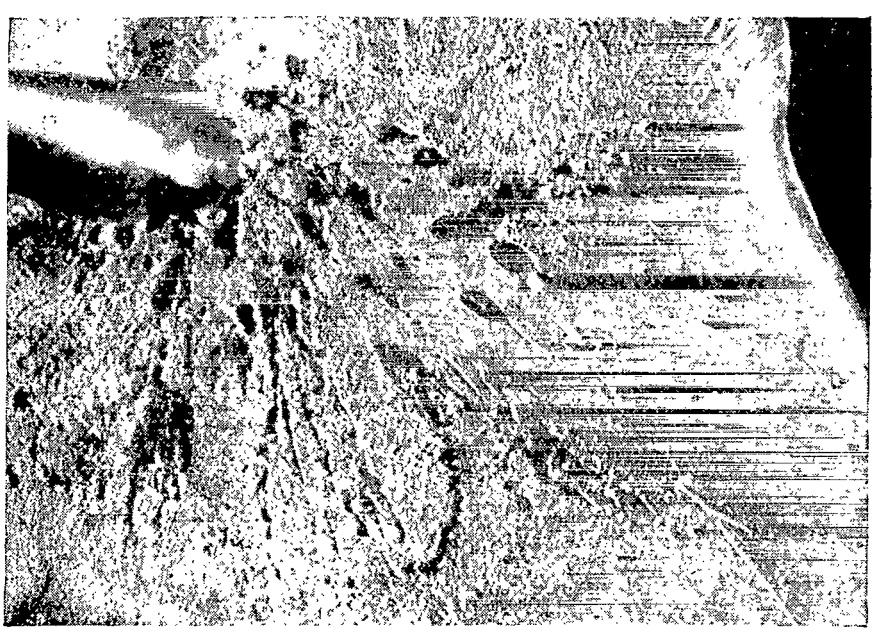

Figure 33. Structure of the fusion crust of the Sikhote-Alinskiy meteor. (according to Ye. L. Krinov)

concerning the predominance of evaporation to larger bodies as well. In his opinion, "The basic mass loss in the case of large 'meteorite-forming' bodies is determined by evaporation, although there are moments when blow-off of the molten layer plays a substantial part. With the slowing down of motion, while fusion is still possible, blowing off of the molten substance takes place" (Ref. 1, p. 77).

Morphological analysis data on the shape of fallen meteors show that either the shape corresponds to the crystalline structure (octahedrons, cubes, etc.), is irregular, or is oriented. The latter shape (Figure 34) apparently results from action of the airstream flowing about the meteorites, and indicates absence of rotation. According to the opinion of Ye. L. Krinov, meteorites that have retained their shape have lost a relatively small portion of their mass in the atmosphere (Ref. 95). The use of a helium method, which permits the original dimensions of the meteorite to be determined on the basis of the relationship of the helium isotopes $He^3$ and $He^4$ in meteorites, and on its distribution along the radius (Ref. 100), has yielded for the Treys meteorite a reduction of the linear dimensions in flight by a factor of 2, i.e., approximately a tenfold reduction in mass. Assuming for the coefficients of meteor-physics equations (Section 2) the following entirely plausible values:

$$\sigma = 1.5 \cdot 10^{-12}, \quad \Gamma = 0.5, \quad \Lambda = 0.015, \quad Q = 1.2 \cdot 10^{10}\ \text{erg/g}$$

(fusion), Martin (Ref. 100) obtained good correspondence with results obtained by the helium method.

In the development of flights at supersonic speeds, and then of space flights, the question of the heat protection of space vehicles returning to earth has become especially acute. One of the means for such protection is utilization of the phenomenon of ablation, which absorbs a considerable quantity of heat. All of this has resulted in considerable research on the theory of ablation,

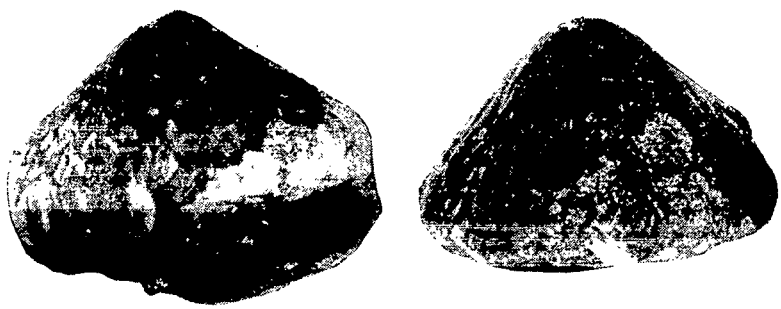

Figure 34. Meteorites of oriented shape: Karakol (left) and Zabrod'ye. Permaglypts are clearly seen on the surface.

as well as in experimental projects. A survey of foreign literature in this field is given by Adams (Ref. 101).

Considering the heating through of meteor bodies inward prior to the beginning of ablation, B. Yu. Levin, on the basis of the problem of the heating of a semi-infinite rod with a given thermal flux at one of its ends, came to the conclusion that if this thermal flux is expressed by an exponential law (in accordance with the increase of air density according to a barometric formula), the following regime of temperature distribution is established in a meteor body:

$$T(x, t) = T(0, t)e^{-x/x_0}, \tag{17.1}$$

where x is the distance from the boundary of the body, and $x_0$ is the so-called heating depth at which the temperature falls by a factor of e. According to the calculations of B. Yu. Levin this value amounts to 0.03–0.06 cm for stone meteorites, and 0.09–0.17 cm for iron meteorites, being inversely proportional to $v^{-1/2}$. Prior to the start of ablation, the temperature of the frontal surface $T(0, t) \sim v^{5/2}$, and thus to a higher velocity of the meteorite body there corresponds a higher temperature at a given depth, in spite of the smaller $x_0$.

If fusion has begun, a steady state sets in quite rapidly, and the front of the fusion wave in the vicinity of the critical point shifts at a constant rate. A precise solution of this case has been obtained by G. A. Tirskiy (Ref. 102). The rate of movement of the fusion wave in the case of constant thermal parameters is equal to

$$u = \frac{q}{\rho c\left(\frac{Q}{c} + T_{\text{fus}} - T_0\right)}, \tag{17.2}$$

where $\rho$, c, Q are the density, heat capacity, and latent heat of fusion of the body; $T_0$ is the initial temperature; $T_{fus}$ is the fusion temperature.

In the work of G. A. Tirskiy (Ref. 110) precise formulas are derived which yield the rate of movement of the fusion wave, the thickness of the fusion film, and the temperature distribution in the body for an arbitrary dependence of the thermophysical properties of the body on temperature.

For very large bodies, it may be assumed that heating spreads into the interior of the body at the same rate as the fusion wave. An important property of fusion is that it in no way influences the thermal flux to the body and has almost no influence on the boundary layer.

In the case of evaporation the pattern changes sharply. In front of the surface of the body a layer of evaporated molecules is formed which interact with the molecules and atoms of the oncoming airstream. The evaporated molecules have a different molecular weight from that of the

molecules and atoms of air (in the case of iron meteorites $\mu = 56$, and in the case of stone meteorites, $\mu = 40$–$72$), and a temperature equal to that of evaporation.

Heat transfer to the body is now no longer independent of the ablation process, as in fusion, since the layer of evaporated molecules creates an effect of thermal blockage (also called sweating out) (Ref. 101), which reduces the thermal flux to the body. The corrective multiplier $\psi$, equivalent to the coefficient of thermal blockage employed in the physical theory of meteors, $\alpha\Lambda \approx \Delta$, is in this case equal to

$$\psi = 1 - \frac{\beta \dot{M}_v (\Delta h)_0}{q_0}, \tag{17.3}$$

where $q_0$ is the thermal flux in the absence of evaporation; $M_v$ is mass rate of evaporation from one unit of area; $(\Delta h)_0$ is the difference of enthalpies across the boundary layer in the absence of evaporation; $\beta$ is the coefficient of thermal blockage, equal to approximately 0.6 for laminar heating, and to 0.2 for turbulent heating. If the effective heat of ablation, $Q_{eff}$, is defined as the energy expended for carrying away a unit of mass of substance, we shall have, in the case of fusion (Ref. 103)

$$Q_{eff} = Q_{fus} + c_p T_{fus} + 0.6 c_{pL} (T_i - T_{fus}), \tag{17.4}$$

and in the case of evaporation

$$Q_{eff} = Q_{evap} + c_p T_i + \beta (\Delta h)_0. \tag{17.5}$$

Increase of the effective heat of ablation in the case of fusion is determined by supplementary absorption of heat by the liquid film, in the case of evaporation, by thermal blockage and absorption of heat by the body due to thermal capacity. By $T_i$ is designated the temperature of the boundary of the division between the liquid and the hard surface with a gas layer; $c_{pL}$ is the specific heat of the liquid.

It has been shown experimentally that in the case of fusion, $Q_{eff}$ increases by about 50 percent due to heating of the liquid film (for pyrex), whereas for evaporation the effect of thermal blockage may, at high velocities, increase $Q_{eff}$ several times. This indicates that for fusion the heat-transfer coefficient $\Lambda$ (see Section 2) is equal to approximately 0.5, whereas for evaporation it is of the order of 0.1, this being in agreement with the data on the physical theory of meteors (Ref. 1). Unfortunately, the experiments so far pertain to comparatively low velocities.

In general, mass removal occurs due both to evaporation and to fusion, which occur simultaneously. The relationship between them is expressed by the "gasification parameter" $\Gamma_*$ ($\Gamma_* = 0$ in pure fusion, and $\Gamma_* = 1$ in pure evaporation). In this case

$$Q_{\text{eff}} = c_p T_i + \Gamma_* \left[ Q_{\text{evap}} + \beta\,(\Delta h)_0 + \frac{1-\Gamma_*}{\Gamma_*} Q'_{\text{fus}} \right], \tag{17.6}$$

where

$$Q'_{\text{fus}} = Q_{\text{fus}} + 0.6 c_{pL}(T_i - T_{\text{fus}}). \tag{17.4a}$$

Obviously, when $\Gamma_* = 0$, the expression (17.6) passes into (17.4), and when $\Gamma_* = 1$, it passes into (17.5).

Calculations carried out by Scala (Ref. 104) for high melting quartz-type oxides have confirmed the fact that when $\Gamma_* \to 1$, the full rate of mass loss, M, is diminished due to the heat-blockage effect, and to the increase of the heat of ablation. The value M is determined by dividing the thermal flux $q_0$ (computed with no account taken of ablation) by the effective heat of ablation $Q_{\text{eff}}$. The latter value, as has already been stated, increases rapidly as the flight velocity increases and, consequently, also as the deceleration enthalpy increases, the latter value entering into the term which expresses the effect of thermal blockage.

The flight altitude influences the ablation process through the deceleration pressure, on which logarithmically depends the temperature (more precisely, the enthalpy) of the liquid film and of the gases at the surface of the division. But since the thermal flux to the body and, at the same time, the surface temperature and the mass loss, increase with the growth of deceleration pressure, the effective heat of ablation (at constant $\Gamma_*$) will remain unchanged. However, under real conditions of $\Gamma_*$, it will change. In the opinion of Scala (Ref. 104), an increase of deceleration pressure will bring about a reduction of $\Gamma_*$ (due to the rapid fall of the viscosity of the molten layer), and some decrease in $Q_{\text{eff}}$.

Thus, at the end of the course the part played by fusion increases not only as a result of diminution of the velocity of the meteorite, but also due to an increase in deceleration pressure due to increasing air density, even if an insignificant slowing down of the meteorite in the final section of the course is taken into account.

An approximate investigation of the conditions of heating and ablation of a flying meteor has been carried out by K. P. Stanyukovich and V. P. Shalimov (Ref. 28). They represented the equation of thermal balance in the following form:

$$S\left(\Lambda \frac{\rho v^3}{2} + q_{rad}\right) = Mc \frac{dT_{\text{av}}}{dt} + \sigma\,(T_i^4 - T_a^4)\,\Sigma + Q_{\text{evap}} mN\,\Sigma, \tag{17.7}$$

where the thermal flux to the body is on the left side, including aerodynamic heating and radiation; M is the mass of the body; m is the mass of one molecule; N is the rate of evaporation

($cm^{-2} \cdot sec^{-1}$); $\Sigma$ is the area of the body; S is the area of the midsection; $T_a$ is the equilibrium temperature of air at a given level; and $T_{av}$ is the average temperature of the body

$$T_{av} = \frac{1}{V}\int_V T(r, t)\, dr. \tag{17.8}$$

In equation (17.7), the first term on the right-hand side takes into account losses for heating; the second right-hand term takes into account losses for radiation; and, the third takes into account those for evaporation. Usually heat expenditures for radiation from the surface of the meteorite body are much smaller than losses for evaporation, therefore, the second term may be disregarded. In subsequent calculations, K. P. Stanyukovich and V. P. Shalimov also disregard heat input due to convective transfer and do not take electron heat conduction into account at all, while for the shock-wave radiation flux they give a very approximate estimate: $(0.1–0.01)\,\sigma T_y^4$.

Heating through of the meteorite body in depth will take place if the condition

$$\frac{dT_{av}}{d\rho} \sim (q - Q_{evap} mN) > 0. \tag{17.9}$$

is fulfilled (q is the overall flux of heat to the body).

Approximate calculations by the authors of Ref. 28 show that for an iron meteorite, traveling at a velocity of 60 km/sec at an angle of 72° to the vertical (R = $10^2$ cm), to an altitude of $H_{equil}$ = 18 km, heat input will be greater than expenditure for evaporation, and the meteorite heats up (primarily at the surface), after which equilibrium sets in and heating-through ceases. On the other hand, at some critical altitude $H_{cr}$ (in the example at hand 12–14 km), the body must become completely destroyed as a result of evaporation. In the case of an iron or stone meteorite $H_{equil} > H_{cr}$; therefore, these bodies may reach earth without being totally destroyed. If, on the other hand, we consider an ice body (such is, for instance, considered to be the Tungusskiy meteorite, which is apparently the nucleus of a small comet (Refs. 105, 106)), in such a case $H_{cr} > H_{equil}$, and warming takes place all of the time (of the order of 0.2 sec) during which the body is destroyed. If the process proceeds at a sufficiently rapid rate, the evaporated particles, in flying asunder, can create a strong shock wave, and this will be analogous to an explosion.

This phenomenon, which the authors of Ref. 28 have called a "thermal explosion," is equivalent to the rapid evaporation of a considerable mass of substance as a result of rapid advancement of the boundary of the evaporating layer deep into the body.

Phenomena of a similar nature have been repeatedly observed in the high-velocity flight of aluminum pellets (Ref. 11), which would suddenly explode without any apparent reason. In this

case, however, intensive burning could have taken place, i.e., the rapid liberation of intrinsic (chemical) energy.

Unfortunately, in the calculation of K. P. Stanyukovich and V. P. Shalimov, account is taken only of integral heating, and not of the temperature distribution along the radius of the body, and the calculation itself is of an excessively approximate nature.

I. V. Nemchinov (Refs. 113, 114) has recently considered the problem of the evaporation of the surface of a meteorite under the influence of a thermal flux transmitted by radiation (in the approximation of radiant heat conduction). In his work it is assumed that in the vicinity of the critical point, the airstream toward the surface of the meteorite and the vapor stream meet at some "contact surface," and are immediately removed "aside." It is assumed in advance that the entire thermal flux goes for evaporation. The effect of thermal blockage brings about an increase of $Q_{eff}$ when T = 50,000° by two orders of magnitude; in other words, the coefficient of blockage, $\alpha\Lambda$, and the almost equal to it heat-transfer coefficient, $\Lambda$, have an order of magnitude of $10^{-2}$. The viscous boundary layer, in which evening out of the velocities takes place, has a thickness hundreds of times less than the thermal boundary layer in which evening out of the temperatures takes place.[1]

In considering the ablation process, I. V. Nemchinov and M. A. Tsikulin (Ref. 114) assume that the mass loss of a meteorite is proportional to the oncoming airstream, in other words,

$$\frac{dM}{dt} = -\alpha S\rho v. \tag{17.10}$$

Let us consider the extent to which formula (17.10) is substantiated. As is known, in the physical theory of meteors (Ref. 1) it is assumed that the mass loss is proportional to the energy, and it is here that equation (2.2) has its origins:

$$\frac{dM}{dt} = -\Lambda \frac{S\rho v^3}{2Q}. \tag{17.11}$$

The coefficient $\alpha$ in equation (17.10) has the following sense:

$$\alpha = \frac{\rho_w v_w}{\rho_s v_s} = \frac{h_s - h_{c+}}{Q_{\text{evap}} + (h_{c-} - h_w)} = \frac{h_s - h_{c+}}{Q_{\text{eff}}}, \tag{17.12}$$

where $\rho$, v, and h are, respectively, the density, velocity, and enthalpy of gas, the subscript w pertains to conditions at the wall, s to the shock-wave front, c to the contact surface (the plus

[1]An analogous result was obtained by Ye. A. Romishevskiy (Ref. 116).

sign from the side of the front; the minus sign from the side of the body, i.e., on the contact surface enthalpy $h_c$ undergoes discontinuity). It is not difficult to express the coefficient $\alpha$ in the following manner:

$$\alpha = \frac{h_s - h_{c+}}{h_s} \frac{Q_{\text{evap}}}{Q_{\text{eff}}} \frac{h_s}{Q_{\text{evap}}} = a\alpha_\Lambda \frac{v^2}{2Q_{\text{evap}}} = \Lambda \frac{v^2}{2Q_{\text{evap}}}, \tag{17.13}$$

and, consequently, equations (17.10) and (17.11) are equivalent.[1] Since $\alpha \sim 1/\rho_s \sim 1/\rho_H$ ($\rho_H$ is the density of air at the altitude H), the mass loss per unit of length of the meteorite course is

$$\frac{dM}{dl} = -\alpha S \rho_H = \text{const}, \tag{17.14}$$

i.e., does not depend upon altitude (at a constant rate of travel).

According to the calculations of I. V. Nemchinov and M. A. Tsikulin, in the case of vertical fall from an altitude of 50 km to the surface of the earth at a velocity of v = 50 km/sec, mass loss due to evaporation for a body with a radius of 10 m amounts to 35 g/cm$^2$. For smaller bodies, mass removal is greater ($\sim\sqrt{R}$) due to reduction of the thickness of the boundary layer and of the vapor layer, which, therefore, heats through more easily.

A precise solution of the problem of the equilibrium and nonequilibrium evaporation of a blunt body in the vicinity of the critical point (in the case of an arbitrary dependence of the physical properties of the body on heat) has been obtained by G. A. Tirskiy (Ref. 111). In distinction from the majority of works on this subject (Refs. 113–115), the evaporation temperature $T_i$ is assumed to be previously unknown and is determined in the course of solving the equations themselves. The heat of evaporation $Q_{evap}$ depends, generally speaking, on $T_i$, the latter being a function of the partial pressure of vapor (in a gas-vapor mixture) on the evaporating surface $p_i$. If the value $p_i = p_{i0}$ (the equilibrium value), then $T_i$ is equal to the surface temperature. In Ref. 111 it is proved that when the accommodation coefficient $\alpha > 0.1$, the equilibrium condition for evaporation is fulfilled. However, "boiling" on the surface of the body, determined by the conditions

$$c_{i0} = 1, \quad p_{i0} = p_{00}, \tag{17.15}$$

where $c_{i0}$ is the mass concentration of vapor at the surface, while $p_{00}$ is the deceleration pressure effected during equilibrium evaporation only in the case of infinitely great thermal flux to the

---

[1] It is possible with a sufficient degree of precision to assume the first multiplier in (17.13) to be equal to the accommodation coefficient $\alpha$, the second equal to the coefficient of thermal blockage $\alpha_\Lambda$ ($\Lambda = a\alpha_\Lambda$), and the enthalpy $h_s$ equal to the kinetic energy of a unit of mass of the oncoming gas $v^2/2$.

body. When "boiling" is attained, $T_i$ becomes equal to the evaporation temperature at the given vapor pressure, $p_i = p_{oo}$. It is specifically for these conditions that most of the approximate solutions were carried out, particularly those in Ref. 115.

In our case, the thermal flux to the body is so great (although it is not infinite), that the condition (17.15) will be fulfilled to a sufficient degree of precision.

In Ref. 112, G. A. Tirskiy solves the problem of simultaneous melting and evaporation of the fusion with account taken of air dissociation. However, the gasification parameter does not enter into his equations in explicit form, although it may be obtained in the course of their solution.

The problem of the ablation of a body flowed about by a stream of ionized gas has not yet been considered by anyone. Meanwhile, the presence of ionization introduces additional new effects, part of which have been mentioned above (Sections 15, 16). This is electron heat conduction, ambipolar or electron diffusion (the precise mechanism of diffusion under conditions of multiple ionization has not yet been ascertained), the catalytic role of the surface of the body in recombination and adhesion of electrons. The interaction of electrons with evaporating molecules must bring about their ionization, and this is observed, as has been demonstrated by meteor spectra, for calcium, magnesium, silicon and iron (Ref. 117). All of these circumstances considerably complicate theoretical consideration of the problem of meteor ablation.

The experimental material at present is also rather small. Experiments in the melting of models of Wood's metal and dry ice carried out by Thomas and Whipple (Ref. 4), yield, but a very approximate conception of the general course of phenomena. Closer to actual conditions are the experiments of I. A. Zotikov (Ref. 118) in the blowing of a supersonic stream about models of iron, the temperature of the material going as high as 2,800°K. In these experiments, indentations characteristic of meteorites—permaglypts (Figure 34)—were obtained; these, in the opinion of the author (Ref. 16), are brought about by turbulent phenomena in the boundary layer. Two facts speak in favor of this supposition: (1) a rather strictly maintained relationship between the dimensions of the permaglypts and those of the meteorite itself; and, (2) high Reynolds number values in the area of meteoric phenomena corresponding specifically to the turbulent boundary layer.

It is possible to count another two or three works of analogous content. Recently, attempts have been made in the United States to simulate meteoric phenomena by shooting aluminum bullets from rockets at high altitudes (at velocities of up to 10 km/sec). However, these experiments were not used to study the course of ablation.

Thus, the problem of the ablation of meteor bodies is still far from a final solution, and requires further research.

# CONCLUSION

What is at present the general state of the problem of the movement of large meteor bodies in the atmosphere?

Unquestionably, the difference in the regimes of flow about meteorites and small meteoric bodies (meteors) brings about substantial differences in the nature of their deceleration, heating and ablation. A meteorite creates a single detached shock wave, and in the case of an irregular shape, a complex system of waves. Behind the wave front there occur various nonequilibrium phenomena, the most important part among which is played by ionization. The large amplitude of the wave brings about a discontinuity in the temperatures of the electron gas and the ion gas, which thereupon gradually even out, but there is not always time enough for the establishment of an equilibrium state behind the wave front. A precise pattern of the temperature distribution behind the shock-wave front has not yet been obtained, and the pattern of current fields with account taken of ionization has also not been obtained.

Although the basic mechanisms of heat transfer to the body are known, and numerical evaluations of them are available, both the question of the influence of the body itself on the temperature distribution, and the question of ionization in the boundary layer for such strong shock waves have as yet been insufficiently studied. Still more complex is the problem of heat transmission to a body undergoing ablation. The mechanism of diffusion in the case of multiple ionization has not been studied, and the influence of ionization on heat transfer has been insufficiently studied. Almost no one has taken into account either electron heat conduction or the catalytic influence of the meteorite surface on heat exchange.

It may be considered doubtless that meteorite ablation takes place both by means of fusion and by means of evaporation. But the relative part played by these processes at various sectors of the flight and at various velocities has not been finally ascertained. And determination of the overall relative mass loss of meteorites in the atmosphere depends on the solution of this problem.

Of great importance to the solution of these problems would be not only subsequent theoretical investigations, but also properly organized photographic observations of bright bolides (in particular, of their spectra), as well as experimental work.

We shall present some specific problems for subsequent research.

1. Theoretical projects.

(1) Subsequent study of the influence of ionization on the parameters of the shock wave and on the heat-transfer mechanism.

(2) Refinement of the mechanism of the initial stage of ionization.

(3) Study of the diffusion process in the presence of multiple ionization.

(4) Study of the influence of the surface properties of a meteorite on recombination and electron adhesion.

(5) Solution of the boundary-layer equations with account taken of evaporation and ionized gas.

(6) Refinement of the temperature distribution in the shock wave with account taken of radiant heat conduction.

(7) Manifold investigation of the process of meteor deceleration in the atmosphere.

2. Observational projects.

(1) Organization of a photographic service for bright bolides and their trails, including spectrography through an obturator.

(2) Investigation of energy distribution in the spectrum of bright bolides to determine the nature of the radiation and its effective temperature.

(3) Subsequent observation of atmospheric bands and lines in the spectra of trails and "tails" of bright meteors with the aim of study of the composition of ions in the trails and the processes of recombination.

3. Experimental projects.

(1) Subsequent investigation of the fusion of models with the aim of studying the process of *permaglypt* formation.

(2) Investigation of the process of mass removal (ablation) of the substance of typical meteorites, in installations that create high-temperature gas streams.

(3) Investigation, in shock-wave tunnels of the structure of shock waves formed by actual meteorites.

(4) The use of rockets for launching artificial meteorites with a previously known mass, composition and velocity.

The present enumeration can undoubtedly be extended, but the accomplishment of even a part of the indicated projects would be of great value not only for meteorite science, but also for the problem of the return to earth of space ships from interplanetary flights.

## REFERENCES


1. Levin, B. Yu. Fizicheskaya teoriya meteorov i meteornoye veshchestvo v solnechnoy sisteme (The Physical Theory of Meteors, and Meteor Substance in the Solar System). Izd-vo AN SSSR, 1956.
2. Fesenkov, V. Meteoritika, No. 9, 3, 1951; No. 12, 72, 1955.
3. Ceplecha, Z. Bulletin of the Astronomical Institute of Czechoslovakia, Vol. 11, No. 1, 9, 1959.
4. Thomas, R. N., Wipple, F. L. Astrophysical Journal, Vol. 114, No. 3, 1951.
5. Jacchia, L. G. Harvard Observatory Technical Report, No. 2, 1949; No. 10, 1952.
6. Bronshten, V. A. Meteoritika, No. 20, 72, 1961.
7. --- Byulleten' VAGO, No. 30 (37), 39, 1961; Meteoritika, No. 22, 42, 1962.
8. Baker, R. L. M. Drag interaction of meteorites with the earth's atmosphere. Dissertation, University of California, Los Angeles, 1959.
9. Stanyukovich, K. P. Meteoritika, No. 7, 39, 1950.
10. --- Izvestiya AN SSSR, Seria mekhaniki i mashinostroyeniya, No. 5, 1960.
11. Pokrovskiy, G. I. Nauchno-metod. sb. VVIA im. Zhukovskogo, No. 23, 1960.
12. Jacchia, L. G. Smithson. Contrib. Astrophys., Vol. 2, No. 9, 1958 (Russian translation in the collection: Meteory, IL, 1959).
13. Ceplecha, Z. Bull. Astron. Inst. Czech., Vol. 12, No. 2, 1961; Meteoritika, No. 20, 178, 1961.
14. Tsien, H. S. Journal of the Aeronautical Sciences, Vol. 13, No. 12, 653, 1946.
15. Schaaf, S. A. Jet Propulsion, Vol. 26, No. 4, 247, 1956.
16. Bronshten, V. A. Geomagnetizm i aeronomiya, Vol. 2, No. 1, 126, 1962.
17. Adams, M. C., Probstein, R. F. Jet Propulsion, Vol. 26, No. 2, 86, 1958.
18. Probstein, R. F., Kemp, N. H. Journal of Aerospace Science, Vol. 27, No. 3, 174, 1960.
19. Probstein, R. F. ARS Journal, Vol. 31, No. 2, 185, 1961.
20. Hayes, W. D., Probstein, R. F. Hypersonic Flow Theory, Acad. Press, New York-London, 1959; Teoriya giperzvukovykh techeniy, IL, 1962.
21. Karma, T. J. Aerospace Sci., Vol. 26, No. 3, 129, 1959 (Russian translation in the collection: Problemy poleta s bol'shimi skorostyami, IL, 1960).
22. Lees, L. Jet Propulsion, Vol. 27, No. 11, 1162, 1957 (Russian translation in the collection: Problemy dvizheniya golovnoy chasti raket dal' nego deystviya, IL, 1959).
23. Ferri, A. First International Congress in the Aeronautical Sciences, Madrid, 1958 (Russian translation in the collection: Problemy poleta s bol'shimi skorostyami, IL, 1960).


24. Patterson, G. N. Canadian Aeronautical Journal, Vol. 4, No. 1, 2, 3, 1958 (Russian translation in the collection: Problemy poleta s bol'shimi skorostyami, IL, 1960).
25. Chernyy, G. G. Techeniye gaza s bol'shoy sverkhzvukovoy skorost'yu (Gas Flow at High Supersonic Velocity). Fizmatgiz, 1959.
26. Stanyukovich, K. P. Meteoritika, No. 14, 1956.
27. Dobrovol'skiy, O. V. Byulleten' Stalinabadskoy observatorii (Bulletin of the Stalinabad Observatory), No. 6, 1952.
28. Stanyukovich, K. P., Shalimov, V. P. Meteoritika, No. 20, 54, 1961.
29. Bond, J. Jet Propulsion, Vol. 27, No. 4, 228, 1958 (Russian translation in the collection: Voprosy raketnoy tekhniki, No. 1, 1959).
30. Selivanov, V. V., Shlyapintokh, I. Ya. Zhurnal fizicheskoy khimii (Journal of Physical Chemistry), No. 3, 670, 1958.
31. Stupochenko, Ye. V., Stakhanov, I. P., Samuylov, Ye. V., Pleshanov, A. S., Rozhdestvenskiy I. V. Termodinamicheskiye svoystva vozdukha v intervale temperatur ot 1,000 do 12,000°K i intervale davleniy ot 0.001 do 1,000 atm (The Thermodynamic Properties of Air in the Temperature Range from 1,000 to 12,000°K and the Pressure Range from 0.001 to 1,000 atm). Sb. Fizicheskaya gazodinamika, Izd-vo AN SSSR, 1959.
32. Predvoditelev, A. S., ed. Tablitsy gazodinamicheskikh velichin potoka vozdukha za pryamym skachkem uploteneniya (Table of Gasdynamic Values of an Airstream behind a Straight Shock Wave). Izd-vo AN SSSR, 1959.
33. Kaplan, S. A., Klimashin, I. A. Astronomicheskogo zhurnal, Vol. 36, No. 3, 1959.
34. Hayes, W. D. Some Aspects of Hypersonic Flow, Ramo-Wooldridge Corp., Los Angeles, 1955.
35. Dorodnitsyn, A. A. Trudy III Vsesoyuznogo matem. s"yegda (Transaction of the III All-Union Mathematical Congress), Vol. 2, Izd-vo AN SSSR, 1946.
36. Belotserkovskiy, O. M. Dokl. AN SSSR, Vol. 113, No. 3, 509, 1957; Prikladnaya matematika i mekhamikha, Vol. 22, No. 2, 1958; Vol. 24, No. 3, 511, 1960.
37. --- Raschet obtekaniya osisimetrichnykh tel s etshedshey udarnoy volnoy (raschetnyye formuly i tablitsy poley techeniy) (Calculation of Flow about Axially Symmetrical Bodies with a Decayed Shock Wave (Calculation Formulas and Tables of Current Fields)). Vych. tsentr AN SSSR, 1961.
38. Chushkin, P. I. Prikl. matem. i mekh., Vol. 24, No. 5, 1960.
39. Katskova, O. N., Naumova, I. N., Shmyglevskiy, Yu. D., Shulishnina, N. P. Opyt rascheta ploskikh i osisimetrichnykh sverkhzvukovykh techeniy gaza metodom kharakteristik (Experience in the Calculation of Plane and Axially Symmetrical Supersonic Gas Currents by the Method of Characteristics). Vych. tsentr AN SSSR, 1961.
40. Chushkin, P. I., Shulishnina, N. P. Tablitsy sverkhzvukovogo techeniya okolo zatuplennykh konusov (Tables of Supersonic Flow about Blunted Cones). Vych. tsentr AN SSSR, 1961.
41. Kogure, T., Osaki, T. Contr. Inst. Astrophys., University of Kyoto, No. 108, 250, 1961.
42. Zel'dovich, Ya. B., Rayzer, Yu. P. Usp. fiz. nauk, Vol. 63, No. 3, 1957.
43. Losev, S. A., Osipov, A. K. Usp. fiz. nauk, Vol. 74, No. 3, 1961.

44. Duff, R., Davidson, N. Journal of Chemical Physics, Vol. 31, No. 4, 1018, 1959 (Russian translation in the collection: Voprosy raketnoy tekhniki, No. 5, 1960).
45. Prokof'yev, V. A. Uch. zap. MGU, No. 172, Mechanika Izd-vo MGU, 1954.
46. Zel'dovich, Ya. B. Zhurnal eksperimental'noy i teoreticheskoy fiziki, Vol. 32, No. 5, 1126, 1957.
47. Rayzer, Yu. P. Zh. eksperim. i teor. fiz., Vol. 32, No. 6, 1528, 1957.
48. Sen, H., Guess, A. The Physical Review, Vol. 108, No. 3, 560, 1957 (Russian translation in the collection: Voprosy raketnoy tekhniki, No. 4, 1958); Sen, H., Guess, A. Vliyaniye vysokikh temperatur na strukturu udarnykh voln (The Influence of High Temperatures on the Structure of Shock Waves). In the collection: Kosmicheskaya gazodinamika, IL, 1960.
49. Stanyukovich, K. P. Neustanovivshiyesya dvizheniya sploshnoy sredy (Unstabilized Motion of a Continuous Medium), Gostekhizdat, 1955.
50. Dorrance, W. N. J. Aerospace Sci., Vol. 28, No. 1, 43, 1961 (Russian translation in the collection: Voprosy raketnoy tekhniki, No. 9, 1961).
51. Baum, F. A., Kaplan, S. A., Stanyukevich, K. P. Vvedeniye v kosmichesknyu gazodinamiku (Introduction to Space Gasdynamics). Fizmatgiz, 1958.
52. Shafranov, V. D. Zh. eksperim. i teor. fiz., Vol. 32, No. 6, 1453, 1957.
53. Landau, L. D. Zh. eksperim. i teor fiz., Vol. 7, No. 2, 209, 1937.
54. Petschek, H. E., Byron, S. Annales de Physique, Vol. 1, No. 3, 270, 1957 (Russian translation in the collection: Opticheskaya pirometriya plazmy, IL, 1960).
55. Bhatnagar, P. L., Krook, M., Menzel, D. H., Thomas, R. N. Vistas in Astronomy, Vol. 1, 296, 1955.
56. Pikel'ner, S. B. Izvestiya Krymskoy astrofizicheskoy observatorii, Vol. 12, 106, 1954.
57. Spitzer, L. Fizika polnost'yu ionizovannogo tela (The Physics of a Completely Ionized Body). IL, 1957.
58. Pikel'ner, S. B. Oxnovy kosmicheskoy elektrodinamiki (Foundations of Space Electrodynamics). Fizmatgiz, 1961.
59. Cohen, R. S., Spitzer, L., Routly, P. M. Phys. Rev., Vol. 80, 320, 1950 (Russian translation in the collection: Problemy sovremennoy fiziki, No. 2, 1956).
60. Ambartsumyan, V. A., Mustel', E. R., Severnyy, A. B., Sobolev, V. V. Teoreticheskaya astrofizika, Gostekhizdat, 1952.
61. Mustel', E. R. Zvezdnyye atmosfery (Stellar Atmospheres). Fizmatgiz, 1960.
62. Ivanov-Kholodnyy, G. S., Nikol'skiy, G. M. Astr. zh., Vol. 37, No. 5, 1960.
63. --- Astr. zh., Vol. 38, No. 1, 1961.
64. Biberman, L. M., Toropkin, Yu. N., Ul'yanov, K. N. Zh. tekh. fiz., No. 7, 1962.
65. Toropkin, Yu. N. K raschetu udarnykh protsessov v goryachem gaze (Calculation of Shock Processes in Hot Gas), (Diploma thesis). Moscow, Energ. In-t., 1961.
66. Brunner, I. Zeitschrift für physik, Vol. 159, 288, 1960.
67. Eckert, G., Weizel, W. Annalen der Physik, Vol. 17, No. 6, 130, 1956.
68. Seaton, M. J. Monthly Notices of the RAS, Vol. 118, 504, 1958; Vol. 119, 81, 1959.
69. Bronshten, V. A. Inzh. zh., Vol. 2, No. 1, 163, 1962.

70. Burgess, A., Seaton, M. J. Reviews of Modern Physics, Vol. 30, 992, 1958; Monthly Notices of the RAS, Vol. 120, 121, 1960 (Russian translation in the collection: Kosmicheskaya gazodinamika, IL, 1960).
71. Biberman, L. M., Norman, G. E. Optika i spektroskopiya, Vol. 8, No. 4, 433, 1960.
72. Biberman, L. M., Norman, G. E., Ul'yanov, N. Optika i spektroskopiya, Vol. 10, No. 5, 565, 1961; Astr. zh., Vol. 39, No. 1, 107, 1962.
73. Zel'dovich, Ya. B., Kompaneyets, A. S., Rayzer, Yu. P. Zh. eksperim. i teor. fiz., Vol. 34, No. 5, 1278, 1958; No. 6, 1447, 1958.
74. Meyerott, R. Combustion and Propulsion, Third AGARD Colloquium, 431–447, 1958 (Russian translation in the collection: Voprosy raketnoy tekhniki, No. 11, 1959).
75. Rayzer, Yu. P. Zh. eksperim. i teor. fiz., Vol. 37, No. 4, 1583, 1959.
76. Zhigulev, B. H., Romashevskiy, Ye. A., Vertushkin, V. K. Inzh. zh., No. 1, 60, 1961.
77. Sobolev, V. V. Perenos luchistoy energii v atmosferakh zvezd i planet (The Transfer of Radiant Energy in the Atmospheres of Stars and Planets). Goztechizdat, 1956.
78. Chapman, S., Cowling, T. Matematicheskaya teoriya neodnorodnykh gazov (The Mathematical Theory of Nonhomogeneous Gases). IL, 1960.
79. Landshoff, R. Phys. Rev., Vol. 76, 904, 1949 (Russian translation in the collection: Problemy sovremennoy fiziki, No. 2, 1956); Vol. 82, 442, 1951.
80. Spitzer, L., Härm, R. Phys. Rev., Vol. 89, 977, 1953 (Russian translation in the collection: Problemy sovremennoy fiziki, No. 2, 1956).
81. Schirmer, H., Friedrich, J. Z. Physik, Vol. 151, No. 2, 174, 1958; Vol. 153, No. 5, 463, 1958 (Russian translation in the collection: Dvizhushcheayasya plazma, IL, 1961).
82. Goldstein, L., Sekiguchi, T. Phys. Rev., Vol. 109, No. 3, 625, 1958; Sekiguchi, T., Herndon, R. S. Phys. Rev., Vol. 119, No. 1, 1, 1958 (Russian translation in the collection: Dvizhushcheayasya plazma, IL, 1961).
83. Lees, L. Jet Propulsion, Vol. 26, No. 4, 259, 1956 (Russian translation in the collection: Nauchnyye problemy iskusstvennykh sputnikov, IL, 1959).
84. Sibulkin, M. J. Aeron. Sci., Vol. 19, No. 8, 570, 1952.
85. Mark, R. Convair Report No. ZA-7-016, San Diego, 1956.
86. Romig, M. Jet Propulsion, Vol. 26, No. 12, 1098, 1956.
87. Fay, J., Riddell, F., Kemp, N. Jet Propulsion, Vol. 27, No. 6, 672, 1957 (Russian translation in the collection: Voprosy raketnoy tekhniki, No. 2, 1958).
88. Kemp, N. H., Riddell, F. R. Jet Propulsion, Vol. 27, No. 2, 132, 1957 (Russian translation in the collection: Nauchnyye problemy iskusstvennykh sputnikov, IL, 1959).
89. Fay, J., Riddell, F. J. Aeron. Sci., Vol. 25, No. 2, 73, 1958 (Russian translation in the collection: Problemy dvizheniya golovnoy chasti raket dal'nego deystviya, IL, 1959).
90. Adams, M. C. ARS Report, No. 1556–60 (Russian translation in the collection: Voprosy raketnoy tekhniki, No. 2, 1962).
91. Engel', A. Ionizirovannyye Gazy (Ionized Gases). Fizmatgiz, 1959.
92. Allis, W. P., Rose, D. S. Phys. Rev., Vol. 93, 84, 1954.

93. Marshall, W. Phys. Rev., Vol. 103, 1900, 1956 (Russian translation in the collection: Problemy sovremennoy fiziki, No. 7, 138, 1957).
94. Chapman, S. Astrophys. J., Vol. 120, 151, 1954.
95. Krinov, Ye. L. Osnovy meteoritiki (Foundations of Meteorite Science). Gostekhizdat, 1955.
96. Kashkay, M. A., Aliyev, V. I. Meteoritika, No. 20, 137, 1961.
97. Ceplecha, Z. Byulleten' Astronomicheskogo instituta Chekhoslovakii, Vol. 8, No. 3, 51, 1957.
98. Anfimov, N. A., Yudelovich, M. Ya. Primeneniye fizicheskoy teorii meteorov k issledovnaiyu protsessa tepleperedachi pri giperzvukovykh skorostyakh (Application of the Physical Theory of Meteors to the Investigation of the Process of Heat Transfer at Hypersonic Velocities). Oborongiz, 1958.
99. Anfimov, N. A. Astr. zh., Vol. 36, No. 1, 1959.
100. Martin, G. R. Geochimica et Cosmochimica Acta, Vol. 3, No. 6, 1953.
101. Adams, M. C. ARS Journal, Vol. 29, No. 9, 625, 1959 (Russian translation in the collection: Voprosy raktnoy tekhniki, No. 4, 1960).
102. Tirskiy, G. A. Doklady AN SSSR, Vol. 125, No. 2, 1959; Vol. 132, No. 4, 1960.
103. Lees, L. ARS Journal, Vol. 29, No. 5, 345, 1959 (Russian translation in the collection: Voprosy raketnoy tekhniki, No. 1, 1960).
104. Scala, S. M. J. Aerospace Sci., Vol. 27, No. 1, 1960 (Russian translation in the collection: Voprosy raketnoy tekhniki, No. 8, 1960).
105. Fesenkov, V. G. Astr. zh., Vol. 38, No. 4, 1961.
106. Stanyukevich, K. P., Bronshten, V. A. Dokl. AN SSSR, Vol. 140, No. 3, 1961.
107. Bond, J. W. Phys. Rev., Vol. 105, No. 6, 1957.
108. Shklovskiy, I. S. Fizika solnechnoy korony (Physics of the Sun's Corona). Fizmatgiz, 1962.
109. Unsel'd, A. Fizika zvezdnykh atmosfer (The Physics of Stellar Atmospheres). Gostekhizdat, 1955.
110. Tirskiy, G. A. Zhurnal vychislitel'noy Matematiki i matematicheskoy fiziki, Vol. 1, No. 3, 1961.
111. --- Vol. 1, No. 5, 1961.
112. --- Zhurnal prikladnoy matematiki i tekhnicheskoy fiziki, No. 5, 1961.
113. Nemchinov, I. V. Zh. prikl. matem. i tekhn. fiz., No. 1, 1960.
114. Nemchinov, I. V., Tsikulin, M. A. Geomagentizm i aeronemiya, Vol. 3, No. 4, 1963.
115. Roberts, L. Journal of Fluid Mechanics, Vol. 4, p. 5, 505, 1958; Technical Report, NASA, R-9, R-10, 1959.
116. Romishevskiy, Ye. A. Inzh. Zh., Vol. 2, No. 1, 170, 1962.
117. Astapovich, I. S. Meteornyye yavleniya v atmosfere zemli (Meteoric Phenomena in the Earth's Atmosphere). Fizmatgiz, 1958.
118. Zotikov, I. A. Meteoritika, No. 17, 35, 1958.
119. Levin, B. Yu. Astr. tsirkyulyar (Astronomical Circular), No. 230, 18, 1962.

120. Makarov, Yu. V., Polyakov, Yu. A. V. sb. "Fizicheskaya gazodinamika, teploovmen i termodinamika gazov vysokikh temperatur" (In the collection: The Physical Gasdynamics, Heat Exchange and Thermodynamics of High-Temperature Gases). Izd-vo AN SSSR, 1962.
121. Rayzer, Yu. P. Zh. eksperim, i teor. fiz., Vol. 33, No. 1 (7), 101, 1957.
122. Chandrasekar, S. Perenos luchistoy energii (The Transfer of Radiant Energy). IL, 1953.
123. Koh, J. C. Y. ARS Journal, Vol. 32, No. 9, 1962 (In Russian under the title: Raketnaya tekhnika i kosmonavtika, IL, 1963).
124. Ferrari, C., Clarke, J. H. Photoionization upstream of a strong shock wave. Brown University, Providence, R. I., USA, 1963.

Translated for the National Aeronautical and Space Administration by John F. Holman & Co. Inc.

NASA-Langley, 1964 TT F-247

*"The aeronautical and space activities of the United States shall be conducted so as to contribute . . . to the expansion of human knowledge of phenomena in the atmosphere and space. The Administration shall provide for the widest practicable and appropriate dissemination of information concerning its activities and the results thereof."*

—NATIONAL AERONAUTICS AND SPACE ACT OF 1958

# NASA SCIENTIFIC AND TECHNICAL PUBLICATIONS

TECHNICAL REPORTS: Scientific and technical information considered important, complete, and a lasting contribution to existing knowledge.

TECHNICAL NOTES: Information less broad in scope but nevertheless of importance as a contribution to existing knowledge.

TECHNICAL MEMORANDUMS: Information receiving limited distribution because of preliminary data, security classification, or other reasons.

CONTRACTOR REPORTS: Technical information generated in connection with a NASA contract or grant and released under NASA auspices.

TECHNICAL TRANSLATIONS: Information published in a foreign language considered to merit NASA distribution in English.

TECHNICAL REPRINTS: Information derived from NASA activities and initially published in the form of journal articles.

SPECIAL PUBLICATIONS: Information derived from or of value to NASA activities but not necessarily reporting the results of individual NASA-programmed scientific efforts. Publications include conference proceedings, monographs, data compilations, handbooks, sourcebooks, and special bibliographies.

***Details on the availability of these publications may be obtained from:***

**SCIENTIFIC AND TECHNICAL INFORMATION DIVISION**

**NATIONAL AERONAUTICS AND SPACE ADMINISTRATION**

**Washington, D.C. 20546**